

INFORMATION TO USERS

This manuscript has been reproduced from the microfilm master. UMI films the text directly from the original or copy submitted. Thus, some thesis and dissertation copies are in typewriter face, while others may be from any type of computer printer.

The quality of this reproduction is dependent upon the quality of the copy submitted. Broken or indistinct print, colored or poor quality illustrations and photographs, print bleedthrough, substandard margins, and improper alignment can adversely affect reproduction.

In the unlikely event that the author did not send UMI a complete manuscript and there are missing pages, these will be noted. Also, if unauthorized copyright material had to be removed, a note will indicate the deletion.

Oversize materials (e.g., maps, drawings, charts) are reproduced by sectioning the original, beginning at the upper left-hand corner and continuing from left to right in equal sections with small overlaps.

Photographs included in the original manuscript have been reproduced xerographically in this copy. Higher quality 6" x 9" black and white photographic prints are available for any photographs or illustrations appearing in this copy for an additional charge. Contact UMI directly to order.

ProQuest Information and Learning
300 North Zeeb Road, Ann Arbor, MI 48106-1346 USA
800-521-0600

UMI[®]

ION CHANNEL LOCALIZATION AND DETERMINANTS OF LOCALIZATION

by

Kevin Petrecca

**Department of Physiology
Faculty of Medicine
McGill University
Montreal, Quebec, Canada**

December 1999

**A thesis submitted to the
Faculty of Graduate Studies and Research
in partial fulfillment
of the requirements for the
Degree of Philosophy**

© Kevin Petrecca, 1999



**National Library
of Canada**

**Acquisitions and
Bibliographic Services**

**395 Wellington Street
Ottawa ON K1A 0N4
Canada**

**Bibliothèque nationale
du Canada**

**Acquisitions et
services bibliographiques**

**395, rue Wellington
Ottawa ON K1A 0N4
Canada**

Your file Votre référence

Our file Notre référence

The author has granted a non-exclusive licence allowing the National Library of Canada to reproduce, loan, distribute or sell copies of this thesis in microform, paper or electronic formats.

L'auteur a accordé une licence non exclusive permettant à la Bibliothèque nationale du Canada de reproduire, prêter, distribuer ou vendre des copies de cette thèse sous la forme de microfiche/film, de reproduction sur papier ou sur format électronique.

The author retains ownership of the copyright in this thesis. Neither the thesis nor substantial extracts from it may be printed or otherwise reproduced without the author's permission.

L'auteur conserve la propriété du droit d'auteur qui protège cette thèse. Ni la thèse ni des extraits substantiels de celle-ci ne doivent être imprimés ou autrement reproduits sans son autorisation.

0-612-64643-2

Canada

to Sarah

ABSTRACT

Ion channels constitute a class of proteins that is ultimately responsible for generating and coordinating electrical signals passing through the brain and heart. In order for ion channels to fulfill these roles a number of coordinated events must ensue at the protein level. Newly translated polypeptides entering the endoplasmic reticulum (ER) must be correctly processed and folded in order to exit. In the case of voltage-dependent ion channels, the channel α subunits, which form the channel pore, oligomerize with like (or unlike) α subunits and/or auxiliary (β) subunits, depending on the channel type. Further posttranslational modifications take place within the Golgi apparatus before the channels embark for their final destination. Once there, or prior to their arrival, they interact with cytoskeletal elements that serve to anchor the channel in place and tether accessory elements involved in ion channel modulation and signaling. Here, I have investigated the role of N-linked glycosylation in the surface membrane expression of a K^+ channel, human *ether-a-go-go* related gene (HERG), mutation of which can give rise to the cardiac disease long QT. Pharmacological and site-directed mutagenesis reveal that N-linked glycosylation is required for proper channel processing and cell surface expression of HERG as determined through immunoblot, immunocytochemical and electrophysiological analysis. Removal of glycosylation leads to an intracellular retention of HERG. Furthermore, I have examined the subcellular localization of the Na^+/H^+ exchanger (NHE1 isoform) in cardiomyocytes using immunocytochemical techniques and found that it exhibits a restricted subcellular localization at the intercalated disc. Along the same line, using the yeast two-hybrid screening technique, I have identified an

actin-binding protein, filamin, that directly interacts with and plays a role in the subcellular localization of a prominent heart and brain K^+ channel, Kv4.2.

RÉSUMÉ

Les canaux ioniques constituent une classe de protéines à l'origine de la génération et de la coordination des signaux électriques du cerveau et du cœur. Pour que les canaux ioniques remplissent ces rôles, un certain nombre d'événements coordonnés doit se produire au niveau protéique. Les polypeptides nouvellement transcrits entrant dans le réticulum endoplasmique (RE) doivent être correctement synthétisés et repliés pour pouvoir en sortir. Dans le cas des canaux ioniques voltage-dépendants, les sous-unités α du canal, qui en forment le pore, s'oligomérisent avec d'autres sous-unités α , identiques ou non, et/ou des sous-unités auxiliaires (β), selon le type de canal. D'autres modifications post-traductionnelles ont lieu dans l'appareil de Golgi avant que les canaux embarquent pour leur destination finale. Une fois arrivés à bon "pore", ou avant leur arrivée, les canaux interagissent avec des composants du cytosquelette qui leur servent d'ancrage et qui leur attachent des éléments accessoires qui modulent les canaux et leur voie de signalisation. Dans mon étude, je me suis intéressé au rôle joué par la glycosylation N-terminale dans l'expression à la surface de la membrane d'un canal potassique, HERG, dont la mutation provoque le syndrome cardiaque du long intervalle QT. Des études pharmacologiques et d'autres de mutagenèse dirigée révèlent que la glycosylation N-terminale est requise pour la synthèse de HERG et son expression à la surface cellulaire. Cela a été déterminé par "immunoblots", immunocytochimie et analyse électrophysiologique. L'élimination de la glycosylation cause la rétention de HERG à l'intérieur de la cellule. De plus, j'ai examiné la localisation subcellulaire de l'échangeur Na^+/H^+ (isoforme NHE1) dans des cardiomyocytes en utilisant des techniques

d'immunocytochimie et j'ai découvert qu'elle est restreinte aux disques intercalaires. Dans le même ordre d'idées, en employant la technique de criblage par système de double hybride de levure, j'ai identifié une protéine liée à l'actine, la filamine, qui interagit directement avec Kv4.2, un canal potassique prédominant du cœur et du cerveau, et qui joue un rôle dans sa localisation subcellulaire.

ACKNOWLEDGEMENTS

I would like to thank my supervisor, Alvin Shrier, for the freedom he afforded me to do the things that I wanted to do and for the trust he must have had to let me do such things. I guess in the end things worked out fine and maybe, but not necessarily, roses can grow in ----. I would like to thank all Shrier lab members who have helped me over the years. Special thanks to Damian G. Wheeler for the neuronal cultures shown in chapter 4.

Importantly, I would like to thank my grandparents for their will, character and determination, and my parents for much too much. I would like to thank Pej and Dam, it wouldn't have been the same without you. Lastly, I would like to thank Myriam for sticking it out for those last few years. You will be happy to know, it's over.

CONTRIBUTION TO PUBLICATIONS

Chapters 2, 3 and 4 of this thesis are duplicates of the following three manuscripts:

1. **Petrecca, K.,** Atanasiu, R., Akhavan, A., and Shrier, A. (1999). N-linked glycosylation sites determine HERG channel surface membrane expression. *J. Physiol. (Lond.)* 515, 41-8.

All experiment in this chapter were performed by myself with the following exceptions; R. Atanasiu generated the HERG-GFP construct and the glycosylation mutants. A. Akhavan was responsible for the electrophysiological experiments.

2. **Petrecca, K.,** Atanasiu, R., Grinstein, S., Orłowski, J., and Shrier, A. (1999). Subcellular localization of the Na⁺/H⁺ exchanger NHE1 in rat myocardium. *Am. J. Physiol.* 276, H709-17.

All experiments in this chapter were performed by myself with the exception of the immunoblot shown in Fig. 1 performed by R. Atanasiu.

3. **Petrecca, K.,** and Shrier, A. Localization of the Kv4.2 potassium channel by interaction with the actin-binding protein, filamin. (Submitted for publication).

All experiments in this chapter were performed by myself.

CONTRIBUTIONS TO ORIGINAL SCIENCE

My findings reported in chapter 2 reveal that N-linked glycosylation is required for efficient surface membrane expression of the K⁺ channel HERG. Mutations in HERG can result in a disorder called Long QT. The findings reported in this chapter sheds light on a novel mechanism for Long QT.

In Chapter 3 I determined the subcellular distribution of the Na⁺/H⁺ exchanger. The NHE1 isoform of the Na⁺/H⁺ exchanger is an integral component of the cardiac intracellular pH homeostatic mechanism that is critically important for myocardial contractility. To gain further insight into its physiological significance, I determined its cellular distribution in adult rat heart. Immunolabelling of NHE1 was detected predominantly at the intercalated disc regions of atrial and ventricular muscle cells. Significant labelling of NHE1 was also observed along the transverse tubular systems, but not the lateral sarcolemmal membranes, of both cell types. These results, in conjunction with other studies, indicate that NHE1 has a distinct distribution in heart and may fulfill specialized roles by selectively regulating the pH microenvironment of pH-sensitive proteins at the intercalated discs (*e.g.*, connexin43) and near the cytosolic surface of sarcoplasmic reticulum cisternae (*e.g.*, ryanodine receptor), thereby influencing impulse conduction and excitation-contraction coupling.

In chapter 4 I identified a novel protein-protein interaction between an ion channel and a cytoskeletal protein. The Kv4.2 K⁺ channel, which plays critical role in postsynaptic excitability, exhibits a somatodendritic expression pattern with a concentration at the PSD; however, the mechanism for this localization is unknown.

Here, I have identified a novel interaction between Kv4.2 and the actin-binding protein, filamin. I mapped the filamin interaction site to a 4 amino acid motif within the Kv4.2 C terminus. I also show that Kv4.2 and filamin interact both in vitro and in brain and that filamin localizes Kv4.2 to cellular specializations in heterologous cells. Moreover, Kv4.2 and filamin share an overlapping synaptic distribution pattern in brain and cultured hippocampal neurons. Thus, filamin may function as a scaffold protein in the postsynaptic density (PSD) mediating a direct link between Kv4.2 and the actin cytoskeleton.

ABBREVIATIONS

A: alanine
aa: amino acid
AChR: acetylcholine receptor
AD: activation domain
AR: adrenergic receptor
Asn: asparagine
 β -gal: β -galactosidase
bp: base pair
cDNA: complementary DNA
CF: cystic fibrosis
CFTR: cystic fibrosis transmembrane regulator
CHP: calcineurin B homologous protein
CO₂: carbon dioxide
cRNA: complementary RNA
Cx: connexin
D: aspartic acid
Dlg: discs large
DNA-BD: DNA binding domain
Endo: endoglycosidase
ER: endoplasmic reticulum
ERM: Ezrin, Radixin, Moesin
F: phenylalanine
GFP: green fluorescent protein
Glc: glucose
GlcNAc: N-acetylglucosamine
GLUT: glucose transporter
GLUT1CBP: GLUT1 C-terminal binding protein
GLYT: glycine transporter
GST: glutathione-S-transferase
H: histidine
hDlg: human discs large
HEK: human embryonic kidney
HERG: human *ether-a-go-go* related gene
His: histidine
I: isoleucine
IP₃: 1,4,5-inositol triphosphate
K: lysine
kDa: kilo Dalton
Kir: inwardly-rectifying K⁺ channel
Kv: voltage gate potassium channel
L: leucine
LQT: long QT

LQTS: long QT syndrome
 LTP: long-term potentiation
 M: methionine
 MAGUK: membrane associated guanylate kinase
 Man: mannose
 MERM: Merlin, Ezrin, Radixin, Moesin
 MuSK: muscle-specific kinase
 N: asparagine
 NHE: Na⁺/H⁺ exchanger
 NHE1BP1: NHE1 binding protein 1
 NHERF: NHE regulatory factor
 NMDA: *N*-methyl-D-aspartate
 NMJ: neuromuscular junction
 O₂: oxygen
 P: proline
 PAGE: polyacrylamide gel electrophoresis
 PBS: phosphate-buffered saline
 PDZ: PSD, Dlg, ZO-1
 PKA: protein kinase A
 PKC: protein kinase C
 PMCA: plasma membrane Ca²⁺ ATPase
 PMSF: phenylmethylsulfonyl fluoride
 PSD: postsynaptic density
 PVDF: polyvinylidene difluoride
 Q: glutamine
 R: arginine
 RATL: receptor associated transmembrane linker
 S: serine
 SAP: synapse associated protein
 SCN: sodium channel
 SDS: sodium-dodecyl-sulphate
 SH2: src homology domain 2
 SH3: src homology domain 3
 T: threonine
 TE: Tris-EDTA
 Thr: threonine
 TNF: tumor necrosis factor
 TRIP: TGFβ receptor interacting protein
 UAS: upstream activation site
 V: valine
 X: any amino acid
 Y: tyrosine
 ZO-1: zona-occludins 1

FIGURES

- Page 52: Effect of tunicamycin on the subcellular localisation of transiently expressed HERG^{GFP} in HEK 293 cells.
- Page 54: Immunoblot analysis of HERG^{GFP} protein stably expressed in HEK 293 cells.
- Page 57: Immunoblot analysis of wild-type and N-linked glycosylation mutant HERG^{GFP}s stably expressed in HEK 293 cells.
- Page 60: Whole-cell outward currents in HEK 293 cells stably expressing wild-type and N-linked glycosylation mutant HERG^{GFP}s.
- Page 64: Subcellular localisation of wild-type and N-linked glycosylation mutant HERG^{GFP}s stably expressed in HEK 293 cells
- Page 83: Detection of rat NHE1 protein in membrane preparations from AP-1 cells and rat heart.
- Page 86: Expression of NHE1 protein in AP-1 cells.
- Page 88: Expression of NHE1 in rat heart.
- Page 90: Comparison of NHE1 protein expression in ventricular and atrial myocardium.
- Page 93: Connexin43 protein expression in ventricular myocardium.
- Page 95: Na⁺,K⁺-ATPase protein expression in ventricular myocardium.
- Page 97: Co-localization of NHE1 and connexin43 protein expression in ventricular myocardium.
- Page 110: The Domain Structure of Filamin and Interaction with Kv4.2.
- Page 113: Coimmunoprecipitation in COS7 cells and Direct Binding of Kv4.2 and Filamin.
- Page 116: Colocalization and Accumulation of Kv4.2 and Filamin at Membrane Ruffles in Transfected COS7 Cells.
- Page 119: Colocalization of Kv4.2 and Filamin at Synapses in Cultured hippocampal Neurons.
- Page 122: Colocalization of Kv4.2 and Filamin at Synapses in Cerebellum.

Page 124: Biochemical Association of Kv4.2 and Filamin in Rat Brain.

TABLE OF CONTENTS

ABSTRACT	I
RESUME	III
ACKNOWLEDGEMENTS	V
CONTRIBUTION TO PUBLICATIONS	VI
CONTRIBUTION TO ORIGINAL SCIENCE	VII
LIST OF ABBREVIATIONS	IX
FIGURES	XI
PERMISSIONS	XIII
TABLE OF CONTENTS	XV
 CHAPTER 1	 1
<i>Introduction</i>	
Overview	2
Part I	3
<i>Long QT Syndrome</i>	3
<i>HERG</i>	4
<i>Functional Consequence of HERG Mutations in Long QT</i>	5
<i>Defective Protein Processing and Disease</i>	7
<i>N-linked Glycosylation and Defective Protein Processing</i>	8
<i>How are N-linked Glycoproteins Formed?</i>	9
<i>Role of N-linked Glycosylation in Protein Folding</i>	10
<i>What Determines N-linked Glycosylation</i>	11
<i>Does N-linked Glycosylation Play a Role in HERG Surface</i>	11
<i>Membrane Expression</i>	
Part II	13
Overview	13
<i>Acetylcholine Receptor Clustering at the Neuromuscular Junction</i>	14
<i>Yeast Two-Hybrid Method For Determining Protein-Protein</i>	16
<i>Interaction</i>	
<i>Cytoskeletal Protein Interactions with Voltage- and Ligand-Gated Ion</i>	17
<i>Channels</i>	
<i>Shaker-type, Kv1.4, K⁺ Channels</i>	18
<i>NMDA Receptor</i>	19
<i>PSD-95 and the Role of PDZ Domains</i>	19
<i>Kir2.1, Kir2.3, Kir4.1 and the Plasma Membrane Ca²⁺ ATPase bind</i>	22
<i>PSD-95</i>	
<i>β2 Adrenergic Receptor</i>	24
<i>Sodium Channels</i>	26
<i>Glucose Transporter</i>	26
<i>K⁺ Channel Kvβ Subunits</i>	27
<i>Functional Implications of Ion Channel Interactions With the</i>	29
<i>Cytoskeleton</i>	
<i>The Synapse is an Adherens Junction</i>	31

<i>Cell Junctions</i>	32
<i>The Intercalated Disc is an Adherens Junction</i>	34
<i>Ion Channels Localize at the Intercalated Disc</i>	35
Part III	37
<i>The Role of N-linked Glycosylation in HERG Surface Membrane Expression</i>	37
<i>Subcellular Localization of NHE1 in Cardiomyocytes</i>	38
<i>The Search for a Kv4.2 Anchoring Protein</i>	39
CHAPTER 2	41
<i>N-Linked Glycosylation Sites Determine HERG Channel Surface Membrane Expression</i>	
Abstract	42
Introduction	43
Materials and Methods	45
<i>DNA Constructs and Transfection of HEK 293 cells</i>	45
<i>Immunocytochemistry</i>	46
<i>Immunoblot Analysis</i>	47
<i>Electrophysiological Analysis</i>	48
Results	50
<i>Role of N-linked Glycosylation in Surface Membrane Expression of HERG^{GFP}</i>	50
<i>Biochemical Analysis of HERG^{GFP} Stably Transfected in HEK 293 Cells</i>	50
<i>Biochemical Analysis of HERG^{GFP} and N-linked Glycosylation Mutant HERG^{GFP}s Stably Transfected in HEK 293 cells</i>	55
<i>Functional Analysis of N-linked Glycosylation Mutants</i>	58
<i>Subcellular Localization of N-linked Glycosylation Mutant Proteins</i>	62
Discussion	65
CHAPTER 3	70
<i>Localization of the Na⁺/H⁺ Exchanger NHE1 to Intercalated Discs and Transverse Tubules of Rat Myocardium</i>	
Abstract	71
Introduction	72
Methods	75
<i>Rat Myocardial Isolation</i>	75
<i>Cell Culture</i>	75
<i>Primary Antibodies</i>	76
<i>Membrane Preparations</i>	76
<i>SDS-Polyacrylamide Electrophoresis and Immunoblotting</i>	77
<i>Immunohistochemistry</i>	78
<i>Immunocytochemistry</i>	79
<i>Confocal Laser Scanning Microscopy</i>	79
Results	81

<i>Myocardial Distribution of the Na⁺/H⁺ Exchanger</i>	81
Discussion	98
<i>The Na⁺/H⁺ Exchanger Isoform is Localized in Rat Cardiac Myocytes at the Intercalated Discs and Transverse Tubules</i>	98
Functional Implications for the Subcellular Localization of NHE1 in Heart	99
 CHAPTER 4	 102
<i>Localization of the Kv4.2 Potassium Channel by Interaction with the Actin-Binding Protein, Filamin</i>	
Abstract	103
Introduction	104
Results	108
<i>Interaction of Kv4.2 with Filamin</i>	108
<i>Association of Kv4.2 and Filamin In Situ and In Vitro</i>	111
<i>Filamin Binds and Localizes Kv4.2 to Membrane Ruffles in Heterologous Cells</i>	114
<i>Kv4.2 Colocalizes with Filamin at Synapses</i>	117
<i>Kv4.2 and Filamin Colocalize in Brain</i>	117
<i>Association of Kv4.2 and Filamin In Vivo</i>	120
Discussion	126
<i>What Determines Filamin Localization?</i>	126
<i>Role of Filamin at the Synapse</i>	128
Materials and Methods	131
<i>Yeast Two-Hybrid Screen and Analysis of Kv4.2-Filamin Interaction</i>	131
<i>Transfections and Immunocytochemistry in Heterologous Cells</i>	132
<i>Coimmunoprecipitations</i>	132
<i>Filter Overlay Assay</i>	134
<i>Neuron Culture, Transfection and Immunocytochemistry</i>	134
<i>Immunohistochemistry</i>	135
 CHAPTER 5	 136
<i>Discussion</i>	
<i>N-linked Glycosylation is Required for HERG Surface Membrane Expression</i>	137
<i>Localization of NHE1 and the Identification of a Cytoskeletal Anchoring Protein</i>	140
<i>Implications of the Kv4.2/filamin Interaction</i>	141
 REFERENCES	 144
 APPENDIX 1	 A1
 APPENDIX 2	 A2

CHAPTER 1

INTRODUCTION

Overview

Ion channels constitute a class of proteins that is ultimately responsible for generating and coordinating electrical signals passing through the brain and heart (Ackerman and Clapham, 1997). In order for ion channels to fulfill these roles a number of coordinated events must ensue at the protein level. Newly translated polypeptides entering the endoplasmic reticulum (ER) must be correctly processed and folded in order to exit. In the case of voltage-dependent ion channels, the channel α subunits, which form the channel pore, oligomerize with like (or unlike) α subunits and/or auxiliary (β) subunits, depending on the channel type. Further posttranslational modifications take place within the Golgi apparatus before the channels embark for their final destination. Once there, or prior to their arrival, they interact with cytoskeletal elements that serve to anchor the channel in place and tether accessory elements involved in ion channel modulation and signaling.

My thesis focuses on two aspects of this pathway. The first part involves investigating factors involved in ion channel surface membrane expression and the second part involves identifying the subcellular localization and determinants of subcellular localization of ion channels in cardiomyocytes and neurons. Specifically, I have investigated the role of N-linked glycosylation in the surface membrane expression of a K^+ channel, HERG, mutation of which can give rise to the cardiac disease long QT (LQT). Also, I have examined the subcellular localization of the Na^+/H^+ exchanger (NHE1 isoform) in cardiomyocytes and found that it exhibits a restricted subcellular localization. Along the same line, I have identified a cytoskeletal protein that directly

interacts with and plays a role in the subcellular localization of a prominent heart and brain K^+ channel, Kv4.2.

PART I

Long QT Syndrome

The long-QT syndrome (LQTS) is a genetic disorder of cardiac electrical repolarization (Vincent, 1998). LQTS is characterized by a prolongation of the QT interval, a measure of the time taken for ventricular repolarization, and is an important but relatively rare cause of sudden death in children and young adults. The majority of LQT sufferers are identified during routine electrocardiographic screening or after the evaluation of a primary relative who is affected. The minority of subjects are identified during a clinical evaluation for unexplained syncope or cardiac arrest. Often, the associated arrhythmia is a torsades de pointes polymorphic ventricular tachycardia triggered by adrenergic arousal (Ackerman and Clapham, 1997).

LQTS is caused by mutations of at least six genes of which four, each encoding ion channels, have been identified: *SCN5A*, encoding the cardiac sodium channel; *KvLQT1*, encoding the α -subunit of a K^+ channel, KVLQT1, that gives rise to the current designated I_{Ks} ; *KCNE1*, encoding minK, an ancillary subunit of the KVLQT1 K^+ channel; and *HERG*, encoding the α subunit of the K^+ channel, HERG, that gives rise to the current designated I_{Kr} (Priori et al., 1999).

The cardiac sodium channel generates the inward current that gives rise to the fast upstroke, phase 0, of the cardiac action potential. In sodium channel-associated LQT, a

deletion of three amino acids in a region thought to control rapid inactivation has been demonstrated (Kass and Davies, 1996). This mutant channel fails to inactivate completely resulting in reopenings of the channel and long-lasting bursts of channel activity. The resulting prolonged inward current thus lengthens the action potential duration. *KvLQT1* and *minK* are thought to combine to form the delayed-rectifier K^+ channel KVLQT1 (I_{Ks}) (Barhanin et al., 1996; Sanguinetti et al., 1996). I_{Ks} is one of the main K^+ conductances responsible for phase 3 repolarization of the action potential. Mutations in either of the subunits that combine to form this channel results in a decreased outward current and a consequent prolongation of the action potential (Vincent, 1998). Lastly, the *human ether-a-go-go gene (HERG)* encodes the α subunit of the delayed-rectifier K^+ channel HERG (Trudeau et al., 1995). HERG, most likely in combination with the ancillary subunit MiRP1 (Abbott et al., 1999), forms the channel that gives rise to the other principle phase 3 repolarizing current I_{Kr} . Mutations in *HERG* similarly result in a decreased outward current and thus, action potential prolongation and LQT (Vincent, 1998).

HERG

HERG is similar in structure to other voltage-dependent K^+ channels in that it is comprised of four α subunits each containing six membrane spanning domains, cytoplasmic N- and C-termini, and a pore formed by the S5 and S6 regions of each subunit. In LQT, at least 30 mutations in *HERG* have been identified, each giving rise to an impairment in channel function (Zhou et al., 1998c). The effect of certain LQT-associated *HERG* mutations on channel function and the role of defective channel

processing as a mechanism underlying HERG loss of function will be reviewed and explored, respectively.

Functional Consequence of HERG Mutations in Long QT

In order to determine the functional consequences of certain LQT-associated *HERG* mutations, Sanguinetti et al. (1996) analyzed the electrophysiological properties of five different mutant channels expressed in *Xenopus* oocytes. The deletion mutant, $\Delta bp1261$, which gives rise to a stop-codon by way of a frameshift within the S1 transmembrane domain, failed, as expected, to generate a current. Another mutation results in the deletion of nine amino acids within the S3 transmembrane region ($\Delta I500-F508$). Again, no current was detected. Three missense mutations, A561V, G628S and N470D, were also analyzed. Two of these mutants, A561V and G628S did not express functional currents. In contrast, the N470D mutant did express a current that exhibited altered voltage dependence of activation. In addition, this mutation decreased the amplitude of the expressed current 70% as compared to that of wild-type HERG. The authors suggest that the decreased current amplitude could arise from a decrease in single channel conductance, a decrease in channel function, or enhanced degradation of the channel protein or cRNA.

To investigate the consequences of *HERG* mutations on channel function in more detail, Zhou et al. (1998), using a combination of electrophysiological, biochemical and immunohistochemical techniques, studied the following LQT-associated mutations in HEK293 cells: T474I; I593R; Y611H; G628S; and V822M. The T474I mutant gave rise to a functional channel with altered gating properties. In contrast, no current was detected

upon expression of the I593R, Y611H, G628S and V822M mutants. Importantly, the I593R and G628S mutant channels were expressed on the cell surface as determined by immunocytochemical localization. Moreover, the G628S mutant channel was sensitive to treatment with proteinase K, a membrane impermeable serine protease that cleaves peptide bonds adjacent to the carboxylic group of aliphatic and aromatic amino acids. Taken together, the authors concluded that although the channel protein was expressed at the cell surface, the mutation rendered it nonfunctional.

Interestingly, the Y611H mutant channel, which also failed to generate a current, exhibited a different phenotype than the other mutant channels examined. This mutant channel was not expressed at the cell surface, but was retained intracellularly. Three lines of evidence point to this conclusion. First, immunoblot analysis revealed that this mutant channel was not sensitive to proteinase K treatment. Second, the mutant channels were sensitive to treatment with Endo H. Endo H digests high mannose oligosaccharides added during core glycosylation of newly synthesized proteins in the ER. Once proteins reach the Golgi apparatus, they undergo complex oligosaccharide modification to become Endo H resistant. Since the mutant channel was Endo H sensitive it can be concluded that it undergoes core glycosylation in the ER but fails to reach the medial Golgi, where it would have undergone complex glycosylation. Lastly, immunocytochemical analysis revealed that the channel exhibited a perinuclear expression pattern with no apparent surface membrane localization.

In summary, these studies demonstrated that certain LQT-associated *HERG* mutations result in the generation of channels that are expressed at the surface membrane but fail to conduct ions, or do so in an altered manner. The Y611H mutant, on the other

hand, does not fit such a classification. The loss of function displayed by this mutant channel is owing to defective channel processing and provides a basis towards our understanding of a novel mechanism for HERG dysfunction in LQT.

Defective Protein Processing and Disease

The majority of integral membrane proteins are synthesized on membrane-bound ribosomes and are translocated into the ER where folding, glycosylation, subunit assembly, and disulfide bond formation takes place. As many proteins contain domains that acquire certain three dimensional structures independent of other protein domains, folding can often begin cotranslationally (Reddy and Corley, 1998). Proper folding continues posttranslationally and is assisted by molecular chaperones. Typically, misfolded proteins, folding intermediates, unassembled subunits, and incompletely assembled oligomers remain in the ER. If they fail to reach the proper conformation they eventually undergo degradation without reaching the Golgi apparatus. By separating native from nonnative proteins, this conformation-based sorting process guarantees that only properly folded proteins will be further posttranslationally modified and expressed. This process, known as the quality control process, which oversees the transport of proteins from the ER to the Golgi apparatus, is one that senses general structural differences between native and nonnative proteins (Sousa and Parodi, 1995; Tatu and Helenius, 1997; Fink, 1999). In some cases, minor protein defects detected by the ER quality control system can lead to human disease (Dobson, 1999).

Cystic fibrosis (CF) is one such example of a disease linked, in part, to defective protein processing. The most common mutation in this disease, resulting in ~70% of CF

cases, is a deletion of a phenylalanine at position 508 in the cystic fibrosis transmembrane conductance regulator. This mutation leads to defective protein folding, retention of the protein within the cell and a consequent absence of protein expression at the cell surface (Cheng et al., 1990). Similarly, analysis of the aquaporin-2 water channel revealed that certain mutations found in patients suffering from nephrogenic diabetes insipidus result from the accumulation of the protein within the ER (Tamarappoo and Verkman, 1998).

N-linked Glycosylation and Defective Protein Processing

Early studies using tunicamycin, a N-linked glycosylation inhibitor, revealed that when N-linked oligosaccharide addition to proteins is blocked, most nonglycosylated forms of the proteins accumulate in the ER, aggregate and do not exit (Olden et al., 1982). For example, tunicamycin treatment of rat brain neurons results in the synthesis of a core sodium channel α subunit that is neither fully processed nor disulfide-linked to $\beta 2$ subunits before being rapidly degraded (Schmidt and Catterall, 1986). Using amino acid substitution to inhibit N-linked glycosylation, the GLYT1 glycine transporter was shown to require N-linked glycosylation for cell surface expression (Olivares et al., 1995). Using the same technique, Ray et al. (1998) showed that N-linked glycosylation of certain sites was critical for proper folding and cell surface expression of the human calcium receptor. Furthermore, in an elegant study, Keller et al. (1998) showed that by inhibiting the glucose trimming of the nicotinic acetylcholine receptor α subunit there was a reduction in its association with ER-resident chaperone calnexin and an increase in proteasomal

degradation. Thus, a role for N-linked oligosaccharides in protein folding and processing of certain integral membrane proteins, including ion channels, has been demonstrated.

How are N-linked Glycoproteins Formed?

The biosynthesis of N-linked oligosaccharide chains begins in the ER where the assembly of the oligosaccharide chain is initiated. The individual sugars, N-acetylglucosamine (GlcNAc), mannose (Man) and glucose (Glc) are sequentially added to the lipid carrier, dolichyl-P, to form the intermediate involved in the addition of the oligosaccharide to the protein, Glc3Man9(GlcNAc)2-PP-dolichol. The oligosaccharide is then transferred from the lipid to specific asparagine residues on the protein that are in the consensus sequence Asn-X-Ser(Thr) by the enzyme oligosaccharyl-transferase (Sousa and Parodi, 1995). This transfer of oligosaccharide to protein occurs as the protein is being synthesized and inserted into the lumen of the ER, thus, a cotranslational event.

As soon as the oligosaccharide is transferred to a protein, and probably before the synthesis of the protein chain has been completed, modification of the oligosaccharide begins. The reaction starts in the ER by the action of the first processing enzyme, glucosidase I, which removes the outermost glucose to give a Glc2Man9(GlcNAc)2-protein. Glucosidase II then sequentially removes the next two glucose moieties to produce the Man9(GlcNAc)2-protein. The glycoprotein, with either a Man8(GlcNAc)2 or a Man9(GlcNAc)2 structure is then transported to the Golgi apparatus where further trimming and posttranslational modification occurs (Fink, 1999).

Role of N-linked Glycosylation in Protein Folding

The role of the glucose residues in protein folding and quality control has now been clarified, in part, by the identification of two lectin-like proteins in the ER: calnexin and calreticulin (Fiedler and Simons, 1995), the former membrane-bound and the latter luminal. Calnexin binds to proteins trimmed down to the innermost glucose residue. This lectin interaction detains monoglucosylated proteins in the ER until they are properly folded. This is achieved by a cycle of glucosidase II action and reglucosylation by the luminal UDP-glucose:glycoprotein glucosyltransferase producing the monoglucosylated form. The key point being that the glucosyltransferase acts preferentially on unfolded or misfolded proteins. The substrate proteins thus undergo controlled on- and off-cycles with selected chaperone components in the ER. Glycoproteins will, for example, associate with calnexin and calreticulin, with glucosidase II and UDP-glucose:glycoprotein glycosyl transferase thereby driving the on- and off-cycle. These interactions may promote folding, suppress irreversible aggregation, and at the same time limit the mobility of the newly synthesized folding and assembly intermediates, preventing their premature exit from the ER (Tatu and Helenius, 1997). Misfolded or incompletely assembled subunits remain associated with calnexin for a prolonged period and are retained in the ER before degradation. As soon as the folding process is complete, the deglucosylated protein is free to leave the ER.

This work has established that N-linked oligosaccharides, immediately after their addition to a polypeptide chain, serve a general and important function in protein folding and quality control. Moreover, oligosaccharides can themselves modify local protein structure to which they are attached and can confer a certain degree of protease resistance

to the protein (Opdenakker et al., 1993). It should be pointed out that the cell is not entirely dependent on the calnexin/calreticulin mediated folding pathway as there are glycoproteins that can bypass this mechanism (Fiedler and Simons, 1995).

What Determines N-linked Glycosylation?

Multiple factors have been implicated in determining the extent to which the consensus glycosylation sequence, Asn-X-Ser(Thr), is glycosylated in a given protein. First, the presence of particular amino acids at or near the Asn-X-Ser(Thr) sequon can preclude glycosylation. For example, proline at either residue flanking the sequon inhibits the attachment of sugars, as does either proline or aspartic acid in the middle of the sequon. Second, the protein exerts an influence on glycosylation through the position of the sequon in the polypeptide. Sequons close to the N- or C-termini are generally less efficiently glycosylated. Finally, the polypeptide sequence may determine the speed with which protein folding renders the sequon inaccessible (Opdenakker et al., 1993). This is believed to result in a competition between the rate of folding and the addition of the dolichol linked precursor. For example, if the Asn-X-Ser(Thr) sequon is rapidly buried within protein domains it will no longer be accessible to the oligosaccharyl-transferase.

Does N-linked Glycosylation Play a Role in HERG Surface Membrane Expression?

Taking the information presented into consideration, at least two scenarios can be envisioned whereby N-linked glycosylation can play a role in the surface membrane expression of HERG. First, mutations that alter the native conformation of HERG may disrupt its ability to be glycosylated. For example, the Y611H mutant channel which was

not expressed at the cell surface was also not glycosylated. Interestingly, this mutation lies between HERG's two glycosylation sites, 598 and 629. This is an example where a mutation may have altered the conformation of the protein rendering the glycosylation sequons inaccessible. Inhibition of glycosylation would lead to decreased association with the ER-resident chaperone calnexin, less opportunity to fold correctly, and subsequent degradation. In fact, mutations at the N629 glycosylation site have been identified in LQT sufferers (Satler et al., 1998; Yoshida et al., 1999). A second, and related, scenario is that since the HERG channel is composed of multiple subunits, including MiRP1 (Abbott et al., 1999), it is conceivable that if glycosylation is inhibited, the conformation of individual subunits may be altered such that they can no longer coassemble. Such an event would also lead to the premature degradation of the individual subunits. In fact, the processes of subunit folding and coassembly have been shown to be interspersed in Shaker K⁺ channel processing (Schulteis et al., 1998)

PART II

Overview

Electrical signaling between neurons and between cardiomyocytes is dependent on the function of a wide variety of ion channels in the plasma membranes of these cells. In neurons, a large and growing body of evidence indicates that these channels do not diffuse freely in the membrane, but typically reside at specific subcellular locations, such as axon terminals, postsynaptic sites, and nodes of Ranvier. Alternatively, little is known about the subcellular localization of ion channels in cardiomyocytes, with the exception of gap junctions proteins which specifically reside at the intercalated disc.

For certain voltage- and ligand-gated ion channels, cytoskeletal elements have been identified that play a role in the anchoring of channels to the cytoskeleton, and the tethering of ion channels to macromolecular complexes. In addition, electrophysiological data supports a role for the cytoskeleton in ion channel function, disruption of the cytoskeleton affects channel function. Thus, cytoskeletal interactions with ion channels may have profound effects on the localization and function of ion channels and thus play a role in excitability and electrical signal transmission.

My interests lie in the identification of ion channels, more specifically K^+ channels and the Na^+/H^+ exchanger (NHE1 isoform), that exhibit discrete subcellular localizations in cardiac myocytes and neurons and the cytoskeletal determinants of this specialized localization. I will first review examples of ion channels, with an emphasis on K^+ channels, that are anchored and clustered through their association with cytoskeletal elements and the functional implications of such an association.

Acetylcholine Receptor Clustering at the Neuromuscular Junction

A classic example of ion channel clustering is that of the acetylcholine receptor (AChR) at the neuromuscular junction (NMJ) where the presynaptic motor neuron synapses with the postsynaptic myocyte. At the NMJ, AChRs are restricted to the crests of the postjunctional folds where they are present at $\sim 10\,000$ receptors/ μm^2 , a density of at least 1000-fold higher than the extrasynaptic membrane (Froehner, 1993). Although many molecules have been implicated in mediating this clustering, including neurally released agrin, the integral membrane receptor tyrosine kinase MuSK and the putative rapsyn associated transmembrane linker (RATL), the protein thought to be most directly responsible is the 43 kDa cytoskeletal protein rapsyn. The reason for this is based primarily on the following evidence. Rapsyn and the AChR are colocalized at the crests of postsynaptic folds in vivo (Sealock et al., 1984). When heterologously expressed in *Xenopus* oocytes, rapsyn forms membrane clusters that are capable of recruiting AChRs (Froehner et al., 1990). Importantly, disruption of the rapsyn gene in mice abolishes AChR clustering at the synapse (Gautam et al., 1995). Moreover, syntrophin, utrophin and dystroglycan, other postsynaptic proteins that cluster at the NMJ, also fail to localize in the rapsyn-deficient mice. Taken together, these data indicate that rapsyn is a cytoskeletal protein that is crucial for the clustering of AChRs at the NMJ and for the molecular organization of the postsynaptic membrane at the NMJ.

Remarkably, more than twenty years after the discovery of rapsyn, no biochemical data demonstrating a direct interaction between rapsyn and the AChR had been reported until very recently. In an attempt to resolve this issue, Fuhrer et al. (1999), using sepharose beads conjugated to α -bungarotoxin, precipitated AChRs and associated

proteins from extracts of myotubes prepared with a mild detergent, electrophoresed the precipitated proteins and performed immunoblotting experiments with antibodies directed against certain proteins implicated in AChR clustering. They demonstrated that large amounts of rapsyn could be coprecipitated with the AChR, adding further support to the notion that rapsyn is associated with AChR complex. More specifically, using a protein overlay assay, Buckel et al. (1998) showed that AChRs and rapsyn can interact revealing a direct association.

Similarly, utrophin and β -dystroglycan were also coprecipitated with AChR. Syntrophin, on the other hand, did not coprecipitate indicating that it may either be weakly associated or not associated with the AChR complex (Fuhrer et al., 1999). Interestingly, by using harsher detergents, they found that the coprecipitation of β -dystroglycan was lost while the association with utrophin and rapsyn was maintained. These data indicate that the association of utrophin and rapsyn to AChR occurs independent of β -dystroglycan. In fact other labs have presented data to support these findings. Rapsyn, when separated from other components of the NMJ by electrophoreses, will bind glutathione-S-transferase (GST)-dystroglycan in a protein overlay assay indicating a direct interaction between these two proteins (Cartaud et al., 1998). Furthermore, Fuhrer et al. (1999) also showed that in rapsyn $-/-$ myotubes there was no evidence for the association of utrophin or β -dystroglycan to the AChR. Taken together, these findings indicate that rapsyn is a cytoskeletal protein that directly interacts with the AChR and is required for mediating the association of utrophin and β -dystroglycan with the AChR.

Yeast Two-Hybrid Method for Determining Protein-Protein Interaction

Rapsyn was identified as a cytoskeletal protein associated with the AChR through the biochemical purification of AChRs (Sobel et al., 1977). This method for isolating and identifying cytoskeletal proteins associated with other ion channels has proven unsuccessful largely because the harsh detergents used to dissociate membrane proteins from the cytoskeleton disrupt protein-protein interactions. An explosion in the field of voltage- and ligand-gated ion channel associated proteins occurred in 1995 largely due to the development of the yeast two-hybrid screening technique. This powerful technique allows for the identification of novel protein-protein interactions. The yeast two hybrid assay is based on the fact that many eukaryotic transcription factors are composed of physically separable, functionally independent domains. Such factors often contain a DNA-binding domain (DNA-BD) that binds to a specific enhancer-like sequence, in yeast this is called an upstream activation site (UAS). One or more activation domains (AD) direct the RNA polymerase II complex to transcribe the gene downstream of the UAS. Both the DNA-BD and the AD are required to activate a gene, and normally, the two domains are part of the same protein. If physically separated and expressed in the same cell, the DNA-BD and AD peptides do not directly interact with each other and thus cannot activate the responsive genes. However, if the DNA-BD and AD can be brought into close enough proximity in the promoter region, the transcriptional activation function will be restored (Bartel and Fields, 1997). Thus, by fusing the DNA-BD of a transcription factor with a protein of interest (bait), one can screen a cDNA library that has been fused to the AD domain region of the transcription factor (prey). Protein-protein interactions can then be determined by the activation of downstream reporter genes.

From a practical perspective, the yeast two-hybrid screening assay is suitable only for baits that encompass non-membrane components of the ion channel as these proteins will be expressed in the yeast nucleus. Bait proteins including transmembrane domains would be expected to take on a non-native conformation in this environment. For ion channels, baits that include the intracellular N- or C-termini would be excellent candidates.

Cytoskeletal Protein Interactions with Voltage- and Ligand-Gated Ion Channels

The yeast two-hybrid method for determining protein-protein interactions has lead to the identification of cytoskeletal elements that interact with a variety of ion channels and transporters. Much of this work has focussed on voltage- and ligand-gated ion channels that have been shown to reside at specific subcellular compartments within neurons, namely the pre- and postsynaptic densities. In cardiomyocytes, ion channels have typically not been thought to exhibit a restricted distribution within the plasma membrane, with the exception of gap junction proteins, as cardiomyocytes do not have obvious morphologically specialized membrane domains such as axons and dendrites in neurons and apical and basolateral domains in epithelial cells. Thus, the little data regarding ion channel associated cytoskeletal elements that mediate channel localization in heart is due to the fact that little data exists regarding cardiac ion channel localization.

What follows is a summary of some of the more recent findings regarding cytoskeletal interactions with ion channels and their implications.

***Shaker*-type, Kv1.4, K⁺ Channels**

At the forefront of identifying ion channel associated proteins using the yeast two-hybrid screening technique was the Sheng lab, who were attempting to identify anchoring proteins associated with the *Shaker*-type K⁺ channel, Kv1.4. These channels have been shown to reside primarily at the presynaptic terminal of neurons (Sheng et al., 1992). They reasoned that since the N-terminal cytoplasmic tail of the ion channel α -subunit contains a proximal domain involved in subunit multimerization, and a putative distal flexible “ball peptide” responsible for the rapid inactivation of the channel, it was most probable that a potential anchoring protein would bind domains to within a cytoplasmic C-terminal tail.

Using the entire cytoplasmic C-terminal tail of Kv1.4 as a bait in a yeast two-hybrid screen they identified PSD-95 as a binding partner (Kim et al., 1995). This finding was confirmed in a protein overlay assay. Successive C-terminal deletion and mutational analysis revealed that the extreme C-terminal amino acids (TDV) were essential for interaction with this protein. More specifically, the valine at the 0 position and the threonine at the -2 position are required for binding. Mutation of the aspartic acid at the -1 had no effect on binding.

Importantly, from a functional perspective, coexpression of Kv1.4 and PSD-95 in COS cells resulted in the coclustering of these proteins. Unlike rapsyn, however, which is able to cluster itself and recruit AChRs to these clusters (Froehner et al., 1990), PSD-95 is unable to cluster in the absence of the interacting ion channel (Kim et al., 1995).

NMDA Receptor

At the same time, the Seeburg lab was asking a similar question regarding the *N*-methyl-D-aspartate (NMDA) receptor, a member of the glutamate receptor family. They noticed that the NR2 subunit of these receptors contained an extended cytoplasmic C-terminal tail. They reasoned, similar to the Sheng lab, that this region may be important for the anchoring of the receptors or play a role in the assembly of a signal-transducing complex for voltage-dependent Ca^{2+} entry through the glutamate-activated ion channel (Kornau et al., 1995).

Using the entire cytoplasmic C-terminal tail as a bait, they performed a yeast two-hybrid screen and identified PSD-95 as an interacting protein (Kornau et al., 1995). This finding was confirmed using a GST pull-down experiment in which GST was fused to the C-terminal 9 residues of NR2 subunit and was incubated with HEK293 cell extracts containing full-length PSD-95. Not surprisingly, the C-terminal tail of the NR2 subunit ends in SXV. These results were later extended by the Sheng lab who demonstrated that the interaction was direct by using a protein overlay assay (Niethammer et al., 1996).

PSD-95 and the Role of PDZ Domains

The studies described above revealed a role for PSD-95 in the binding and clustering of Kv1.4 and NMDA receptors (NR2 subunits) mediated through interactions with their cytoplasmic C-termini. The PSD-95 family of proteins in mammals contains PSD-95/SAP90, chapsyn-110/PSD-93, hDlg/SAP97 and SAP102 (Sheng et al., 1996). In their N-terminal half, this family of proteins is characterized by the presence of three domains with a length of approximately 90 amino acids. These domains are termed PDZ domains

because they were initially recognized as sequence repeats in PSD-95, the *Drosophila* septate junction protein discs-large (Dlg), and the tight junction protein zona occludins 1 (ZO-1). In addition, these proteins contain an SH3 domain and a guanylate kinase-like (GK) domain in their C-terminal region, defining them as a subclass of the MAGUK (membrane-associated guanylate kinase) superfamily of proteins (Mitic and Anderson, 1998).

PDZ repeats are modular protein-binding domains that recognize a short consensus peptide sequence, analogous to the better known SH2 or SH3 domains (Pawson and Scott, 1998). Similar to SH2 and SH3 domains, PDZ domains show specificity of binding. For instance, the Kv1.4/NR2 C-terminal E-S/T-D-V sequence motif does not bind to PDZ domains of other PDZ domain-containing proteins. Moreover, the specificity of interaction can be demonstrated by the fact that the C-terminal binding motif (E-S/T-D-V) shows different affinities for the three PDZ domains of PSD-95 family proteins (Hseuh et al., 1997).

The X-ray crystallographic structure of a PDZ domain from PSD-95, complexed with its peptide ligand, has shed light on the basis of PDZ domain peptide recognition (Doyle et al., 1996). A loop formed by the conserved -G-L-G-F- sequence in the PDZ domain binds to the carboxylate group of the terminal valine, explaining the specificity for an extreme C-terminal peptide sequence. The side chain of the C-terminal valine is buried in a deep hydrophobic pocket. Further side chain interactions explain the specific recognition of serine or threonine at the -2, and glutamine at the -3 positions. The penultimate (-1) residue of the peptide, however, makes only a backbone contact with the PDZ pocket.

Even more significantly, several of the critical contact residues defined in the crystallized PDZ domain from PSD-95 (Doyle et al., 1996) are different in other more distantly related PDZs, leading to the prediction that the various subclasses of PDZ domains will recognize different C-terminal peptide sequences. Using an oriented peptide library approach, Songyang et al. (1997) demonstrated that PDZ domain-containing proteins can be divided into two major groups based on the amino acid selected at the -2 position. Group I, including PSD-95, selected peptides with amino acids that contain hydroxyl groups (serine, threonine or tyrosine). Group II, including the PDZ domain-containing protein p55 and CASK, selected peptides with hydrophobic amino acids at this position. Most members of this group preferred a phenylalanine at this position, although tyrosine was also selected. This finding has been confirmed in a number of studies. For example, the PDZ domain CASK binds to the C-terminal tail of neuexins (-E-Y-Y-V; Hata et al., 1996), syndecans (-E-F-E-A, Cohen et al., 1998) and the transforming growth factor β -receptor II interacting protein, TRIP (-E-F-E-A, unpublished observation). Importantly, Songyang et al. (1997) also determined that PDZ domains do not bind internal sequences.

PDZ domains have been observed in more than 40 cytosolic proteins, many of which are located at specific regions of cell-cell contacts such as tight and adherens junctions, septate junctions and synaptic junctions. Roles of PDZ domain-containing proteins include ion channel clustering (Kim et al., 1995), protein localization (Simske et al., 1996), and mediating the assembly of macromolecular signaling complexes (Westphal et al., 1999). Given the divergence of PDZ domains and the number of PDZ domain-containing proteins thus far identified, it is engaging to envision a large

submembrane network that anchors integral membrane proteins such as ion channels and adhesion molecules to intracellular molecules such as signaling and cytoskeleton elements. In fact, a large number of ion channels that terminate in putative PDZ-binding motifs could potentially be interacting with a number of PDZ domain-containing proteins.

Many labs have taken advantage of the yeast two-hybrid screening technique in order to identify proteins that interact with integral membrane protein cytoplasmic C-termini. Indeed, it turns out that many ion channels, receptors and adhesion molecules bind PDZ domains. Examples include certain K^+ channels, Na^+ channels, the cystic fibrosis transmembrane conductance regulator (CFTR), several G protein coupled receptors, AMPA receptors, metabotropic glutamate receptors, adhesion molecules including neurexin, neuroligin and fasciclin II, neuronal nitric oxide synthase, and the list continues to expand. In the following sections of this review I will highlight some of these interactions and their functional implications that are more directly relevant to this review.

Kir2.1, Kir 2.3, Kir 4.1 and the Plasma Membrane Ca^{2+} ATPase bind PSD-95

The inwardly rectifying K^+ current (Kir) is the predominant conductance of a resting cell (Hille, 1992). To date, seven Kir families have been identified, Kir1-7 (Coetzee et al., 1999). Of these seven families, both Kir2.0 and Kir4.0 subfamilies contain C-termini that terminate in consensus PDZ binding motifs, SXI and SXV respectively.

Kir2.0 channels are highly expressed in heart and brain. Kir2.1 and 2.2 terminate in SEI, while Kir2.3 terminates in SAI. Using coimmunoprecipitation analysis from brain

and HEK293 cells, Kir2.1 and 2.3 were shown to interact with PSD-95 (Cohen et al., 1996). Interestingly, this study also demonstrated that the serine at the -2 positions is a substrate for phosphorylation by protein kinase A (PKA), and, upon phosphorylation, the interaction with PSD-95 is abolished (Cohen et al., 1996). This study revealed that the interaction of Kir2.0 with PSD-95 may be a dynamic and regulated event in a physiological environment.

Kir4.1, which is predominantly expressed in glial cells (Coetzee et al., 1999), has a sequence of SXV at its C-terminus. As expected, Horio et al. (1997) demonstrated that when Kir4.1 and PSD-95 were coexpressed in HEK293 cells they coclustered. Moreover they demonstrated that they could be coimmunoprecipitated from these cells. Importantly, electrophysiological analysis revealed that the magnitude of the whole cell current was increased 2-fold in cells expressing Kir4.1 and PSD-95 as compared to cells expressing Kir4.1 alone. They reasoned that since there was no difference in the single channel conductance, the increase current most likely arose from a stabilization of the channel at the cell surface by PSD-95.

The plasma membrane Ca^{2+} ATPase (PMCA) is a ubiquitous Ca^{2+} transporting enzyme that extrudes Ca^{2+} from the cell. To date, four PMCA isoforms in human and rat have been cloned. Expression of the PMCA1, 2 and 4 isoforms has been reported in heart (Hammes et al., 1998). The extreme C-termini of alternatively spliced "b"-type isoforms resemble those of K^+ channels and NMDA receptor (NR2) subunits that interact with the PDZ domains of certain MAGUKS. The "b"-type alternatively spliced forms of human PMCA terminate in the conserved sequence -SL/VETSL/V that matches the minimal -T/SXV consensus motif for PDZ interaction. The -ETSV of hPMCA4b matches the

consensus precisely whereas that of the other three PMCA b splice forms (ETSL) deviates conservatively from the consensus of the last residue. Western blot analysis using isoform specific antibodies have shown that human heart and brain express both PMCA 4a and 4b isoforms (Caride et al., 1996). With this information in mind, Kim et al. (1998) demonstrated that PMCA 4b and PSD-95 could be coimmunoprecipitated from COS7 cells and that PMCA4b and 2b could interact with a GST fusion protein containing all three PDZ domains of hDlg.

β2-Adrenergic Receptor

The β2-adrenergic receptor (AR), which is highly expressed in heart, belongs to the class of seven-transmembrane domain receptors for hormones and neurotransmitters that possess extracellular N-termini and intracellular C-termini. In an effort to determine binding partners for this receptor, Hall et al (1998b), instead of using the yeast two-hybrid screening technique, used a protein-protein overlay assay. To do so, they generated a GST-fusion protein containing the C-terminal tail of the β2-AR. This fusion protein was then subjected to electrophoresis and blotted with extracts from various organs. A single prominent band at 50 kDa was observed which was greatly enriched in kidney extracts. Amino acid sequencing of this protein revealed that it encoded the Na⁺/H⁺ exchanger regulatory factor (NHERF). NHERF contains two PDZ domains. Analysis revealed that the first PDZ domain is sufficient to bind the C-terminal region of the receptor that terminates in the amino acids DSLL. Importantly, in a functional context, when heterologously expressed, the β2-AR seemed to cocluster with NHERF but

only when the cells were stimulated with the B2-AR agonist isoprenaline. Thus, the interaction between these two proteins is agonist dependent.

NHERF was originally identified as a protein required for PKA mediated inhibition of the small intestine and renal proximal tubule brush border Na^+/H^+ exchanger (NHE) -3 isoform (Weinman et al., 1998; Yun et al., 1997). Yun et al. (1998) demonstrated that the entire second PDZ domain plus the C-terminal domain of NHERF is necessary to interact with NHE3, although the mode of interaction is presently unclear. Furthermore, NHERF has been demonstrated to bind the MERM family of cytoskeletal actin binding proteins, merlin, ezrin, moesin and radixin (Murthy et al., 1998). Since ezrin is a PKA anchoring protein, a macromolecular complex has been suggested whereby NHERF binding to both ezrin and NHE3 localizes PKA in the vicinity of the cytoplasmic domain of NHE3. Thus, the scaffolding properties of the cytoskeletal protein NHERF indirectly recruits PKA to NHE3 through the binding of ezrin.

To add a further level of complexity to this system, Hall et al. (1998b) demonstrated that the agonist-dependent interaction of the β 2-AR and NHERF results in a decreased inhibition of NHE3 activity. In summary, and not unlike the Kir2.0/ PSD-95 interaction, the physiological environment can regulate protein-protein interactions resulting in direct functional consequences for the ion channel. In this case, β 2-AR stimulation results in a recruitment of NHERF from NHE3, thus limiting the availability of NHERF to associate with NHE3, resulting in a decreased PKA-mediated inhibition of NHE3 activity.

Sodium Channels

Voltage-dependent sodium channels are concentrated in the postsynaptic membrane of the NMJ where they are confined primarily to the deeper portions of the folds and the perijunctional membranes. Conflicting data exists regarding their subcellular localization in heart. Cohen (1996) reported that these channels are localized to the intercalated disc while Petrecca et al., (1997) and Jurevicius et al. (1997) reported that they are more uniformly distributed along the sarcolemmal membrane.

Skeletal muscle and heart sodium channels, SkM1 and rH1 respectively, terminate in the consensus ESLV, a putative PDZ binding motif. Syntrophins, a PDZ domain-containing family of intracellular peripheral membrane proteins, are components of the dystrophin-associated protein complex in skeletal muscle that is relatively concentrated at the NMJ. Gee et al. (1998), using coprecipitation and protein-protein overlay analysis demonstrated that sodium channels and syntrophins directly interact and that they can be copurified from tissue. At the same time, using a very different approach, Shultz et al. (1998), also demonstrated that the C-terminal motif of these sodium channels interacts with the PDZ domain of α -syntrophin. This was accomplished by determining the solution structure of the α -syntrophin PDZ domain and applying peptide library searches. Whether sodium channel interaction with syntrophins mediates localization and/or tethering of other elements into a macromolecular complex has not been reported.

Glucose Transporter

Glucose transporters are required for efficient movement of glucose across the plasma membrane of mammalian cells. GLUT1 is a ubiquitously expressed transporter. Recently,

it was shown that GLUT1 in erythrocyte ghosts could be activated by agents that disrupt the actin cytoskeleton (Zhang and Ismail-Beigi, 1998). Thus a link between the transporter and the cytoskeleton seems likely. Interestingly, GLUT 1 is localized to the intercalated disc in heart (Doria-Medina et al., 1993). Bunn et al. (1999), who reasoned that there is more than likely a cytoskeletal element involved in this localization, used the yeast-two hybrid screening technique to identify GLUT1-associated proteins. They identified a novel protein that they called GLUT1 C-terminal binding protein (GLUT1CBP). Not surprisingly, considering the extreme C-terminal amino acids of GLUT1, the interaction is mediated by a PDZ motif. The C-terminal amino acids of GLUT1 are DSQV which directly bind the PDZ domain of GLUT1CBP. Western blot analysis revealed that this protein is expressed in all tissues examined with the exception of the small intestine. They also found that GLUT1CBP dimerizes and that the PDZ domain of GLUT1CBP also binds α -actinin-1, potentially directly linking GLUT1 to the actin cytoskeleton.

K⁺ Channel Kv β Subunits

Many voltage-dependent K⁺ channels associate with nonintegral membrane components known as Kv β subunits (Pongs et al., 1999). Four Kv α subunits oligomerize to form the ion conducting transmembrane pore (Hille, 1992), whereas Kv β subunits are attached to the cytoplasmic face of the Kv α subunits. Three closely related Kv β subunits, Kv β 1-3, have been identified containing a conserved C-terminal region and variable N-terminal region (Pongs et al., 1999). These Kv β subunits oligomerize with α subunits in the ER before transport to the Golgi apparatus (Nagaya and Papazian, 1997).

The role of Kv β subunits has followed three avenues of investigation. First, a chaperone function has been suggested for these subunits as they have been shown to influence the cell surface expression of Kv α subunits when coexpressed in heterologous cells (Shi et al., 1996; Nagaya and Papazain, 1997). Although this finding has added insight into K $^{+}$ channel processing, it is most likely not the primary role of the Kv β subunit. The reasoning for this is that since Kv α and Kv β subunits together form a functional complex in the cell membrane, it is not surprising that one would influence the others abundance. A simple comparison can be made to the Kv α subunits. It is clear that Kv α subunits oligomerize in the ER prior to their transport to the Golgi apparatus (Shulteis et al., 1998). The fact that additional subunits (Kv β subunits) also oligomerize in the ER and that this interaction influences channel processing follows a similar paradigm.

A second, and very novel, role for Kv β subunits has been proposed by the MacKinnon lab. They have determined the structure of a Kv β subunit by X-ray crystallography. Remarkably, its structure is related to that of aldo-keto reductases (Gulbis et al., 1999). These authors propose that the primary role of the Kv β subunit is that of an enzyme. Specifically, they suggest that the reduction/oxidation chemistry of a cell is intrinsically linked to changes in membrane potential via the interaction of Kv α and Kv β subunits of voltage-dependent K $^{+}$ channels.

The most well-characterized function of the Kv β subunit is with respect to its role in K $^{+}$ channel inactivation. Coexpression of Kv β 1 was found to greatly accelerate the rate of inactivation of K $^{+}$ currents expressed from the Kv1.1 or Kv1.4 α -subunits. Similarly,

Kv β 3 accelerates the rate of inactivation of K⁺ currents expressed from Kv1.4 or Kv1.5 α subunits (Pongs et al., 1999). As was mentioned previously, Kv β subunits contain a conserved C-terminal region and a variable N-terminal region. Kv β 1 and Kv β 3 subunits contain a similar N-terminal region that encodes an extreme N-terminal “ball” peptide postulated to play a role in N-type inactivation. This “ball” peptide is similar to that encoded by the Kv α subunit N-terminus. Kv β 2 subunits, on the other hand, do not encode such a “ball” peptide and thus have no effect on channel inactivation. Taken together, the notion that the main function of Kv β subunits is its role in channel inactivation may be suspect simply because it is not conserved throughout all Kv β subunits identified to date.

A role for Kv β subunits that has not been characterized, but is directly relevant to this review, is one of K⁺ channel anchoring. In COS cells, Kv β 1.1 associates with large bundles of actin filaments (Nakahira et al., 1999). Colocalization of this subunit and F-actin is seen at the cell cortex where actin filaments and actin binding proteins such as α -actinin form a fibre network. Importantly, Kv β 1.1 is not only colocalizing with these cytoskeletal elements, it is associating with them since its interaction with the actin based cytoskeleton is resistant to extraction with nonionic detergents, a trait characteristic of actin-associated membrane proteins (Nakahira et al., 1999). Thus, Kv β subunits may serve as an anchorage point in the K⁺ channel complex.

Functional Implications of Ion channel Interaction With the Cytoskeleton

Agents that disrupt the actin cytoskeleton have long been known to alter ion channel function. Electrophysiological studies have demonstrated that upon breakdown of the cytoskeleton, changes can be seen in the electrophysiological characteristics of NMDA channel activity (Rosenmund and Westbrook, 1993), inactivation of L-type Ca^{2+} channels (Galli and DeFelice, 1994), and epithelial (Cantiello et al., 1991) and cardiac (Undrovinas et al., 1995; Maltsev and Undrovinas, 1997) Na^{+} channels. These changes were presumed to be owing to cytoskeletal attachments to the ion channels.

Although our understanding of ion channel associated cytoskeletal elements has advanced greatly in the past five years, very few studies revealing a direct relationship between ion channel associated cytoskeletal proteins and ion channel function have been reported. One study reported that when the association of Kv1.1 and a PSD-95-like protein was disrupted, the extent of channel inactivation was decreased (Jing et al., 1997). A second reported that Kir4.1 and PSD-95 coexpression in heterologous cells resulted in a two-fold increase in the whole cell current that could not be accounted for by channels in single channel conductance (Horio et al., 1997).

One explanation for the lack of data regarding ion channel function and cytoskeletal proteins is that these interactions are not binary, in fact they are complex. Cytoskeletal ion channel anchoring proteins not only bind and cluster ion channels, they also mediate the assembly of complex macromolecular complexes involved in roles such as signaling and structural organization. An example of a signaling complex mediated through interactions with a cytoskeletal protein is that of NMDA receptors, type 1 protein phosphatase, and PKA. Yotiao, a cytoskeletal protein that binds NMDA receptors (Lin et al., 1998), also binds type 1 protein phosphatase and PKA, both of which directly

regulate channel activity (Westpal et al., 1999). An elegant example of structural organization is typified by the MAGUK proteins PSD-95 and CASK. CASK is a presynaptic cytoskeletal protein that binds the adhesion molecule β -neurexin through its PDZ domain. Beta-neurexin heterophilically adheres to the postsynaptic adhesion molecule neuroligin, which in turn, through a PDZ mediated interaction, binds the third PDZ domain of PSD-95. PSD-95 can then, through PDZ domains 1 and 2, bind the NMDA receptor and ensure that it is properly localized within the PSD (Irie et al., 1997).

In summary, ion channel associated proteins are critical for clustering and immobilizing ion channels at appropriate locations, and, since they are often multimodular, mediate the assembly of structural and signaling complexes at junctional specializations typified by the neuronal synapse.

The Synapse is an Adherens Junction

It is generally overlooked that the synaptic complex is built around an adhesive junction, not dissimilar from an epithelial adherens junction (Fannon and Colman, 1996). This, not well documented feature of synapses has received more attention recently as studies taking advantage of *Drosophila* genetics have shed some light on the structural organization of the synapse.

One of the three original PDZ containing proteins identified, discs large (Dlg), was found to localize to septate junctions (Woods and Bryant, 1991), the equivalent of the vertebrate tight junction. Mutation of the gene encoding Dlg leads to neoplastic overgrowth of larval imaginal discs, defective adhesion between epithelial cells, and abnormal cell polarity (Woods and Bryant, 1991). The *Drosophila* homologue of Dlg,

DlgA, is found at synaptic boutons at the neuromuscular junction, mutation of which disrupts synaptic bouton structure (Lahey et al., 1994). Thus, disruption of this cytoskeletal MAGUK protein leads to ultrastructural changes at both septate and synaptic junctions. Furthermore, the human Dlg homologue, hDlg/SAP97, localizes at points of epithelial cell contact and, similar to PSD-95, binds to ion channels via the extreme C-terminal S/TXV motif (Kim and Sheng, 1996). Importantly, in an ultrastructural context, it also binds ezrin/radixin/moesin (ERM) cytoskeletal proteins, which in turn bind to the actin cytoskeleton (Lue et al., 1996). The precise role of DlgA and hDlg/SAP97 in junctional assembly is not known.

Other components of epithelial adherens junctions, including N-cadherin, and α - and β -catenin, are present in the synaptic membrane adjacent to transmitter release zones where cadherins have been proposed to "lock-in" nascent synaptic connections (Fannon and Colman, 1996). Taken together, it is reasonable to think of the synapse as a highly specialized cell junction that is similar, at least at the ultrastructural level, to the epithelial adherens junction.

Cell Junctions

Cell junctions can be classified into three functional groups: tight junctions; anchoring junctions; and gap junctions (Alberts et al., 1994). Tight junctions create a barrier to diffusion of solutes between vertebrate epithelial and endothelial cells. They also act as a fence within the membrane lipid bilayer to separate distinct lipid and protein components of the apical and basolateral surface domains of polarized epithelial cells (Mitic and Anderson, 1998). The major cellular constituents of tight junctions are the

transmembrane protein occludin and the intracellular proteins that couple occludin to the cytoplasm. Occludin is a 65 kDa transmembrane protein that contains extracellular loops and intracellular N- and C-termini. The extracellular loops are implicated in the tight junction's barrier function and in cell adhesion. The intracellular proteins that link occludin to the actin cytoskeleton are the MAGUK proteins zona occludins 1 and 2 (Mitic and Anderson, 1998).

Anchoring junctions are a widely distributed junction type which link the cytoskeletal elements of one cell to those of a neighbouring cell or to the extracellular matrix (Alberts et al., 1994). Three types of anchoring junctions exist: adherens junctions, which connect actin filaments from one cell to the next by linkage through a transmembrane protein; desmosomes, which connect intermediate filaments from one cell to the next by linkage through a transmembrane protein; and hemidesmosomes, which link intermediate filaments of one cell to the extracellular matrix.

Lastly, gap junctions, which are found in most tissues, are formed from transmembrane proteins, connexins, that form channels called connexons. Gap junctions allow inorganic ions and other small water-soluble molecules to pass directly from the cytoplasm of one cell to the cytoplasm of its neighbouring cell thereby coupling the cells both electrically and metabolically (Alberts et al., 1998).

In the heart, excluding the vasculature, two of these types of junctions exist, anchoring junctions (primarily the adherens type) and gap junctions. Not coincidentally, they both can be found at the same site, the intercalated disc, the site where neighbouring cardiomyocytes connect.

The Intercalated Disc is an Adherens Junction

In general, cardiomyocytes are joined end to end by specialized structures called intercalated discs containing two types of anchoring junctions; adherens junctions and desmosomes. There is now a sizeable and growing list of proteins that are components of adherens junctions. At present, most remain as markers without known function or protein association.

Adherens junctions are formed by members of the cadherin family of calcium-dependent adhesion molecules. Cadherins mediate cell-cell adhesion mainly through homophilic interactions. Most cadherins, including the N-cadherins found in cardiomyocytes and neurons, function as transmembrane linker proteins that mediate interactions between the actin cytoskeletons of the cells they join. A highly conserved cytoplasmic region of the cadherins interact with the actin cytoskeleton by means of associated linker proteins called catenins (Mitic and Anderson, 1998).

Biochemical analyses using purified catenins and recombinant cadherin cytoplasmic tails, as well as expression studies with deletion mutants of β -catenin have shown that β -catenin binds directly to the cadherin cytoplasmic tail and serves as a linker to α -catenin. Alpha-catenin, in turn, directly binds actin filaments and thus forms the actin link between adjacent cells. Gamma-catenin (also called plakoglobin) sometimes substitutes for β -catenin in the cadherin-catenin complex, but its physiological significance is obscure. In addition, other cytoskeletal proteins including vinculin, talin, α -actinin and the ERM family cluster at the intercalated disc each playing an incompletely understood role in the organization of this complex region (Mitic and Anderson, 1998).

Recent studies have demonstrated that the PDZ-domain containing protein ZO-1 is also recruited to adherens junctions by interacting with α - or β -catenin; both of these proteins have the potential to interact with ZO-1 and target it to the plasma membrane. Recently, ZO-1 was also shown to link directly the actin cytoskeleton to the cadherin-catenin based adherens junction (Mitic and Anderson, 1998).

Thus, since the neuronal synapse and the cardiac intercalated disc share many features at the ultrastructural level, much information regarding the organization of intercalated disc can be gleaned from knowledge of the neuronal synapse. Specifically, how cytoskeletal proteins are involved in tethering ion channels and intracellular elements necessary for signaling within this highly specialized region.

Ion Channels Localize at the Intercalated Disc

It has been well established that cardiac gap junction proteins, connexins, are localized to the intercalated disc in cardiomyocytes (Beyer et al., 1989). The clustering of connexin43 has been reported to be owing to an interaction with ZO-1, and this interaction, although questionable, is thought to occur through an interaction of the Cx43 C-terminus and the PDZ domain of ZO-1 (Toyofuku et al., 1998). Similarly, the localization of the glucose transporter 1 at the intercalated disc is due to an interaction with the PDZ domain-containing protein GLUT1CBP (Bunn et al., 1999).

The subcellular localization of other ion channels in cardiomyocytes has only recently been determined. The first report of an ion channel to exhibit a discrete subcellular localization at the intercalated disc in isolated cardiomyocytes is the voltage-dependent K^+ channel Kv4.2 (Barry et al., 1995). This localization has also found to be

true in the intact myocardium (unpublished observation). Around the same time, another voltage-dependent K^+ channel, Kv1.5, was also found to be expressed at the intercalated disc in the intact myocardium (Mays et al., 1995; unpublished observation). Conflicting reports have been reported regarding the localization of the cardiac sodium channel, rH1. Cohen et al. (1996) reported a localization at the intercalated disc while, Petrecca et al. (1997) and Jurevicius et al. (1997) found that they were more evenly distributed throughout the plasma membrane. In contrast, the, $Na^+/K^+/ATPase$ and L-type Ca^{2+} channels are not localized at the intercalated disc. The $Na^+/K^+/ATPase$ is evenly distributed throughout the plasma membrane (Sweadner et al., 1994, Petrecca et al., 1999) while L-type Ca^{2+} channels are evenly distributed throughout T-tubular membranes (Carl et al., 1995; Gao et al., 1997; Takagishi et al., 1997).

In order to determine if other K^+ channels, in addition Kv1.5 and Kv4.2, exhibit an intercalated disc specific localization, I screened cardiac tissue using monospecific antisera and confocal microscopy. My findings indicated that HERG (Pond et al., In Press) was uniformly distributed throughout the surface membrane and T-tubules. On the other hand, minK, Kv1.4, and Kv2.1 exhibited an intercalated disc specific localization (unpublished observation). Thus, the intercalated disc, like the neuronal synapse is a site where many ion channels accumulate.

Interestingly, the ubiquitous sodium-hydrogen exchanger, NHE1, has been shown to cluster at focal adhesion sites in adherent fibroblast in culture, colocalizing with a variety of cytoskeletal proteins that are constituents of the intercalated disc including vinculin and talin (Grinstein et al., 1993). NHE is that main transporter responsible for maintaining pH_i . In mammals, at least six NHE isoforms are known to exist. Cardiac

tissue from rats, rabbits and humans expresses predominantly NHE1 mRNA; hence, it is the main NHE isoform responsible for controlling myocardial pH_i. NHE1, a putative 12 transmembrane domain spanning protein, contains intracellular N- and C-termini that acts as an electroneutral transporter exchanges an intracellular H⁺ for an extracellular Na⁺ (Petrecca et al., 1999).

Part III

The Role of N-linked Glycosylation in HERG Surface Membrane Expression

Hypothesis and Rationale

Defective protein processing has been determined to play a role in certain ion channel-associated diseases. The genetic cardiac disease LQT is a prime example. Certain LQT-associated HERG mutations render the channel nonfunctional due to an inability of the channel to conduct ions at the cell surface whereas others reduce surface membrane expression due to defective channel processing. The role of N-linked glycosylation in protein processing has been well established and has been shown to be crucial for the surface membrane expression of certain ion channels. My hypothesis is that certain mutations that alter the extent of N-linked glycosylation may lead to the misfolding of the channel within the ER and premature degradation.

Experimental Outline

To determine if N-linked glycosylation plays a role in HERG processing initial experiments will be carried out to determine the effects of tunicamycin, an N-linked glycosylation inhibitor, on HERG surface membrane expression. If an effect is observed, both of the HERG consensus N-linked glycosylation sites will be removed either singly

or in combination. The effects of these mutations, and thus the role of N-linked glycosylation in channel processing and surface membrane expression, will be determined through immunoblotting, electrophysiological analysis and immunocytochemistry.

Subcellular Localization of NHE1 in Cardiomyocytes

Hypothesis and Rationale

Two factors lead me to the hypothesis that NHE1 may be localized at the intercalated disc. First, it has been shown that the exchanger localizes at focal adhesion sites in adherent fibroblasts. Since many components of this focal adhesion complex are also found at the intercalated disc, I reasoned that one of these cytoskeletal elements may be anchoring the exchanger and thus it seems likely that the same would be true at the intercalated disc. Second, since the function of the exchanger is to regulate pH, I reasoned that if the intercalated disc is a structure where many critical signaling elements gather, it would be appropriate to have the pH regulator localized in this vicinity. In fact, Cx43, the major gap junction protein that is localized at the intercalated disc, is gated by intracellular pH (Spray et al., 1985; Burt et al., 1988; White et al., 1990; Liu et al., 1993; Ek et al., 1994).

Experimental Outline

To determine the localization of the NHE1 in cardiac tissue I will use a NHE1-specific antibody to immunolabel fresh-frozen cryosections of rat heart. The subcellular distribution of NHE1 will be visualized using confocal microscopy.

The Search for a Kv4.2 Anchoring Protein

Hypothesis and Rationale

Kv4.2 has been shown to be highly expressed in brain and heart and is thought to be the $Kv\alpha$ subunit that gives rise to I_A in neurons and I_{to} in heart. It is localized to dendrites, primarily the postsynaptic density (Sheng et al., 1992; Alonso et al., 1997), in neurons and intercalated discs in isolated cardiomyocytes (Barry et al., 1995) and cardiac tissue (unpublished observations). Due to its restricted localization in these tissues I reasoned that it may have a cytoskeletal protein association that may be responsible for its anchorage or localization at these sites.

Experimental Outline

As all reported cytoskeletal protein interactions with ion channels have involved the C-terminus of these ion channels, I reasoned that the same might hold true for Kv4.2. The extreme C-terminal amino acids of Kv4.2 are VSAL, a putative PDZ motif. Although it would be logical to search for PDZ domain-containing proteins in order to identify a binding partner, I am more interested in identifying a protein that plays a role in Kv4.2 localization and not clustering. Although PDZ domain-containing proteins have been reported to mediate clustering and scaffolding, they are not, by themselves, sufficient for localization. Arnold et al. (1999) elegantly demonstrated that the Kv1.4 interaction with PSD-95 was not sufficient for its localization to the presynaptic terminal. Similarly, the entire C-terminal tail of Kv1.4 was shown to be significantly more efficient for localization of the ion channel to the synapse than the last seven or nine amino acids indicating the PDZ-domain interactions is not sufficient for localization (Zito et al., 1997). Lastly, a 120 amino acid region in the C-terminal tail of Kv2.1 was shown is

required for the localization of this channel (Scannevin et al., 1996). Taken together, these studies demonstrated that PDZ interactions are not sufficient for channel localization and that upstream regions in the C-terminal tail are required for localization.

In order to identify a Kv4.2 interacting protein that may play a role in its localization I will use the yeast two-hybrid screening method. Taking the three studies cited above into consideration, I will use the entire C-terminal tail of Kv4.2 as a bait to screen a human heart cDNA library.

CHAPTER 2

N-linked Glycosylation Sites Determine HERG Channel Surface Membrane Expression

Abstract

Long QT syndrome (LQT) is an electrophysiological disorder that can lead to sudden death from cardiac arrhythmias. One form of LQT has been attributed to mutations in the human *ether a-go-go* related gene (*HERG*) that encodes a voltage-gated cardiac K⁺ channel. While a recent report indicates that LQT in some patients is associated with a mutation of HERG at a consensus extracellular N-linked glycosylation site (N629), earlier studies have failed to identify a role for N-linked glycosylation in the functional expression of voltage-gated K⁺ channels. In this study we use pharmacological agents and site-directed mutagenesis to assess the contribution of N-linked glycosylation in the surface localisation of HERG channels. Tunicamycin, an inhibitor of N-linked glycosylation, blocked normal surface membrane expression of a HERG-GFP fusion protein (HERG^{GFP}) transiently expressed in HEK 293 cells imaged with confocal microscopy. Immunoblot analysis revealed that N-glycosidase F shifted the molecular mass of HERG^{GFP}, stably expressed in HEK 293 cells, indicating the presence of N-linked carbohydrate moieties. Mutations at each of the two putative extracellular N-linked glycosylation sites (N598Q and N629Q) lead to a perinuclear subcellular localisation of HERG^{GFP} stably expressed in HEK 293 cells, with no surface membrane expression. Furthermore, patch clamp analysis revealed that there was a virtual absence of HERG current in the N-glycosylation mutants. Taken together, these results strongly suggest that N-linked glycosylation is required for surface membrane expression of HERG. These findings may provide insight into a mechanism responsible for LQT2 due to N-linked glycosylation related mutations of HERG.

Introduction

Long QT syndrome (LQT) is a disorder that can cause sudden death from cardiac arrhythmias, torsade de pointes and ventricular fibrillation. Mutations in the human *ether a-go-go* related gene (*HERG*) underly chromosome 7-linked LQT (Satler, Vesely, Duggal, Ginsburg & Beggs, 1998). *HERG*, the human *ether-a-go-go* (*eag*) related gene, is a member of the *eag* family of potassium channels (Warmke & Ganetzky, 1994). Family members contain six putative transmembrane spanning domains, an ion-conducting pore region and a putative cyclic nucleotide-binding domain. Expression of wild-type *HERG* protein in *Xenopus* oocytes revealed that *HERG* encodes the rapidly activating, inwardly rectifying K^+ channel responsible for the cardiomyocyte current, I_{Kr} (Sanguinetti, Jiang, Curran & Keating, 1995), an important component of ventricular repolarization. These findings have led to the proposal that reduced I_{Kr} , resulting from mutations in *HERG*, can prolong cardiomyocyte action potential duration thereby giving rise to LQT (reviewed in Roden, Lazzara, Rosen, Schwartz, Towbin & Vincent, 1996).

It has recently been reported that *HERG* mutations Y611H and V822M result in an incompletely glycosylated form of the protein exhibiting a restricted perinuclear distribution with no detectable current (Zhou, Gong, Epstein & January, 1998a). In addition, it has been demonstrated that N-linked oligosaccharides can act as determinants for cell surface transport of certain membrane proteins (Gut, Kappeler, Hyka, Balda, Hauri & Matter, 1998). The *HERG* amino acid sequence contains two extracellular consensus N-linked glycosylation sites, N598 and N629. In this study, we set out to determine if N-linked glycosylation is required for surface membrane expression of *HERG* in a mammalian cell line, HEK 293. To do so, we generated stably transfected cell

lines expressing green fluorescent protein (GFP) tagged HERG (HERG^{GFP}), and singly and doubly mutated HERG^{GFP}s that have had either one or both of the conserved N-linked glycosylation sites removed. The wild-type and N-linked glycosylation mutant HERG^{GFP}s were analysed for their biochemical and electrophysiological properties as well as subcellular localisation. We found that the wild-type protein exhibited a surface membrane localisation and normal electrophysiological function; however, both single (N598Q, N629Q) and double (N598Q/N629Q) mutants showed an intracellular localisation, with no detectable current. These results strongly suggest that N-linked glycosylation is required for surface membrane expression of HERG channels.

Materials and Methods

DNA Constructs and Transfection of HEK 293 cells

HERG cDNA (kindly provided by Dr. G.A. Robertson, University of Wisconsin) was subcloned into *Bam*HI/*Eco*RI sites of the pBK-CMV expression vector (Stratagene). GFP cDNA was subcloned into the *Not*I/*Xba*I sites of the pBK-CMV expression vector (Stratagene). The HERG-GFP fusion construct (designated HERG^{GFP}) was generated by ligating the 3' end of the HERG cDNA with the 5' end of the GFP cDNA. In order to do so, a *Not*I site at the 3' end of the HERG cDNA was introduced by PCR and the GFP cDNA was subcloned into *Not*I/*Xba*I sites of the pBK-CMV/HERG expression vector. The final fusion construct was sequenced (Sheldon Biotechnology, Montreal, Quebec) in order to verify its integrity and purified using a Wizard Plus Midiprep Purification System (Promega).

The following primers were used to mutate either singly or in combination the two N-linked glycosylation sites located in the extracellular loop between transmembrane segments S5 and S6 using the unique site elimination technique (Deng & Nickoloff, 1992): N598Q, 5'-GGCAAACCCTACCCAGAGCAGCGGCCTG; N629Q, 5'-GTGGGCTTCGGCCCAGGTCTCTCCCAAC. The N-linked glycosylation mutant HERG^{GFP} fusion constructs were then purified using a Wizard Plus Midiprep DNA Purification System (Promega) and sequenced (Sheldon Biotechnology, Montreal, Quebec).

HEK 293 cells were transfected with wild-type and mutant constructs using Lipofectamine (Gibco). After selection in 800 µg/ml of geneticin (G418, 50% active; Gibco) for 10-15 days, single colonies were selected, grown and assayed for HERG^{GFP}

expression. The stably transfected cells were maintained in α -minimum essential medium, 10% fetal bovine serum, 1% penicillin/streptomycin (Gibco) and 800 μ g/ml geneticin.

Immunocytochemistry

For transient transfections, native GFP fluorescence was used to localise HERG^{GFP}. Cells plated on coverslips were rinsed in phosphate buffered saline (PBS), fixed in 4% paraformaldehyde for 20 min at room temperature, rinsed in PBS and mounted using Immuno Fluore (Fisher Scientific). For tunicamycin (Sigma) treatment, 1 μ g/ml of tunicamycin was added to cells 20 h post-transfection for an additional 18 h. Cells were then fixed as above.

For the stable transfectants; however, an anti-HERG antibody was used to localise HERG^{GFP} as the native GFP fluorescence was too low to allow for subcellular localisation. The low level of native GFP fluorescence is due not to a low level of fusion protein expression but to a reduction in the absorption, and thus emission, of the chromophore due to dimerization of the GFP molecule. This dimerization results from high levels of fusion protein expression (Clontech). Briefly, stably transfected cells plated on coverslips were fixed in 2% paraformaldehyde for 30 min followed by five rinses in PBS. Cells were then incubated in 0.5% Triton X-100/0.5% BSA in PBS for 30 min followed by incubation with an anti-HERG antibody generated against the amino terminus of HERG, anti-N, (kindly provided by Drs. A. Pond and J.M. Nerbonne, Department of Pharmacology and Molecular Biology, Washington University, St. Louis, Mo; Pond & Nerbonne, 1996) for 1 h and subsequently rinsed in PBS. The cells were

then incubated with FITC-conjugated goat anti-rabbit IgG (Jackson ImmunoResearch Laboratories, Inc.) for 1 h followed by three rinses in PBS. All incubations were performed at room temperature. Coverslips were mounted using Immuno Floures (Fisher Scientific).

All imaging was performed using a Zeiss LSM 410 inverted confocal microscope. GFP and FITC were imaged by exciting the sample with a 488 nm line from an argon/krypton laser and the resulting fluorescence was collected on a photomultiplier after passage through FT510 and BP515-540 filter sets. Optical sections were taken using a x25, 0.8 NA (optical thickness = 3.1 μ m) objective and a x63, 1.4 NA (optical thickness = 1.0 μ m) objective. All images were printed on a Kodak XLS8300 high resolution (300 DPI) printer.

Immunoblot Analysis

Parallel 100 mm plates of similarly confluent cultures were used to isolate crude membrane fractions. All steps were performed at 4 °C. Briefly, the cells were rinsed 5 times with PBS, lysed with 2 mls of a solution containing 200 mM NaCl, 33 mM NaF, 10 mM EDTA, 50 mM HEPES (pH 7.4) and Complete protease inhibitor cocktail (Boehringer), and harvested with the aid of a rubber scraper. Cells were then homogenized and centrifuged at 3600 x g for 10 min. The supernatants were collected and the membrane fractions were pelleted by centrifugation at 110 000 x g for 40 min. The membrane enriched pellets were solubilized in 50 mM Tris-HCl, 15 mM β -mercaptoethanol and 1% SDS. The membrane proteins were then heated to 70 °C in sample buffer (0.12 M Tris-HCl (pH 6.8), 2% SDS, 2% β -mercaptoethanol, 20%

glycerol, and 0.001% bromophenol blue) for 2 min and resolved on a 6.25% SDS polyacrilamide gel. The proteins were then transferred onto a PVDF membrane (Amersham) overnight. Membranes were quenched in PBS with 5% dried milk/0.1% Tween 20 for 1 h at room temperature and subsequently incubated with the anti-N antibody at a 1:500 dilution for 2 h at room temperature followed by three 10 min rinses in PBS with 0.1% Tween 20. Membranes were then incubated in a 1:3000 dilution of horseradish peroxidase-conjugated goat anti-rabbit IgG (Jackson ImmunoResearch Laboratories, Inc.) for 1 h at room temperature. Horseradish peroxidase conjugated secondary antibodies were detected using the chemiluminescence ECL⁺ detection kit (Amersham).

For N-glycosidase F treatment, 1% NP-40, Complete protease inhibitor cocktail (Boehringer), and 2 units of N-glycosidase F (Boehringer) were added to ~30 µg of the resuspended membrane fractions. The mixture was then incubated at 37 °C for 21 h. The reaction was stopped by adding sample buffer and boiling for 2 min.

Electrophysiological Analysis

The whole-cell patch clamp technique was used to record membrane currents. Cells were plated on 35 mm petri dishes and placed on the stage of an inverted microscope (Zeiss IM35, Oberkochen, Germany). All experiments were carried out at 35 ± 1 °C. Patch clamp electrodes were filled with medium containing (in mM): 130 KCl, 1 MgCl₂, 5 EGTA, 5 MgATP, 10 HEPES (pH 7.2 with KOH). The pipette tip resistance was 2-4 MΩ. The external medium contained (in mM): 137 NaCl, 4 KCl, 1.8 CaCl₂, 1 MgCl₂, 10 glucose and 10 HEPES (pH 7.4 with NaOH). Membrane currents were recorded using an

Axopatch amplifier (Axopatch-1D; Axon Instrument Corp., Foster City, CA). Voltage clamp pulses were delivered from a custom-designed software package (Alembic Software Co., Montreal, Canada) implemented on a personal computer equipped with an analog-to-digital card (Omega Corp., Stanford, CT). The data were stored on a computer hard disc and analysed using the same software. A two-step voltage clamp protocol was imposed from a holding potential of -80 mV to assess the presence of HERG current. The first step, which served to activate HERG current, consisted of a 4 sec depolarizing pulse to potentials between -60 to +50 mV in increments of 10 mV. At the end of the first step the membrane was repolarized back to -60 mV for 2 sec, in order to assess HERG tail currents, before returning to the -80 mV holding potential. Cell capacitance was estimated by analog measurements using the patch clamp amplifier. Graphics and statistical analysis were carried out using Origin software (Microcal). E-4031 was a generous gift from Eisai Co. (Tsukuba research Laboratories, Japan).

Results

Role of N-linked Glycosylation in Surface Membrane Expression of HERG^{GFP}

Fluorescence confocal microscopy was used to determine the subcellular localisation of HERG^{GFP} transiently expressed in HEK 293 cells. Native GFP fluorescence reveals that HEK 293 cells transiently expressing HERG^{GFP} show abundant surface membrane expression of HERG^{GFP} (Fig. 1A, arrows indicate localisation between cells; Fig. 1B, arrows indicate surface membrane expression). When the cells were treated for 18 h with tunicamycin, an inhibitor of N-linked glycosylation, the transfected protein was no longer seen at the surface membrane but showed an intracellular accumulation with a predominant perinuclear subcellular localisation (Fig. 1C, the arrow indicates an endoplasmic reticulum (ER)-Golgi-like distribution pattern; Fig. 1D). These results indicate that treatment of cells with tunicamycin results in an intracellular retention of HERG^{GFP} with no surface membrane expression.

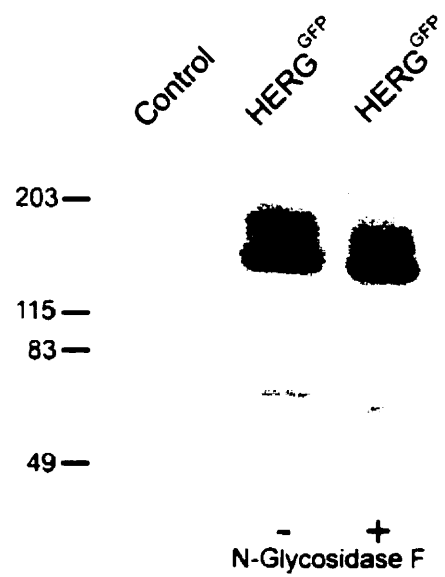
Biochemical Analysis of HERG^{GFP} Stably Transfected in HEK 293 Cells

Immunoblot analysis of HERG^{GFP} stably transfected in HEK 293 cells is shown in Fig. 2. An antibody directed against the amino terminus of HERG, anti N, was used to probe for HERG^{GFP} protein. The anti-N antibody recognizes multiple species of HERG^{GFP} in stably transfected cells, an upper band with an apparent molecular mass of ~185 kDa and a lower band with an apparent molecular mass of ~165 kDa, a degradation product at ~70 kDa is also evident (Fig. 2, lane 2). Neither band was present in untransfected HEK 293 cells (Fig 2A, lane 1). Similarly, Zhou, Gong, Ye, Fan, Makielski, Robertson, *et al.* (1998b) reported that two bands of HERG are evident upon Western blot analysis. An

Figure 1. Effect of tunicamycin on the subcellular localisation of transiently expressed HERG^{GFP} in HEK 293 cells. A. Subcellular localisation of HERG^{GFP}. Native GFP fluorescence overlayed on a transmitted-light image. Arrows indicate HERG^{GFP} localisation at surface membranes. B. Fluorescence image revealing the subcellular localisation of HERG^{GFP}. Arrows indicate HERG^{GFP} localisation at surface membranes. C. Subcellular localisation of HERG^{GFP} in cells treated with 1 µg/ml of tunicamycin for 18 hours. Native GFP fluorescence overlayed on a transmitted-light image. Arrows indicate the perinuclear localisation HERG^{GFP}. D. Fluorescence image revealing the subcellular localisation of HERG^{GFP} in cells treated with 1 µg/ml of tunicamycin for 18 hours. Representative images of three separate experiments are shown.



Figure 2. Immunoblot analysis of HERG^{GFP} protein stably expressed in HEK 293 cells. Enriched membrane fractions were prepared as described in the Material and Methods. Each lane was loaded with ~30 µg of protein. An anti-HERG antibody was used to probe for HERG^{GFP}. The control lane shows results with untransfected cells. The HERG^{GFP} lanes show results with cells stably expressing HERG^{GFP} before (-) and after (+) treatment with N-glycosidase F. The data is representative of four separate experiments.



upper band with an apparent molecular mass of 155 kDa and a lower band with an apparent molecular mass of 135 kDa. This is consistent with our results as we have an ~ 30 kDa GFP molecule tagged to the carboxyl terminus of HERG.

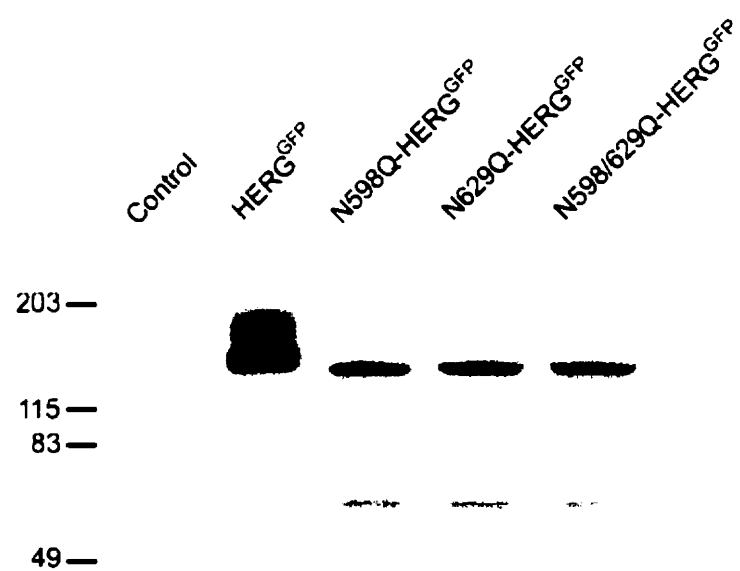
To determine the extent of N-linked carbohydrate modification, protein isolated from HEK 293 cells stably expressing HERG^{GFP} was treated with N-glycosidase F, which removes N-linked carbohydrate from proteins. This treatment converted the 185 kDa band to an ~ 170 kDa band and shifted the lower 165 kDa band to an ~ 162kDa band (Fig. 2, lane 3). The ~70 kDa degradation product was also shifted suggesting that it is derived from a glycosylated portion of the protein. These results suggest that both molecular mass species of HERG^{GFP} undergo N-linked glycosylation with the upper molecular mass species most likely representing a fully glycosylated form of the protein.

Biochemical Analysis of HERG^{GFP} and N-linked Glycosylation Mutant HERG^{GFP}s Stably Transfected in HEK 293 cells

HERG contains two potential extracellular consensus N-linked glycosylation sites. One site (Asn-598), near the putative pore region, and the second (Asn-629), within the pore region. To determine the role of N-linked glycosylation at each of these sites three constructs were generated by site-directed mutagenesis, N598Q, N629Q and N598Q/N629Q. Each of these three N-linked glycosylation mutant HERG^{GFP} fusion proteins was stably expressed in HEK 293 cells.

Immunoblot analysis of total membrane protein isolated from wild-type HERG^{GFP}, N598Q-HERG^{GFP}, N629Q-HERG^{GFP}, and N598Q/N629Q-HERG^{GFP} stably expressed in HEK 293 cells is shown in Fig. 3. For each of the three N-linked

Figure 3. Immunoblot analysis of wild-type and N-linked glycosylation mutant HERG^{GFP}s stably expressed in HEK 293 cells. Enriched membrane fractions were prepared as described in the Material and Methods. Each lane was loaded with ~30 µg of protein. An anti-HERG antibody was used to probe for HERG^{GFP}. The control lane shows results with untransfected cells. Results from protein isolated from cells stably expressing either HERG^{GFP}, N598Q-HERG^{GFP}, N629Q-HERG^{GFP} or N598Q/N629Q-HERG^{GFP} are shown in their respective lanes. The data is representative of four separate experiments.



glycosylation mutant HERG^{GFP} proteins the anti-N antibody recognizes a protein species with an apparent molecular mass of ~162 kDa (Fig. 3, lanes 3,4,5). The apparent molecular mass of each of the mutant HERG^{GFP} proteins is similar to the lower band of the enzymatically deglycosylated wild-type HERG^{GFP} protein (Fig. 2, lane 3) suggesting that none of the mutant proteins are glycosylated and that both N-linked glycosylation sites must be available for either site to be glycosylated as mutations at either N-linked glycosylation site lead to a nonglycosylated form of the protein. An ~70 kDa degradation product is also evident for the wild-type protein and a shifted correlate product is also evident for all three mutant proteins indicating that the degradation product is derived from a glycosylated portion of the protein.

Functional Analysis of N-Linked Glycosylation Mutants

To evaluate the functional role of N-linked carbohydrate modification of HERG^{GFP}, whole-cell patch clamp technique was used to study the membrane currents in HEK 293 cells stably expressing wild-type HERG^{GFP} and the N-linked glycosylation mutants. Figure 4A (top left) shows current traces recorded during a series of depolarizing voltage clamp steps from a -80 mV holding potential to potentials ranging from -60 mV to +50 mV. A tail current can be observed at the termination of the initial depolarizing step when the membrane is suddenly stepped to -60 mV. Figure 4A (bottom left) shows that the time-dependent current induced during the step and the current tail were almost completely blocked by E-4031, a selective inhibitor of I_{K_r} and I_{HERG} (Sanguinetti *et al.* 1995). In the presence of E-4031 a small amplitude rapidly activating transient outward current persists along with a residual steady-state background current. Control

Figure 4. Whole-cell outward currents in HEK 293 cells stably expressing wild-type and N-linked glycosylation mutant HERG^{GFP}s. A two-step voltage clamp protocol was imposed from a holding potential of -80 mV to assess the presence of HERG current in HEK 293 cells stably transfected with HERG^{GFP} or HERG^{GFP} mutants. The outward currents were evoked during an initial 4 sec depolarizing pulse to potentials between -60 to +50 mV in increments of 10 mV. At the end of the first step the membrane was repolarized back to -60 mV for 2 sec before returning to the -80 mV holding potential. A) Left Top: A series of current traces recorded in HEK 293 cells stably transfected with HERG^{GFP} showing an inwardly rectifying delayed rectifier current. Left Bottom: In the presence of E-4031 (1 μ M) the HERG^{GFP} induced delayed rectifier current was completely blocked. The residual transient outward current and background current was similar to that observed in untransfected cells. Right: Current-voltage relationship of untransfected HEK 293 cells (n=6, solid triangles) and in HEK 293 cells stably transfected with HERG^{GFP} (n=6, solid squares) normalized to the cell capacitance (16.3 ± 1.5 pF; n=6). B) Each panel shows a series of current traces recorded from HEK 293 cells stably transfected with N598Q-HERG^{GFP}, N629Q-HERG^{GFP} and N598Q/N629Q-HERG^{GFP}. HERG^{GFP} current was absent in all three mutants.

A

HERG^{GFP}

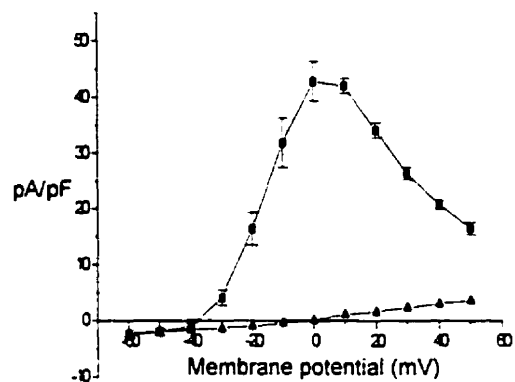


HERG^{GFP} + E-4031



500 pA

1 sec



B

N598Q-HERG^{GFP}



N629Q-HERG^{GFP}



N598Q/N629Q-HERG^{GFP}



500 pA

1 sec

experiments carried out using untransfected HEK 293 cells (n=32) showed that the small amplitude transient current was present in most cells but the large time-dependent outward current observed in HERG^{GFP} transfected cells was never observed. These results indicate that HERG^{GFP} fusion protein is functional and that the time-dependent outward current in HERG^{GFP} transfected cells ($I_{\text{HERG}^{\text{GFP}}}$) has properties similar to I_{HERG} . This is further illustrated in Fig. 4A (right) which shows the current-voltage relationship measured at the end of the initial 4 sec depolarization step in HEK 293 cells stably transfected with HERG^{GFP} and in control untransfected cells. The current-voltage relationship indicates that $I_{\text{HERG}^{\text{GFP}}}$ is activated at membrane potentials positive to -40 mV. At potentials positive to 0 mV the current-voltage relationship showed a marked inward rectification with a negative slope conductance. In untransfected cells a small residual linear background current persists with reversal close to 0 mV suggesting a degree of non-selectivity. The above observations are very similar to those recently reported for HERG transfected HEK 293 cells (Zhou et al. 1998b) and demonstrate that HERG^{GFP} encodes an ion channel with pharmacological and electrophysiological characteristics similar to the current expressed by native HERG.

The current recordings from HEK 293 cells stably expressing the N-linked glycosylation mutants (N598Q-HERG^{GFP}, N629Q-HERG^{GFP} or N598Q/N629Q-HERG^{GFP}) are shown in figure 4B. The currents were induced using the same voltage clamp protocol as in figure 4A. It was found that the large $I_{\text{HERG}^{\text{GFP}}}$ evident in wild-type HERG^{GFP} stably transfected cells was absent in all three N-linked glycosylation mutants (n=40 for each mutant). The recordings indicate that HEK 293 cells transfected with the mutants retain the small transient outward current. Current-voltage plots of the three

mutants (data not shown) were similar to those observed in untransfected HEK 293 cells (Fig. 4A, right), consistent with the presence of a small amplitude endogenous background current.

Subcellular Localisation of N-Linked Glycosylation Mutant Proteins

Fluorescence confocal microscopy was used to determine the subcellular localisation of the wild-type and N-linked glycosylation mutant HERG^{GFP}s stably expressed in HEK 293 cells. Wild-type-HERG^{GFP} exhibited a surface membrane distribution pattern (Fig 5A), consistent with the functional electrophysiological recordings. In contrast, N598Q-HERG^{GFP}, N629Q-HERG^{GFP} and N598Q/N629Q-HERG^{GFP} revealed a perinuclear subcellular localisation consistent with the absence of a HERG current upon electrophysiological analysis (Fig. 5B-D) indicating that both N-linked glycosylation sites must be available for surface membrane expression of HERG^{GFP}.

Figure 5. Subcellular localisation of wild-type and N-linked glycosylation mutant HERG^{GFP}s stably expressed in HEK 293 cells. Cells were immunolabelled with an anti-HERG antibody followed by a FITC-conjugated goat anti-rabbit IgG antibody. Representative immunofluorescence images are overlayed on transmitted-light images. A. Surface membrane localisation of wild-type HERG^{GFP}. B. Perinuclear localisation of N598Q-HERG^{GFP}. C. Perinuclear localisation of N629Q-HERG^{GFP}. D. Perinuclear localisation of N598Q/N629-HERG^{GFP}. Representative images of four separate experiments are shown.

A

B

C

D

Discussion

In the present study we set out to determine the role of N-linked glycosylation in surface membrane expression of HERG. In part, this was assessed using an inhibitor of N-linked glycosylation, tunicamycin. As a means to visualize the subcellular localisation of HERG, we constructed a HERG^{GFP} fusion protein. We found that treatment of HERG^{GFP} transiently expressed in HEK 293 cells with tunicamycin lead to an absence of surface membrane expression of the protein and an intracellular accumulation exhibiting a perinuclear subcellular distribution. In order to determine if the HERG^{GFP} fusion construct functions normally, whole-cell patch clamp recordings of HERG^{GFP} stably expressed in HEK 293 cells were performed. The HERG^{GFP} current that was generated revealed similar properties to HERG stably expressed in the same cell line (Zhou *et al.* 1998b). These findings indicate that GFP tagged to the carboxyl terminus does not affect HERG^{GFP} targeting to its final destination nor its function.

Immunoblot analysis of HERG^{GFP} reveals that it exists as two molecular mass species, ~ 185 kDa and ~165 kDa. Upon enzymatic deglycosylation with N-glycosidase F, the larger molecular mass species shifts from ~185 kDa to ~170 kDa, and the smaller molecular mass species shifts from ~165 kDa to ~162 kDa. These findings are consistent with those of Zhou *et al.* (1998b) and indicate that the upper band most likely represents the fully glycosylated form of HERG. Since treatment with the enzyme did not convert both protein bands to a single band indicates that post-translational modifications other than N-linked glycosylation may be involved. Possibilities include palmitylation,

sulfation, phosphorylation or acylation. O-linked glycosylation does not seem to be a possibility as HERG does not contain such a consensus site.

In order to elucidate the role of each consensus N-linked glycosylation site, N598 and N629, we constructed three N-linked glycosylation mutants, N598Q-HERG^{GFP}, N629Q-HERG^{GFP} and N598Q/N629Q-HERG^{GFP}, and stably expressed them in HEK 293 cells. Substitution of the asparagine at amino acid 598 with a glutamine resulted not only in the loss of glycosylation at site 598, but also at 629, yielding a molecular mass species of ~162 kDa. Similarly, substitution of the asparagine at amino acid 629 with glutamine resulted in the loss of glycosylation at site 629 and 598 yielding a molecular mass species of ~162 kDa. The double mutant also resulted in a molecular mass species of ~162 kDa. These findings indicate that both glycosylation sites, N598 and N629, must be available for glycosylation to occur. Immunofluorescence analysis revealed that each of the N-linked glycosylation mutants showed an absence of surface membrane expression with a perinuclear subcellular distribution. Moreover, no HERG current was detectable in any of the three N-linked glycosylation mutants. These results indicate that N-linked glycosylation is required for proper trafficking of HERG^{GFP} as the unglycosylated 162 kDa form of the protein does not appear to exit the ER-Golgi apparatus. An alternative explanation is that the substitution of the asparagine with a glutamine yields a three-dimensional configuration of the protein rendering it susceptible to degradation prior to exiting the ER-Golgi apparatus. However, treatment of cells with tunicamycin resulted in a ER-Golgi-like retention of HERG^{GFP} that is similar to that observed with the N-linked glycosylation mutants. This further supports the notion that N-linked carbohydrate is required for trafficking of HERG^{GFP} to its final destination at

the cell surface. Moreover, in one of the N598Q-HERG^{GFP} stable cells we were able to record a small HERG-like current indicating that at least some of the protein retains its proper three-dimensional configuration in the nonglycosylated state and that a small percentage is able to reach the surface membrane. Thus it appears that for HERG^{GFP}, the consensus N-linked glycosylation sites must both be available for glycosylation to occur and that a nonglycosylated form of the protein is retained intracellularly.

To date, 19 different *HERG* mutations in LQT patients have been reported (Curran, Splawski, Timothy, Vincent, Green & Keating, 1995; Akimoto, Furutani, Kasanuki, Imamura, Furutani, Takao *et al.* 1996; Benson, MacRae, Vesely, Walsh, Seidman, Seidman *et al.* 1996; Dausse, Berthet, Denjoy, Andre-Fouet, Cruaud, Bennaceur *et al.* 1996; Satler, Walsh, Vesely, Plummer, Ginsburg & Jacob, 1996; Tanaka, Nagai, Tomoike, Takata, Yano, Yabuta *et al.* 1997; Satler *et al.* 1998). Importantly, it was recently reported that HERG protein resulting from mutations Y611H and V822M is incompletely glycosylated and no current was detectable (Zhou *et al.* 1998a). In addition, a recent study has demonstrated that N-linked oligosaccharides can act as determinants for cell surface transport of certain membrane proteins (Gut *et al.* 1998). Recently two mutations resulting in LQT were found at a consensus extracellular N-linked glycosylation site, N629D and N629S (Satler *et al.* 1998). Taken in context of the results in this paper, these observations suggest that mutations at N-linked glycosylation sites or mutations that inhibit N-linked glycosylation may effect HERG protein trafficking and surface expression.

The role of carbohydrates in the trafficking and function of certain ion channels has been reported by several groups. Waechter, Schmidt & Catterall (1983) demonstrated

that tunicamycin reduced the number as well as function of sodium channels on the cell surface. The effect of tunicamycin was not mediated solely by increasing the rate of proteolytic degradation of internalized sodium channels but must also reduce the rate of sodium channel appearance on the cell surface and/or increase the rate of internalization of channels from the cell surface. Merlie, Sebanne, Tzartos & Lindstrom (1982) reported that when muscle cells were treated with tunicamycin, the $\alpha 1$ subunit of the muscle-type nicotinic acetylcholine receptor failed to assemble into toxin-binding receptors on the cell surface. In addition, Mishina, Tobimatsu, Imoto, Tanaka, Fujita, Fukuda *et al.* (1985) reported that when the asparagine at amino acid 141 of the *Torpedo* $\alpha 1$ subunit was replaced with an aspartic acid, there was no acetylcholine response and no detectable α -bungarotoxin binding sites on the cell surface. N-linked glycosylation has also been shown to be necessary for proper trafficking of the GLYT1 glycine transporter to the plasma membrane (Olivares, Aragon, Gimenez & Zafra, 1995)

The role of N-linked glycosylation has not been clearly established for K^+ channels. Santacruz-Tolosa, Huang, John & Papazian (1994) reported that for the Shaker K^+ channel, N-linked glycosylation is not required for the assembly of functional channels nor for their transport to the cell surface. Similarly, Deal, Lovinger & Tamkun (1994) reported that glycosylation at the single extracellular N-linked glycosylation site is not required for subunit assembly, transport to the surface, protein stability or function of the Kv1.1 channel.

Early studies with tunicamycin, demonstrated that when N-linked carbohydrate addition to protein is blocked, most nonglycosylated forms of the proteins accumulated in the ER, aggregated, and did not exit. This led to the concept that carbohydrate addition

aids protein folding and stabilizes the protein conformation rendering it less susceptible to proteolytic degradation (Fiedler & Simons, 1995). Further studies have demonstrated that glycoproteins associate with ER resident chaperones, some of which include calnexin, calreticulin, PDI, Bip and Grp94, and that this association promotes correct folding, oligomeric assembly, prevents degradation and supports quality control (Hammonds & Helenius, 1995; Hebert, Zhang, Chen, Foellmer & Helenius, 1997). ER retention of misfolded or unassembled proteins has been demonstrated for the $\Delta F508$ cystic fibrosis transmembrane conductance regulator, the truncated α chain of β -hexosaminidase and unassembled subunits of the T cell receptor (Bonifacino & Lippincot-Schwartz, 1991; Ward & Kopito, 1995).

In summary, we report that inhibition of N-linked glycosylation using tunicamycin results in a perinuclear accumulation of HERG^{GFP} in HEK 293 cells. Substitution of the asparagines at the each of the consensus N-linked glycosylation sites with glutamine leads to a similar perinuclear accumulation of HERG^{GFP} with no surface membrane expression and no detectable current. These findings may help to provide insight into a mechanism responsible for the lack of HERG current resulting from certain mutations observed in individuals with LQT2.

The data provided in chapter 2 demonstrate that N-linked glycosylation is required for the surface membrane expression of the ion channel HERG. The question addressed in the following chapter is that once ion channels are trafficked to the cell surface are they uniformly distributed or are they localized to a specific subcellular region.

CHAPTER 3

Localization of the Na^+/H^+ Exchanger NHE1 to Intercalated Discs and Transverse Tubules of Rat Myocardium

Abstract

The NHE1 isoform of the Na^+/H^+ exchanger is an integral component of the cardiac intracellular pH homeostatic mechanism that is critically important for myocardial contractility. To gain further insight into its physiological significance, we determined its cellular distribution in adult rat heart. Immunolabelling of NHE1 was detected predominantly at the intercalated disc regions of atrial and ventricular muscle cells. Significant labelling of NHE1 was also observed along the transverse tubular systems, but not the lateral sarcolemmal membranes, of both cell types. By contrast, the Na^+,K^+ -ATPase $\alpha 1$ - subunit was readily labelled by a specific mouse monoclonal antibody (McK1) along the entire ventricular sarcolemma and intercalated disc region, and to a lesser extent in the transverse tubules. These results, in conjunction with other studies, indicate that NHE1 has a distinct distribution in heart and may fulfill specialized roles by selectively regulating the pH microenvironment of pH-sensitive proteins at the intercalated discs (*e.g.*, connexin43) and near the cytosolic surface of sarcoplasmic reticulum cisternae (*e.g.*, ryanodine receptor), thereby influencing impulse conduction and excitation-contraction coupling.

Introduction

The continuous contractile activity of the myocardium generates metabolic acid which must be extruded in order to maintain cardiac function. This is exemplified by experimentally-induced decreases in intracellular pH (pH_i) which result in marked reductions in myocardial contractility (Orchard and Kentish, 1990). The precise mechanism of this inotropic effect is not well defined, but is associated with reduced myosin-ATPase activity (Kentish and Neyler, 1979), decreased ionic current through voltage-activated Na^+ and Ca^{2+} channels (Irisawa and Sato, 1986; Sato et al., 1985; Zhang and Siegelbaum, 1991), diminished binding of Ca^{2+} to troponin C of the contractile apparatus (Blanchard and Solaro, 1984), and reductions in gap junction conductance (Spray et al., 1985). Hence, regulation of pH_i is of critical importance for normal myocardial function.

At least three different ion transporters contribute to myocardial pH_i regulation; the $\text{Cl}^-/\text{HCO}_3^-$ exchanger (Liu et al., 1993; Vaughn-Jones, 1979), the $\text{Na}^+-\text{HCO}_3^-$ cotransporter (Laradic-Gossmann et al., 1992) and the Na^+/H^+ exchanger (NHE) (Lazdunski et al., 1985). Of these, the NHE is the main mechanism responsible for returning myocardial pH_i to the neutral range (pH_i 7.1 to 7.3) following an acid load. In mammals, at least six NHE isoforms (NHE1 to NHE6) are known to exist and they exhibit distinct differences in their primary structures (~20-60% amino acid identity), patterns of tissue expression, membrane localization, functional properties, and physiological roles (Orlowski and Grinstein, 1997; Wakabayashi et al., 1997). Cardiac tissue from rat (Orlowski et al., 1992; Yu et al., 1993), rabbit (Tse et al., 1993) and human (Fliegel et al., 1993) expresses predominantly the NHE1 mRNA; hence it is the

main NHE isoform responsible for controlling myocardial pH_i . The heart also expresses NHE6, but it is localized to the mitochondria inner membrane (Numata et al., 1998) where it contributes primarily to matrix cation (Na^+ and indirectly Ca^{2+}) homeostasis (Crompton and Heid, 1978).

Aside from its role in normal myocardial pH_i regulation, accumulating evidence points to NHE1 as a contributing factor in the pathophysiology of cardiac ischemia and reperfusion injuries. Metabolic alterations that create large pH gradients across the sarcolemma lead to hyper-activation of NHE1 during the early stages following ischemia and reperfusion, causing a dramatic influx of Na^+ which secondarily elevates intracellular Ca^{2+} (Duff, 1995; Fliegel and Dyck, 1995; Karmazyn and Moffat, 1993; Pierce and Meng, 1992; Scholz and Albus, 1993). This disturbance in Ca^{2+} homeostasis is generally believed to contribute to cardiac arrhythmias, necrosis and eventually contractile failure. The role of NHE1 in ischemic and reperfusion injuries, however, is most convincingly demonstrated by animal studies showing that treatment with amiloride, a relatively non-specific inhibitor of NHE1, significantly reduces Na^+ and Ca^{2+} overload and thus has cardioprotective properties (Karmazyn, 1988). Similar protective effects are obtained with amiloride analogues (Duff et al., 1991; Kaplan et al., 1995; Karmazyn et al., 1993; Moffat and Karmazyn, 1993; Myers and Karmazyn, 1993; Pierce et al., 1993; Tani et al., 1996) and new benzoyl guanidinium compounds (*e.g.*, HOE694 (Harper et al., 1993; Myers, 1990; Scholz et al., 1993; Yasutake et al., 1994) and HOE642 (cariporide) (Scholz et al., 1995; Xue et al., 1996) which are more potent and selective antagonists of NHE1. The antiarrhythmic action of amiloride has also been demonstrated in human clinical studies, where it suppressed inducible ventricular tachycardia (Duff et al., 1989)

and spontaneous ventricular premature beats (Myers et al., 1995). These studies highlight the importance of examining the molecular and cellular properties of NHE1 in order to further understand its physiological importance in myocardial function.

NHE1 activity has been demonstrated in isolated sarcolemmal vesicles (Pierce and Philipson, 1985), though its precise location in cardiac tissue is unknown. Recent immunolocalization and subcellular fractionation studies in other cell types have provided initial indications that NHE1 is not distributed homogeneously throughout the plasma membrane. For example, though present throughout the surface membrane of adherent fibroblasts, NHE1 preferentially accumulates along the border of lamellipodia in close association with vinculin, talin and F-actin, suggesting that it can be localized to specialized regions by interacting with the cytoskeleton (Grinstein et al., 1993). Likewise, NHE1 is restricted to the basolateral surface of polarized epithelial cells (Biemesderfer et al., 1992; Tse et al., 1991). In this study, we examined the hypothesis that NHE1 is localized to discrete regions of the myocardial membrane. An NHE1 isoform-specific polyclonal antibody was used in conjunction with confocal immunofluorescence. The data show that NHE1 is selectively targeted to the intercalated discs and transverse tubules, suggesting that it may fulfill specialized physiological roles at these sites.

Methods

Rat Myocardial Isolation

Adult Sprague-Dawley rats (250-350 g) were anesthetized with CO₂. A mid-line thoracotomy was performed and the heart was rapidly removed. The preparation, containing the entire heart was placed in a tissue bath superfused with Tyrode's solution (in mmol/L: 121 NaCl, 5 KCl, 15 NaHCO₃, 1 Na₂HPO₄, 2.8 Na-acetate, 1 MgCl₂, 2.2 CaCl₂ and 5.5 glucose) and gassed with a 95% O₂ and 5% CO₂ mixture. Temperature was maintained at 37.0 °C and the pH was 7.4. The preparation was pinned down in its proper orientation and then frozen in isopentane previously cooled to -40 °C. The frozen preparation was then trimmed into small blocks containing the various regions under investigation. The blocks were mounted on a cryostat tissue holder using Histo Prep (Fisher Scientific), placed on the rapid-freeze stage of a Microm cryostat (Carl Zeiss) and cut into 20 µm thick sections.

Cell Culture

AP-1 cells are Na⁺/H⁺ exchange-deficient Chinese hamster ovary cells that were created by random chemical mutagenesis and selected by the proton-suicide technique (Rotin and Grinstein, 1989). AP-1^{NHE1} cells were obtained by stable transfection of AP-1 cells with the complete coding region of the rat NHE1 isoform, as described in detail elsewhere (Orlowski, 1993). The AP-1 cells were maintained in complete -minimal essential medium supplemented with 10% fetal bovine serum, 100 units/mL penicillin, 100 µg/mL streptomycin, and 25 mmol/L NaHCO₃ (pH 7.4), and incubated in an humidified atmosphere of 95% air and 5% CO₂ at 37 °C.

Primary Antibodies

Isoform-specific polyclonal antibodies to NHE1 were raised by injecting rabbits with a fusion protein constructed with β -galactosidase of *Escherichia coli* and the last 157 amino acids of the hydrophilic (C-terminal) domain of the human exchanger, and affinity purified as described (Grinstein et al., 1993). Gap junctions were identified using a monoclonal antibody directed against residues 252-270 of the C-terminus of the rat connexin43 molecule (Chemicon International). The Na⁺,K⁺-ATPase was identified using a mouse monoclonal antibody, McK1, directed against the amino acids DKKSKK near the N-terminus of the rat Na⁺,K⁺-ATPase α 1-subunit (generously provided by Dr. Kathy Sweadner, Massachusetts General Hospital) (Sweadner et al., 1994).

Membrane Preparations

Adult Sprague-Dawley rats were anesthetized with CO₂, killed by cervical dislocation and the chest cavity was open. The heart was transected below the major vessels, rinsed in PBS at 4 °C and frozen at -70 °C. Rat heart membranes were prepared according to the method of Hosey *et al.* (Hosey and Fields, 1981) with minor modifications. All procedures were performed at 4 °C and all solutions contained the Complete™ protease inhibitor cocktail (Boehringer Mannheim, Germany). Hearts were minced, diluted in 10 volumes of TE buffer (Tris 10 mmol/L, EDTA 1 mmol/L, pH 7.4) and homogenized three times (10 sec each) with a Brinkman Polytron (Brinkman Instruments, Westbury, N.Y.) at a setting of 9. Nuclei and cell debris were pelleted by centrifugation at 1000g for 10 min. The pellet was rehomogenized in TE buffer and the centrifugation step repeated. The supernatants from both low-speed spins were pooled and centrifugated at 30,000g for 30 min. In order to

depolymerize the actin, the pellet was resuspended in TE containing 0.6 mol/L KI and incubated on ice for 30 min. After centrifuging at 30,000g for 30 min, the resulting pellet was resuspended in TE and washed two times to completely remove the KI. The final pellet was solubilized by boiling in TE containing 1% SDS and the insoluble material centrifuged at 13,000g for 30 min.

Confluent AP-1 cells were washed three times with PBS, scraped off from the plates, lysed in RIPA buffer (NaCl 150 mmol/L, Tris HCL 20 mmol/L, SDS 0.1%, deoxycholate 0.5%, Triton X-100 1%, pH 8.0) supplemented with protease inhibitor cocktail, and spun down at 2,400g for 5 min. The supernatant was collected as a crude membrane fraction.

The protein concentration of all of the membrane preparations was measured using the Bio-Rad *DC* Protein Assay kit. Solubilized membranes were aliquoted and stored at -70 °C until use.

SDS-Polyacrylamide Gel Electrophoresis and Immunoblotting

Samples containing AP-1 (20 µg protein) and rat heart (40 µg protein) membranes were resolved on 10% SDS-polyacrylamide gels and electrophoretically transferred to Polyscreen PDVF membranes (DuPont, NEN Research Products). After transfer, the PDVF membranes were quenched in phosphate buffered saline (PBS) containing 5% nonfat dry milk and 0.1% w/v Tween 20 for 1 h. Polyclonal NHE1 antiserum was added to a final dilution of 1:5000 and the incubation was allowed to proceed for another 2 h at room temperature. The membranes were further incubated with goat anti-rabbit IgG conjugated with horseradish peroxidase (New England BioLabs) for 1 h at room temperature and the

labeled proteins detected by enhanced chemiluminescence (ECL) using a Western blotting detection kit (Amersham).

To demonstrate the specificity of the immunoreactivity, duplicate samples were submitted to the same protocol except that the primary antibody was preincubated for 1 h with the NHE1 fusion protein (1 $\mu\text{g/mL}$ final concentration) used to generate the antiserum.

Immunohistochemistry

Cryostat sections, 20 μm thick, prepared from the frozen hearts were mounted onto slides and air-dried at room temperature for 1 h. After permeabilizing and blocking with 0.2% Triton X-100/0.5% BSA in phosphate-buffered saline (PBS), sections were incubated for 2 h at room temperature with primary antibody diluted in 0.2% Triton X-100/0.5% BSA/PBS. After three washes in phosphate-buffered saline (pH 7.2), sections were incubated with secondary antibody (Texas Red-conjugated goat anti-rabbit IgG or FITC-conjugated goat anti-mouse IgG, Jackson ImmunoResearch Laboratories, Inc.) diluted in 0.2% Triton X-100/0.5% BSA/PBS for 1 h at room temperature followed by three rinses in PBS. Sections were then mounted using Immuno Flore (ICN). Controls include omission of the primary antibodies directed against NHE1, Connexin43 and Na^+, K^+ -ATPase, and NHE1 antibody competition with the fusion protein that the antibody was generated against.

Immunocytochemistry

Cells grown on coverslips were fixed in 1% paraformaldehyde for 15 min at room temperature followed by three rinses in PBS (pH 7.2). Cells were then permeabilized and blocked by incubation in 0.2% Triton X-100/0.5% BSA in PBS for 30 min at room temperature. Cells were subsequently rinsed in PBS and incubated with appropriately diluted primary antibody in 0.2% Triton X-100/0.5%BSA/PBS for 1 h at room temperature. After three rinses in PBS, cells were incubated in secondary antibody (Texas Red-conjugated goat anti-rabbit IgG, Jackson ImmunoResearch Laboratories, Inc.) diluted in 0.2% Triton X-100/0.5%BSA/PBS for 1 h at room temperature followed by three rinses in PBS. Sections were then mounted using Immuno Flore (ICN).

Confocal Laser Scanning Microscopy

For confocal microscopy, sections from nine hearts were analyzed for immunolocalization of NHE1. An additional four hearts were analyzed for localization of Na^+/K^+ -ATPase and colocalization of NHE1 and connexin43. All imaging was performed using a Zeiss LSM 410 inverted confocal microscope. Texas Red-conjugated secondary antibodies were excited with a helium/neon (543 nm) laser and were imaged on a photomultiplier after passage through FT560 and LP590 filter sets. FITC-conjugated secondary antibodies were imaged by exciting the sample with a 488 nm line from an argon/krypton laser and the resulting fluorescence was collected on a photomultiplier after passage through FT510 and BP515-540 filter sets. All images were printed on a Kodak XLS8300 high resolution (300 DPI) printer. Optical sections were taken using a x25, 0.8 NA (optical thickness = 3.1 μm) objective or a x63, 1.4 NA

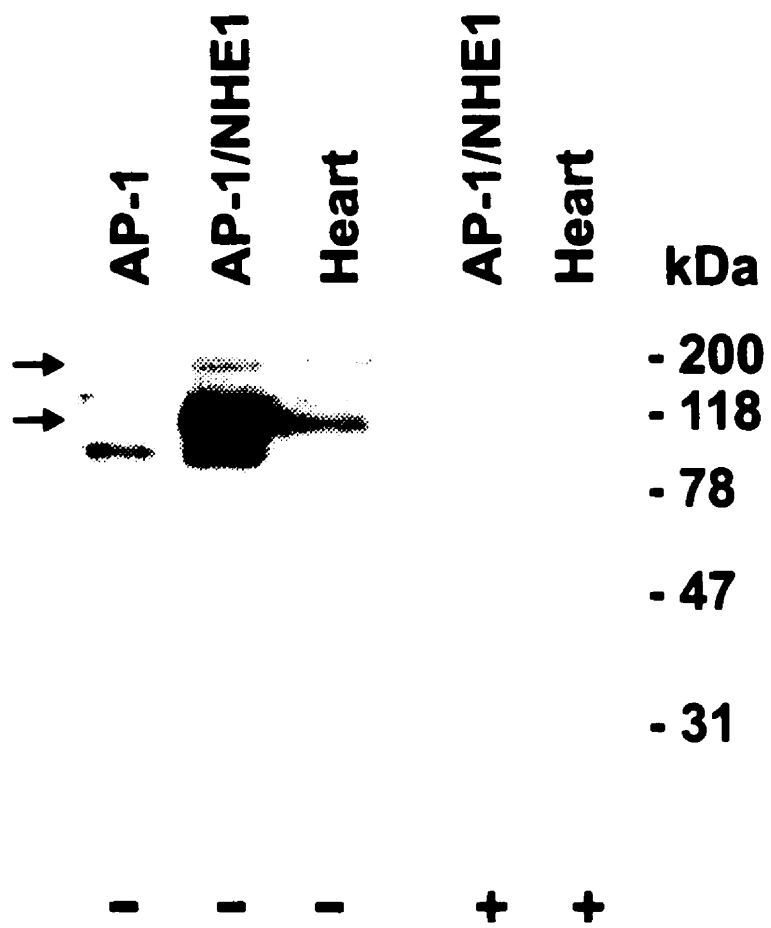
objective (optical thickness = 1.0 μm). The imaging parameters, including contrast and brightness and acquisition times, were similar for all positive and negative experiments within each figure. The data presented in this study are identical to, and representative of, all experiments.

Results

Myocardial distribution of the Na⁺/H⁺ exchanger

To determine the cellular location of NHE1 in the intact rat myocardium, we used confocal immunofluorescence microscopy and an isoform-specific anti-human NHE1 antibody that has been successfully used for the detection of NHE1 by immunocytochemistry and Western blotting (Fukushima et al., 1996; Grinstein et al., 1993). Rat NHE1 has a high degree of sequence similarity with human NHE1 and was therefore anticipated to react with the anti-human NHE1 antibody. Fig. 1 illustrates the specificity of the antibody by immunoblotting of protein extracts from NHE1-transfected fibroblasts and heart tissue: a prominent immunoreactive band of ~110 kDa (fully glycosylated form) and smaller amounts of dimerized (~200 kDa) and unglycosylated (~90 kDa) forms were observed in crude cell extracts from stably transfected AP-1 cells overexpressing rat NHE1 (AP-1^{NHE1}; lane 1), consistent with previous reports (Fafournoux et al., 1994; Fukushima et al., 1996). By comparison, enriched membranes isolated from rat heart (lane 2) contained smaller amounts of the fully glycosylated NHE1 and minor amounts of the dimerized form, but the unglycosylated protein was absent or below the detection sensitivity of the antibody. These bands could be competed off by incubation of the primary antibody with excess soluble NHE1 fusion protein (lanes 3 and 4), demonstrating the specificity of this detection system. Other smaller, fainter bands were also detected in extracts from AP-1^{NHE1} cells and heart tissue. Some of these were competed off by excess soluble NHE1 fusion protein, suggesting that they may be proteolytic products of NHE1 that arose during tissue processing. Other bands are neither consistently observed between different experiments nor are they effectively

Figure 1. Detection of rat NHE1 protein in membrane preparations from AP-1 cells and rat heart. Membrane fractions were prepared from AP-1 cells stably transfected with rat NHE1 (AP-1^{NHE1}) and rat hearts as described in “Materials and Methods”. The proteins were resolved by SDS-polyacrylamide gel electrophoresis and then detected by immunoblotting. The blots were preincubated with the NHE1 antiserum (final dilution 1:5000) either in the absence (-) or presence (+) of soluble NHE1 fusion protein (final concentration 1 µg/mL) used to generate the antiserum, followed by incubation with goat anti-rabbit IgG conjugated with horseradish peroxidase. The labeled proteins were detected by enhanced chemiluminescence. The positions of monomeric (unglycosylated (~ 90 kDa) and fully glycosylated (~ 110 kDa)) and dimeric (~ 200 kDa) forms of NHE1 are indicated by *arrows* at the *left* of the figure. The positions of prestained molecular weight markers are indicated at the *right* of the figure.



quenched by the soluble NHE1 fusion protein, and hence are likely of nonspecific origin. Further analysis showed significant labelling of NHE1 throughout the cell surface and to a lesser extent in the perinuclear region of transfected AP-1^{NHE1} cells (Fig. 2A), whereas in nontransfected AP-1 cells surface-associated and perinuclear immunofluorescence was extremely faint and diffuse (Fig. 2B), in agreement with an earlier report using whole cells (Grinstein et al., 1993). These initial experiments suggested that the fluorescence pattern generated by this antibody is a valid indicator of the distribution of NHE1 in cells and tissues.

Immunolabelling of longitudinal sections of rat ventricle revealed that NHE1 preferentially accumulated at the intercalated disc region and less intensely along parallel lines corresponding to the transverse tubular system (Fig. 3A, B). By contrast, no labelling was detected along the lateral sarcolemma regardless of the optical plane. Control sections treated with the secondary antibody alone (Fig. 3C,D) or with both the primary and Texas Red-conjugated secondary antibodies in the presence of the NHE1 fusion protein used to generate the antibody (Fig. 3E,F) gave no signals, confirming the specificity of the immunoreactivity. The lack of signal in the presence of competing soluble NHE1 antigen also indicates that the minor non-specific bands detected in the Western blot were not a contributing factor to the immunofluorescence signal. Similar results were obtained for both ventricular (Fig. 4A,B) and atrial (Fig. 4C,D) tissue shown at two higher magnifications.

To establish the validity of these observations, we examined the locations of two other previously characterized proteins in cardiac tissue; connexin43, which is confined to gap junctions at the intercalated discs (Beyer et al., 1989), and the Na⁺,K⁺-ATPase α 1

Figure 2. Expression of NHE1 protein in AP-1 cells. *A*, immunofluorescence image of AP-1^{NHE1} cells incubated with anti-NHE1 antibody. Arrows indicate plasma membrane labelling. *B*, immunofluorescence image of untransfected AP-1 cells incubated with anti-NHE1 antibody. Bar = 20 μ m.

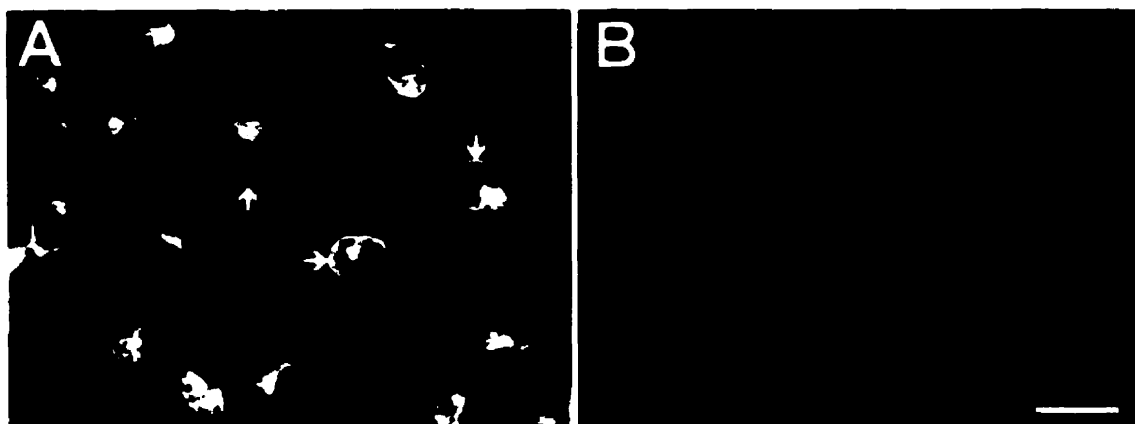


Figure 3. Expression of NHE1 in rat heart. *A*, transmitted light image of a 20 μm thick section of ventricle. *B*, immunofluorescence image of the ventricular section in *A* (inset b) incubated with anti-NHE1 antibody followed by Texas Red-conjugated goat anti-rabbit IgG. *C*, transmitted light image of a 20 μm thick section of ventricle. *D*, immunofluorescence image of the ventricular section in *C* (inset d) incubated in the presence of Texas Red-conjugated goat anti-rabbit IgG only. *E*, transmitted light image of a 20 μm thick section of ventricle. *F*, immunofluorescence image of the ventricular section in *E* (inset f) incubated in the presence of anti-NHE1 antibody and the NHE1 fusion protein that the primary antibody was generated against followed by Texas Red-conjugated goat anti-rabbit IgG. Magnification in *A*, *C* and *E* is identical. Magnification in *B*, *D* and *F* is identical. Bars: *E* = 62.5 μm , *F* = 25 μm .

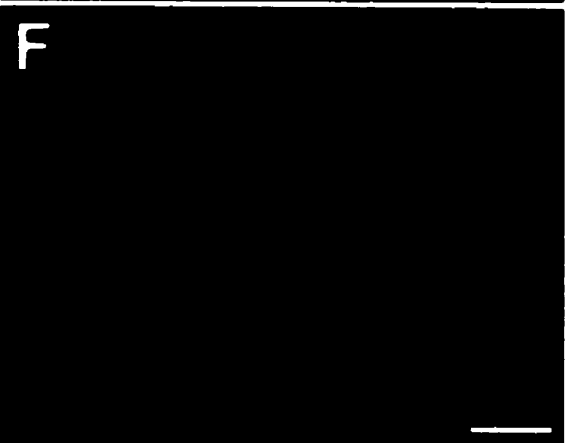
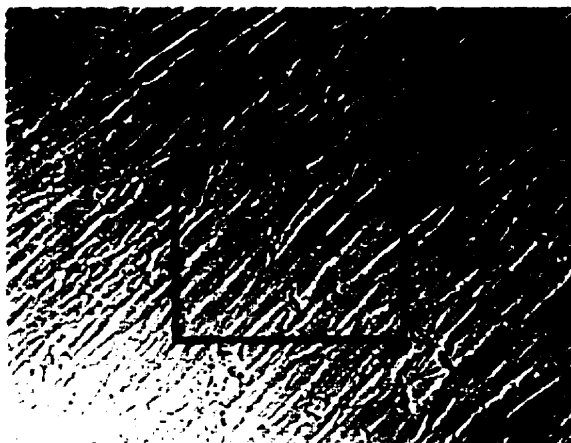
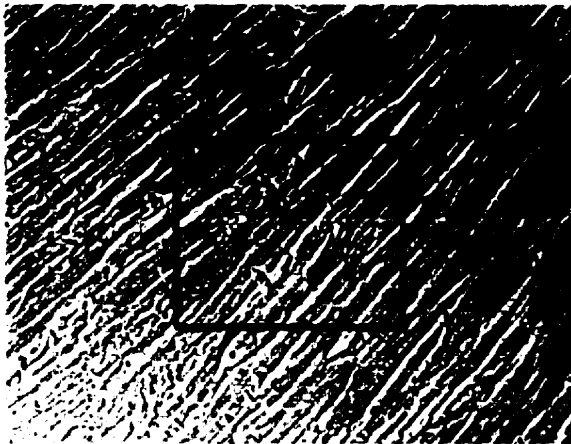
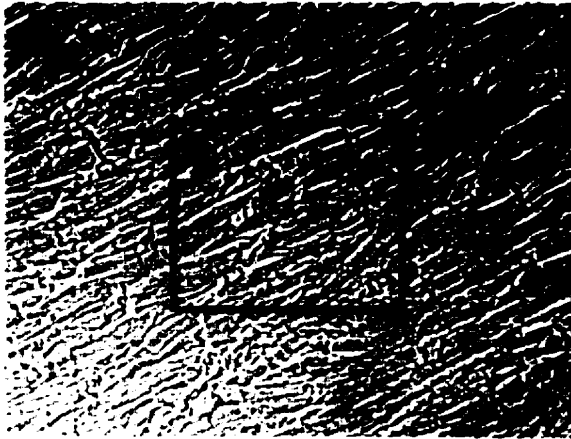
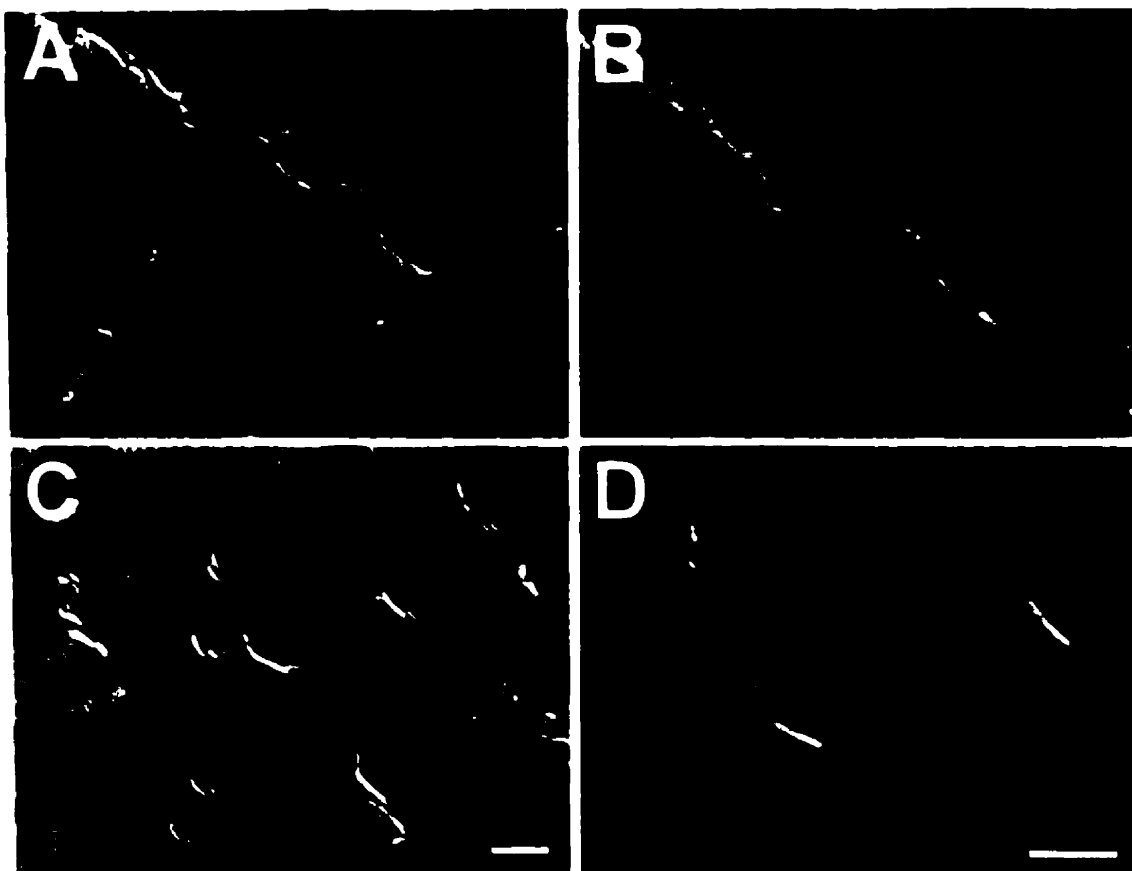


Figure 4. Comparison of NHE1 protein expression in ventricular and atrial myocardium. *A*, immunofluorescence image of ventricular tissue incubated in the presence of anti-NHE1 antibody. *B*, high magnification image of panel *A*. *C*, immunofluorescence image of atrial tissue incubated in the presence of anti-NHE1 antibody. *D*, high magnification of panel *C*. Magnification in *A* and *C* is identical. Magnification in *B* and *D* is identical. Bars: *C* = 10 μm , *D* = 10 μm .



subunit, which is distributed along the surface sarcolemma and transverse tubules (McDonough et al., 1996; Moffat and Karmazyn, 1993). As shown in Fig. 5 at low (Fig. 5A,B) and high (Fig. 5C) magnification, labelling longitudinal sections of rat ventricular muscle with a mouse monoclonal antibody directed against rat connexin43 revealed clusters of transversely-oriented gap junctions at the intercalated discs, in agreement with other studies (Beyer et al., 1989). Labelling was not detected in control sections treated with the FITC-conjugated secondary antibody alone (Fig. 5D). However, when ventricular tissue was labelled with a specific monoclonal antibody (McK1) raised against the rat Na⁺,K⁺-ATPase α 1 subunit, it showed a more uniform distribution along the entire sarcolemma and intercalated disc region (Fig. 6A,B). Less prominent labelling was also observed in the transverse tubules, which is more visible at higher magnifications (Fig. 6C). Again, control sections treated with the secondary antibody alone (Fig. 6D) were negative. These latter results are consistent with other reports using the same anti-Na⁺,K⁺-ATPase α 1 antibody (McDonough et al., 1996; Moffat and Karmazyn, 1993). Dual labelling experiments of NHE1 (Fig. 7A: NHE1 label) and connexin43 (Fig. 7B: connexin43 label) confirm that they are co-localized to the intercalated disc regions (Fig. 7C: NHE1 + connexin43), although they do not appear to occupy the same sites.

Figure 5. Connexin43 protein expression in ventricular myocardium. *A*, transmitted light image of a 20 μm thick section of ventricle. *B*, low magnification of an immunofluorescence image of the ventricular section in *A* incubated with anti-connexin43 antibody followed by Texas Red-conjugated goat anti-mouse IgG. *C*, higher magnification of an immunofluorescence image of a ventricular section incubated with anti-connexin43 antibody followed by Texas Red-conjugated goat anti-mouse IgG; Bar = 10 μm . *D*, immunofluorescence image of a ventricular section incubated with Texas Red-conjugated goat anti-mouse IgG only at an identical magnification to panels *A* and *B*; Bar = 50 μm .

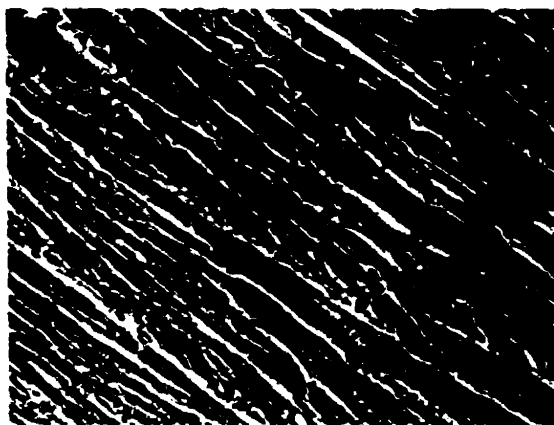


Figure 6. Na⁺,K⁺-ATPase protein expression in ventricular myocardium. *A*, transmitted light image of a 20 µm thick section of ventricle. *B*, immunofluorescence image of the ventricular section in *A* (inset b) incubated with McK1 followed by Texas Red-conjugated goat anti-mouse IgG. Vertical arrows indicated lateral membrane labelling. Horizontal arrows indicate labelling at the intercalated disk region. *C*, immunofluorescence image of a 20 µm thick section of ventricle incubated with McK1 followed by Texas Red-conjugated goat anti-mouse IgG at higher magnification (Bar = 10 µm). *D*, Immunofluorescence image of a ventricular section incubated with Texas Red-conjugated goat anti-mouse IgG only. Magnification in *B* and *D* is identical. Bar in *D* = 25 µm.

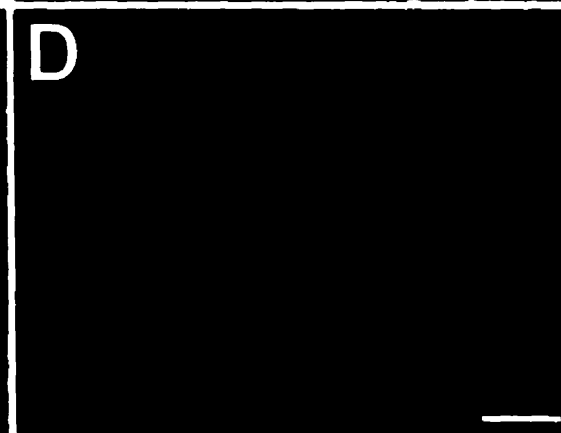
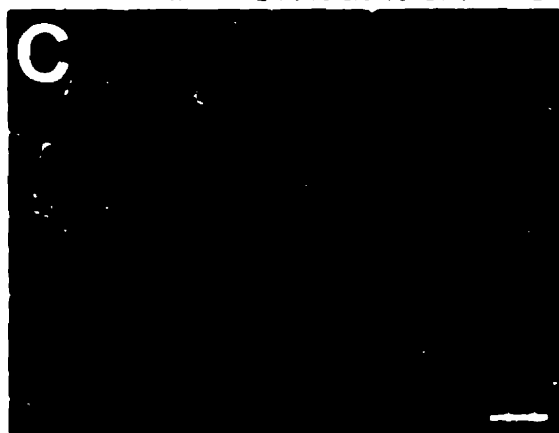
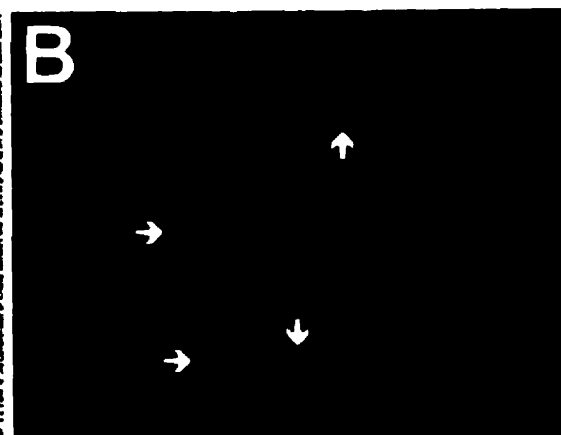
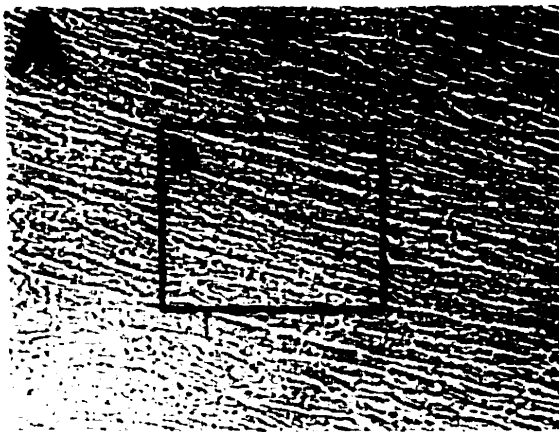
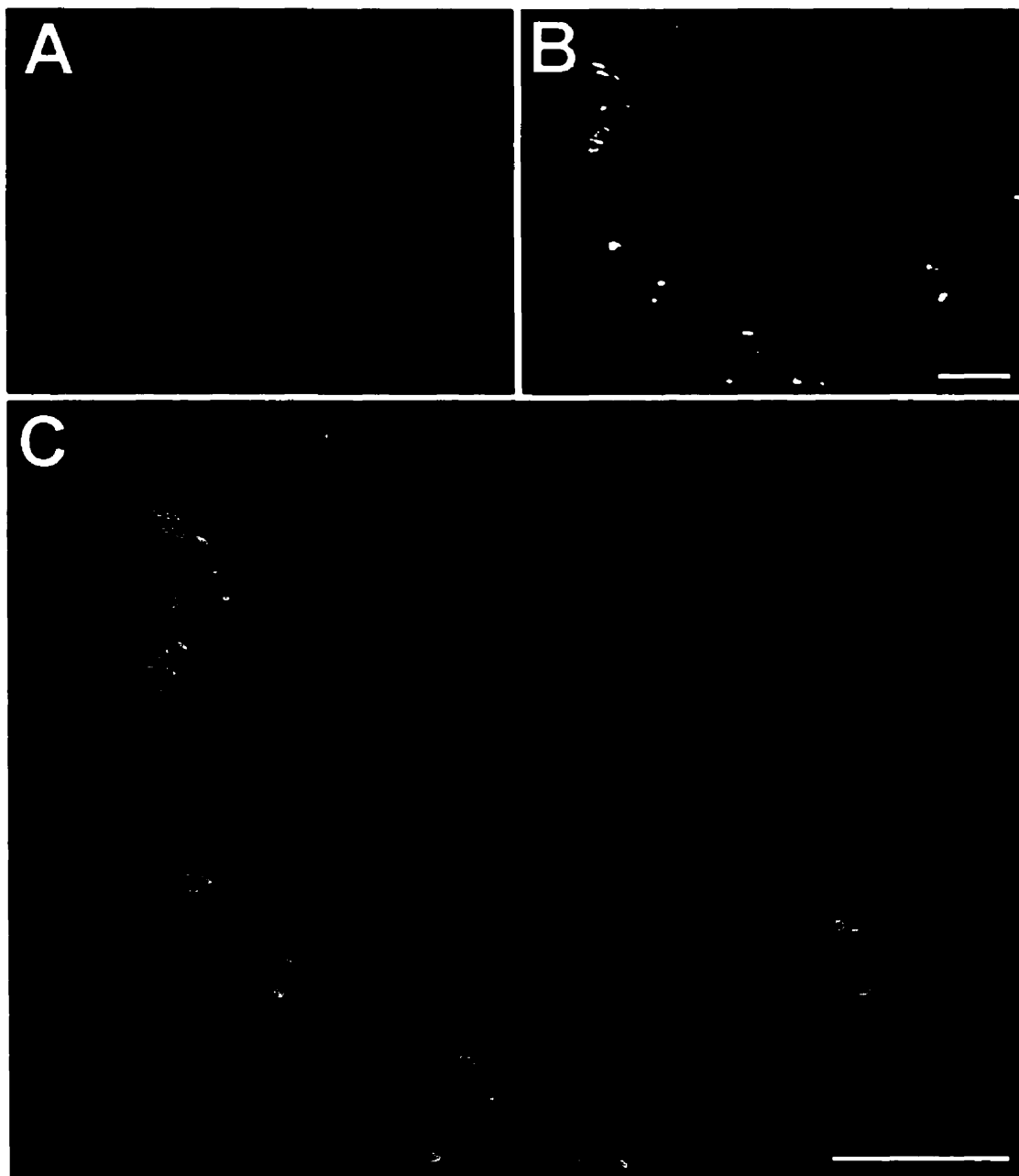


Figure 7. Co-localization of NHE1 and connexin43 protein expression in ventricular myocardium. *A*, immunofluorescence image of ventricular tissue incubated in the presence of anti-NHE1 antibody. *B*, immunofluorescence image of ventricular tissue, identical region as panel *A*, incubated in the presence of anti-connexin43 antibody. *C*, overlay of panels *A* and *B*. NHE1 protein expression is visible as red labelling. Connexin43 protein expression is visible as green labelling. Magnification in *A* and *B* is identical. Bars: *B* = 10 μm , *C* = 10 μm .



Discussion

The Na⁺/H⁺ exchanger NHE1 isoform is localized in rat cardiac myocytes at the intercalated discs and transverse tubules

Biochemical studies have indicated that Na⁺/H⁺ exchanger activity (*i.e.*, the NHE1 isoform) is present in isolated sarcolemmal vesicles (Pierce and Philipson, 1985). By using an isoform-specific anti-NHE1 polyclonal antibody and confocal immunofluorescence microscopy, we show that NHE1 is preferentially localized at the intercalated disc regions and transverse tubular system of adult rat atrial and ventricular muscle cells. In this study, the specificity of immunolabelling in rat heart is demonstrated by the lack of a detectable signal in the presence of a competing soluble form of the NHE1 antigen added during incubation with the primary antibody, and the absence of a signal in the presence of secondary antibody alone. Taken together, these data strongly suggest that the observed immunolabelling represents localization of NHE1 protein to the intercalated discs and transverse tubules.

Immunolabelling of NHE1 at the intercalated discs appears more intense than that of the transverse tubular system. This could represent selective clustering and higher densities of NHE1 protein per unit area of membrane, analogous to the preferential accumulation of NHE1 along the border of lamellipodia in fibroblasts (Grinstein et al., 1993). Alternatively, the intense signals may reflect increased membrane surface area due to the infolding of the sarcolemma at the intercalated discs (Page and McCallister, 1973).

Unexpectedly, NHE1 was not observed along the lateral sarcolemma. The possibility that this membrane compartment was inaccessible to antibodies under the

given experimental conditions was excluded by our ready detection of the Na^+, K^+ -ATPase $\alpha 1$ subunit in the lateral sarcolemma. While the absence of labelling of NHE1 may reflect a level of abundance that is below the detection sensitivity of the antibody, the data are more readily explained by the selective targeting of NHE1 to the intercalated disc and transverse tubular membranes. This distribution differs somewhat from that of the $\text{Na}^+/\text{Ca}^{2+}$ exchanger which, like the Na^+, K^+ -ATPase $\alpha 1$ subunit, is present throughout the sarcolemma, the transverse tubules and the intercalated discs of isolated ventricular myocytes from adult guinea pig and rat hearts (Frank et al., 1992; Kieval et al., 1992). Other pH regulatory transporters also appear to exhibit preferential membrane targeting in heart. An antibody which recognizes both the AE1 and AE3 isoforms of the $\text{Cl}^-/\text{HCO}_3^-$ exchanger revealed that they accumulated mainly at the lateral sarcolemma and transverse tubules of isolated adult rat ventricular myocytes (Puceat et al., 1995), although it was not established whether these isoforms were differentially targeted to these membrane surfaces. The location of the other major cardiac pH regulatory protein, the $\text{Na}^+/\text{HCO}_3^-$ cotransporter, is currently unknown. Thus, the distribution of the NHE1 isoform in cardiac myocytes appears distinct from that of other known exchangers and pumps. The mechanisms responsible for this differential membrane localization are unknown.

Functional implications for the subcellular localization of NHE1 in heart

The immunofluorescence data revealed that NHE1 accumulates at the intercalated discs in close proximity to the predominant cardiac gap junction protein connexin43, which suggests that a functional relationship may exist between the two proteins. It is well

known that small changes in pH_i within the physiological range regulate gap junction conductance (Spray et al., 1985; White et al., 1990). The molecular basis for this phenomenon is not fully understood, but electrophysiological studies have shown that decreasing pH_i reduces the open probability of individual cardiac gap junction channels (Burt and Spray, 1988). Recent structural studies have implicated His95 (Ek et al., 1994) and the carboxy tail (Liu et al., 1993) of connexin43 as critical components involved in “ H^+ gating” of the cardiac gap junction. Thus, it is reasonable to suggest that neighboring NHEs may play a role in this regulation. Indeed, pretreatment of rat neonatal paired cardiomyocytes with amiloride (1 mmol/L), a nonselective inhibitor of NHE1, enhanced the inhibitory effects of acidic pH_i on conductance of gap junctions presumably by retarding extrusion of protons (Firek and Weingart, 1995). The caveat to this study is that the effects of amiloride could have been secondary to inhibition of other transporters and channels (Kleyman and Cragoe, 1988), thus making it difficult to firmly establish a functional link between NHE1 activity and gap junction conductance. Nevertheless, the data are consistent with the hypothesis that the high density of NHE1 in the intercalated disc region serves to regulate the pH_i environment of gap junctions, particularly connexin43; thereby influencing intercellular communication.

Aside from NHE1, other ion transport proteins are also concentrated at the intercalated disc region of cardiac myocytes, such as voltage-gated Na^+ channels (H1 subtype) (Cohen, 1996), voltage-gated K^+ channels (Barry et al., 1995; Mays et al., 1995), and inositol 1,4,5-triphosphate Ca^{2+} release channels (*i.e.*, IP_3 receptors) (Kijima et al., 1993). Whether these ion channels are similarly influenced by physiologically relevant changes in pH_i is unknown.

Likewise, it is attractive to speculate that the presence of NHE1 along the transverse tubules is functionally coupled to the rapid release of Ca^{2+} by the sarcoplasmic reticulum Ca^{2+} release channel (*i.e.*, ryanodine receptor) which is highly pH_i -sensitive (Xu et al., 1996); a minor cytosolic acidification decreases the rate of Ca^{2+} release which is directly involved in triggering the contractile process.

In conclusion, the data show that NHE1 is specifically targeted to distinct regions of cardiac myocytes. We speculate that NHE1 may fulfill specialized roles in heart by selectively regulating the pH microenvironment of pH-sensitive proteins at the intercalated discs (*e.g.*, connexin43) and near the cytosolic surface of sarcoplasmic reticulum cisternae (*e.g.*, ryanodine receptor), thereby influencing impulse conduction and excitation-contraction coupling.

The data provided in chapter 3 demonstrate that the NHE1 is not uniformly distributed throughout the cell surface of cardiac myocytes but exhibits a site-specific localization at the intercalated disc region. The question addressed in the following chapter is proteins that interact with ion channels play a role in this site-specific localization.

CHAPTER 4

Localization of the Kv4.2 Potassium Channel by Interaction with the Actin-Binding Protein, Filamin

Abstract

The Kv4.2 K⁺ channel, which plays critical role in postsynaptic excitability, exhibits a somatodendritic expression pattern with a concentration at the PSD; however, the mechanism for this localization is unknown. Here, we report a novel interaction between Kv4.2 and the actin-binding protein, filamin. We have mapped the filamin interaction site to a 4 amino acid motif within the Kv4.2 C terminus. We show that Kv4.2 and filamin interact both in vitro and in brain and that filamin localizes Kv4.2 to cellular specializations in heterologous cells. Moreover, Kv4.2 and filamin share an overlapping synaptic distribution pattern in brain and cultured hippocampal neurons. Thus, filamin may function as a scaffold protein in the postsynaptic density (PSD) mediating a direct link between Kv4.2 and the actin cytoskeleton.

Introduction

Appropriate synaptic transmission is dependent upon the precise localization of ion channels and neurotransmitter receptors at specific subcellular sites (Sheng, 1996; Ziff, 1997; Colledge and Froehner, 1998; Craven and Bredt, 1998). Voltage-gated K⁺ channels are expressed within neurons in a variety of spatial distributions (Sheng et al., 1992; Wang et al., 1994; Veh et al., 1995) where they function as regulators of membrane excitability and synaptic transmission (Hille, 1991; Magee et al., 1998). Fast transient (A-type) K⁺ channels, members of the voltage-gated K⁺ channel family found in a wide variety of excitable cells, have been implicated in the control of action potential frequency and threshold, action potential configuration, neurotransmitter release and postsynaptic excitability (Jan and Jan, 1997; Magee et al., 1998). Kv1.4 and Kv4.2, fast transient K⁺ channel family members, are differentially segregated in neurons. Kv1.4 is localized to axons exhibiting a concentration at the presynaptic terminal (Sheng et al., 1992; Zito et al., 1997; Arnold and Clapham, 1999), whereas Kv4.2 is localized to the somatodendritic compartment exhibiting a concentration at the postsynaptic terminal (Sheng et al., 1992; Maletic-Savatic et al., 1995; Alonso and Widmer, 1997).

The PSD-95/SAP90 subfamily of MAGUK (membrane associated guanylate kinase) proteins has been implicated in the synaptic clustering of several classes of neuronal ion channels. In their N-terminal half, this family of proteins is characterized by three PDZ domains that function as modules for specific protein–protein interactions. PDZ domains have been shown to bind short peptide motifs at the extreme C-terminus of proteins including Shaker K⁺ channels and NR2 subunits of NMDA receptors (Kim et al., 1995; Kornau et al., 1995). PSD-95 colocalizes with Shaker K⁺ channels and NMDA

receptors in central neurons, and coexpression of PSD-95 leads to the clustering of Shaker K⁺ channels in heterologous cells (Kim et al., 1995, Hsueh et al., 1997).

Recent studies suggest that the Kv1.4/PSD95 interaction is not sufficient for the precise localization of this complex at the presynaptic terminal. Expression of PSD-95:GFP in pyramidal cells results in a predominant dendritic localization. When neurons are cotransfected with both Kv1.4 and PSD-95:GFP, PSD-95:GFP appears in both axons and dendrites, while Kv1.4 exhibits a restricted axonal localization. Disruption of the domains that mediate the interaction of Kv1.4 with PSD-95 results in a non-specific Kv1.4 localization (Arnold and Clapham, 1999). Similarly, Zito et al. (1997) showed that the C-terminal 11 amino acids of the Shaker K⁺ channel are sufficient to direct synaptic localization of a heterologous protein *in vivo*; however, this synaptic localization is not as efficient as that directed by the entire C-terminal sequence. Finally, the subcellular localization of Kv2.1 in epithelial cells has been shown to be dependent upon a motif within its cytoplasmic tail rather than the very C-terminus (Scannevin et al., 1996). Taken together, these data suggest that although interaction with PDZ containing proteins is critical for the clustering of certain K⁺ channels, it is not sufficient for their proper localization and that the mechanism responsible for their localization may be mediated by C-terminal protein interactions that remain largely unknown.

In this study we set out to identify Kv4.2 C-terminal interacting proteins involved in Kv4.2 localization. Here, we report the identification and characterization of a novel interaction between Kv4.2 and filamin, a member of the α -actinin/spectrin/dystrophin family of actin-binding proteins. Filamin was originally identified as a protein isolated from motile alveolar macrophage that caused purified muscle actin to gel and precipitate

(Hartwig et al., 1975). It is a widely distributed member of a family of actin-binding proteins capable of cross-linking actin filaments into orthogonal arrays and contributes substantially to the formation and structure of the actin meshwork situated immediately subjacent to the surface membrane (Marti et al., 1997). A large body of evidence implicates filamin in the regulation of the actin cytoskeleton in dynamic regions of the cell periphery in a manner that is regulated, directly and indirectly, through cell surface receptors. Filamin, which directly links membrane receptors (eg., β integrin) to the actin cytoskeleton, has been shown to play a crucial role in mechanoprotection by reinforcing the cell membrane in order to maintain cell integrity in a protein kinase C (PKC)-dependent manner (Glogauer et al., 1998). Moreover, filamin plays a role in the induction of filopodia that is dependent upon its interaction with the small GTPase RalA (Ohta et al., 1999), and, mutation of filamin results in human periventricular heterotopia, a disorder in which neurons fail to migrate (Fox et al., 1998). Importantly, filamin is a component of the neuromuscular junction (NMJ) that has been implicated in stabilizing acetylcholine receptor (AChR) clusters (Shadiak and Nitkin, 1991). Furthermore, filamin has been shown to mediate the assembly of macromolecular signaling complexes. In the *Drosophila* dorsoventral signaling cascade filamin links the membrane receptor Toll to its downstream mediator Tube (Edwards et al., 1997). Filamin also participates in TNF- α signal transduction to stress-activated protein kinases by interacting with SEK-1 (Marti et al., 1997).

Here, we show that Kv4.2 and filamin can be coimmunoprecipitated from both heterologous cell and brain extracts. Mapping studies reveal that a four amino acid (aa) motif located ~ 30 aa upstream of the Kv4.2 C-terminus is required for Kv4.2-filamin

interaction. We also show that Kv4.2 and filamin share an overlapping synaptic expression pattern in brain and that Kv4.2 and filamin colocalize at synaptic sites in cultured hippocampal neurons. Importantly, we demonstrate that filamin not only colocalizes with Kv4.2 at cellular specializations in heterologous cells, it is responsible for Kv4.2 localization at these sites. These findings suggest that filamin is a Kv4.2-interacting protein that colocalizes with Kv4.2 at neuronal synapses and plays an important role in the localization of Kv4.2 at cellular specializations in heterologous cells.

Results

Interaction of Kv4.2 with Filamin

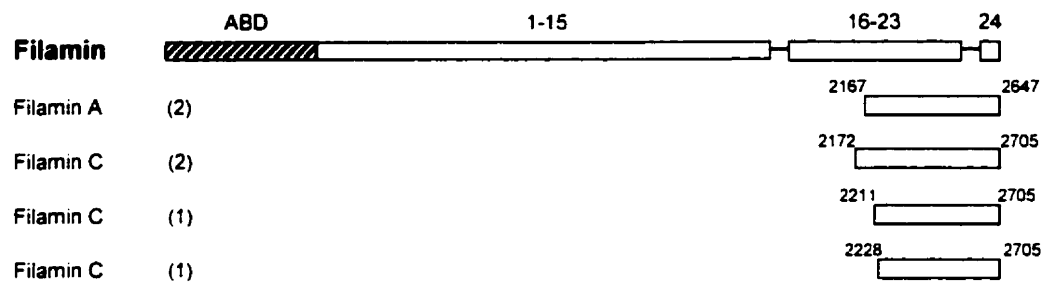
In an effort to search for molecules that may be involved in the localization of Kv4.2, we used the entire C terminus of Kv4.2 as a bait to screen a human heart cDNA library using the yeast two-hybrid method. The screen yielded multiple copies of four distinct cDNAs encoding polypeptides that interacted specifically with the C terminus of Kv4.2. No other clones were isolated in this screen. Furthermore, an unrelated bait encoding the C terminus of HERG did not interact with any of the isolated clones. Sequence analysis revealed that one of the cDNAs was derived from filamin A, while the other three cDNAs were derived from distinct but overlapping sequences of a highly homologous polypeptide, filamin C (Figure 1A).

Three filamin isoforms (A, B and C) have been identified exhibiting an overall aa homology of 70-72%. Each isoform shares three common functional domains; a N-terminal actin-binding domain that is structurally similar to that of the - actinin/spectrin/dystrophin family of cytoskeletal proteins, a semiflexible rod domain composed of 24 repeats interrupted by two short sequence inserts of 20-40 aa between repeats 15-16 and 23-24 which are proposed to form flexible hinges, and a C-terminal self-association domain (Xie et al., 1998). All partial filamin cDNA fragments isolated in this screen began at variable starting points within repeat 20 and were complete to the C-terminus (Figure 1A).














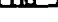





To define the site of interaction between Kv4.2 and filamin we began by examining successively larger C-terminal deletions of Kv4.2 that bind filamin using yeast two-hybrid analysis. Deletion of the C-terminal 25 aa did not affect binding (Figure 1B).

Figure 1. The Domain Structure of Filamin and Interaction with Kv4.2. (A) Human cDNA clones isolated a yeast two-hybrid screen using the Kv4.2 C-terminal region (aa 395-630) as a bait are shown aligned below a schematic representation of the filamin domain structure. ABD, actin binding domain; 1-15, 16-23, and 24 represent ~96 aa repeats, each separated by hinge regions. Partial cDNAs from filaminA and filaminC genes were isolated. Numbers in parentheses indicate the number of times each clone was isolated using the yeast two-hybrid screen. (B) Sequence requirements in the Kv4.2 C-terminal region for interaction with filamin. FilaminC (aa 2172-2705) binding to Kv4.2C1 (aa 395-630) and deletion derivatives were assayed by HIS3/ β -gal induction in the yeast two-hybrid system. Residues 601-604 are required for interaction with filamin, deletion and/or mutation of this region abolishes the interaction. Kv4.3, which contains the identical binding region, also interacts with filamin. The HERG C-terminal region (aa 864-1165) does bind filamin. The various bait fragments were tested for filamin binding by semi-quantitative yeast two-hybrid interaction assays based on the degree of induction by reporter genes HIS3 and β -Gal. HIS3 activity was measured by the percentage of colonies growing on histidine lacking medium as compared to the full-length Kv4.2 bait (Kv4.2C1): +++, >75%; ++, > 50%; +, >25%. β -Gal activity was determined from the time taken for colonies to turn blue in X-gal filter lift assays performed at room temperature: +++, < 2h; ++, < 3h; +, < 4h; -, no significant activity. H6, sixth transmembrane domain

A



B

		<u>HIS3</u>	<u>β-Gal</u>
 630	Kv4.2C1 (395-630)	+++	+++
 621	Kv4.2C2 (395-621)	+++	+++
 615	Kv4.2C3 (395-615)	+++	+++
 612	Kv4.2C3.01 (395-612)	+++	+++
 610	Kv4.2C3.02 (395-610)	+++	+++
 608	Kv4.2C3.03 (395-608)	+++	+++
 606	Kv4.2C3.04 (395-606)	+++	+++
 604	Kv4.2C3.05 (395-604)	+++	+++
 600	Kv4.2C3.1 (395-600)	++	-
 585	Kv4.2C3.2 (395-585)	++	-
 570	Kv4.2C3.3 (395-570)	++	-
 555	Kv4.2C3.4 (395-555)	++	-
 539	Kv4.2C4 (395-539)	++	-
 531	Kv4.2C5 (395-531)	+	-
 500	Kv4.2C6 (395-500)	+	-
 450	Kv4.2C7 (395-450)	+	-
 ATAA 630	Kv4.2C1 P601/603/604A	++	-
 475 636	Kv4.3C (475-636)	+++	+++
 1165	HERGC (864-1165)	+	-

However, deletion of the next four aa (601-604) completely abolished the interaction suggesting that these aa (PTPP), are critical for Kv4.2 interaction with filamin.

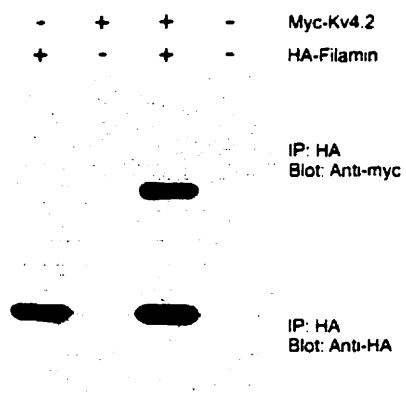
We next generated point mutations of the putative Kv4.2-interaction domain using the entire C-terminal Kv4.2 bait fragment (Kv4.2C1). Substitution of the prolines in the 601-604 aa region to alanines (PTPP→ATAA) completely abolished the interaction (Figure 1B). These observations indicate that this proline-rich region is a critical domain for interaction with filamin. This sequence was noted to be identical in Kv4.3, consistent with it representing a site of interaction with both members of the Kv4 family. Subsequently, using yeast two-hybrid analysis, we found that filamin also interacts with Kv4.3 (Figure 1B).

Association of Kv4.2 and Filamin In Situ and In Vitro

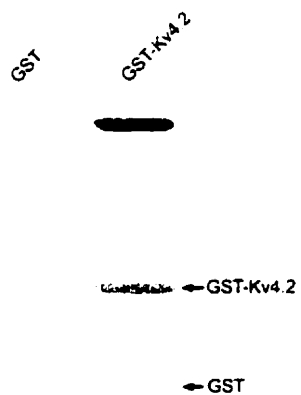
To further investigate the interaction of Kv4.2 and filamin, we tested whether these proteins form a complex in transfected heterologous cells. COS7 cells, transfected either singly or doubly with HA epitope-tagged filamin (HA-filamin) and myc-tagged Kv4.2 (myc-Kv4.2), were solubilized and immunoprecipitated with an anti-HA antibody. The immunoprecipitates were resolved by SDS-PAGE and immunoblotted with anti-HA and anti-myc antibodies. As shown in Figure 2A, myc-Kv4.2 was coimmunoprecipitated with HA-filamin from cells cotransfected with myc-Kv4.2 and HA-filamin, indicating a Kv4.2/filamin association. In contrast, when cells were singly transfected with HA-filamin or myc-Kv4.2, myc-Kv4.2 was not detected in the immunoprecipitates isolated with the anti-HA antibody indicating the specificity of the coimmunoprecipitation. In

Figure 2. Coimmunoprecipitation in COS7 cells and Direct Binding of Kv4.2 and Filamin. (A) Extracts from COS7 cells transfected singly or doubly with myc-Kv4.2 and HA-filamin were immunoprecipitated with anti-HA antibodies. The immunoprecipitates were immunoblotted with anti-myc (upper panel) and anti-HA antibodies (lower panel). (B) Filter overlay assay showing direct in vitro binding of [³⁵S]filamin to Kv4.2. Glutathione-S-transferase (GST) and GST-Kv4.2 (aa 417-630) fusion proteins were prepared as crude bacterial lysates and purified with glutathione-Sepharose beads. Five µg of protein was resolved by SDS-PAGE and transferred to a PVDF membrane. Upper Panel: Renatured membrane overlayed with [³⁵S]filamin showing specific binding to GST-Kv4.2. Lower Panel: Ponceau S stained membrane showing the position and similar abundance of proteins in each lane.

A



B



these experiments we were unable to coimmunoprecipitate HA-filamin using the anti-myc antibody as the immunoprecipitating antibody. The reasons for this are unclear.

Direct interaction of Kv4.2 and filamin was tested in a filter overlay assay using a GST-Kv4.2 bacterial fusion protein and in vitro translated [³⁵S]filamin. A purified GST-Kv4.2 (aa 471-630) fusion protein and GST alone were separated by SDS-PAGE and transferred to a polyvinylidene difluoride (PVDF) membrane. The proteins were renatured on the membrane and probed with in vitro translated [³⁵S]filamin. Filamin bound to the GST-Kv4.2 fusion protein but did not bind GST alone (Figure 2B, upper panel). Moreover, when the overlay assay was performed on non-renatured membranes, the interaction was abolished indicating that Kv4.2 must be in a native conformation for association with filamin. Taken together, these data show that Kv4.2 and filamin form a complex in heterologous cells and that they directly interact in an in vitro assay.

Filamin Binds and Localizes Kv4.2 to Membrane Ruffles in Heterologous Cells

To examine if filamin colocalizes with Kv4.2 in heterologous cells, we transfected HA-filamin and myc-Kv4.2 into COS7 cells and analyzed their distribution immunocytochemically. Our results, consistent with previous reports (Schwarzman et al., 1999; Ohta et al., 1999), show that filamin localizes to membrane ruffles in transfected cells (Figure 3B). Kv4.2 exhibits a general nonuniform cell surface distribution with a striking accumulation at membrane ruffles where it colocalizes with filamin (Figure 3A-C). In order to examine the specificity of this colocalization and to determine the functional significance of the interaction, a myc-Kv4.2 deletion construct (Kv4.2/600) in which the last 30 aa including

Figure 3. Colocalization and Accumulation of Kv4.2 and Filamin at Membrane Ruffles in Transfected COS7 cells. COS7 cells were doubly transfected with myc-Kv4.2 and HA-filamin (A-C), myc-Kv4.2/600 and HA-filamin (D-F) or myc-Kv4.2/ATAA and HA-filamin (H-I). Cells were double immunolabeled using anti-myc (Cy3; A, D, and G) and anti-HA (Oregon Green; B, E, and H) antibodies. (A-C) Kv4.2 exhibits a nonuniform cell surface distribution with a striking accumulation at filamin-rich membrane ruffles. (D-F) Deletion of the C-terminal 30 aa of Kv4.2, including the filamin binding site (Kv4.2/600), and (G-I) substitution of the prolines with alanines within the filamin binding site of Kv4.2 (Kv4.2/ATAA) results in a nonuniform cell surface distribution of Kv4.2 with a marked absence at the filamin-rich membrane ruffles. Arrows indicate membrane ruffles.



the PTPP binding site had been removed, was also cotransfected with filamin. Figure 3D-F show that Kv4.2 no longer accumulates nor colocalizes with filamin at membrane ruffles even though it is abundantly expressed on the cell surface. Similarly, a myc-Kv4.2 construct in which the PTPP binding motif has been substituted with ATAA (Kv4.2/ATAA), was cotransfected in COS7 cells with filamin. Similar to the Kv4.2/600, Kv4.2/ATAA also failed to accumulate or colocalize with filamin at membrane ruffles even though it was abundantly expressed on the cell surface (Figure 3G-H). These data demonstrate that Kv4.2 colocalizes with filamin in heterologous cells and that the accumulation of Kv4.2 at cellular specializations is dependent upon their interaction.

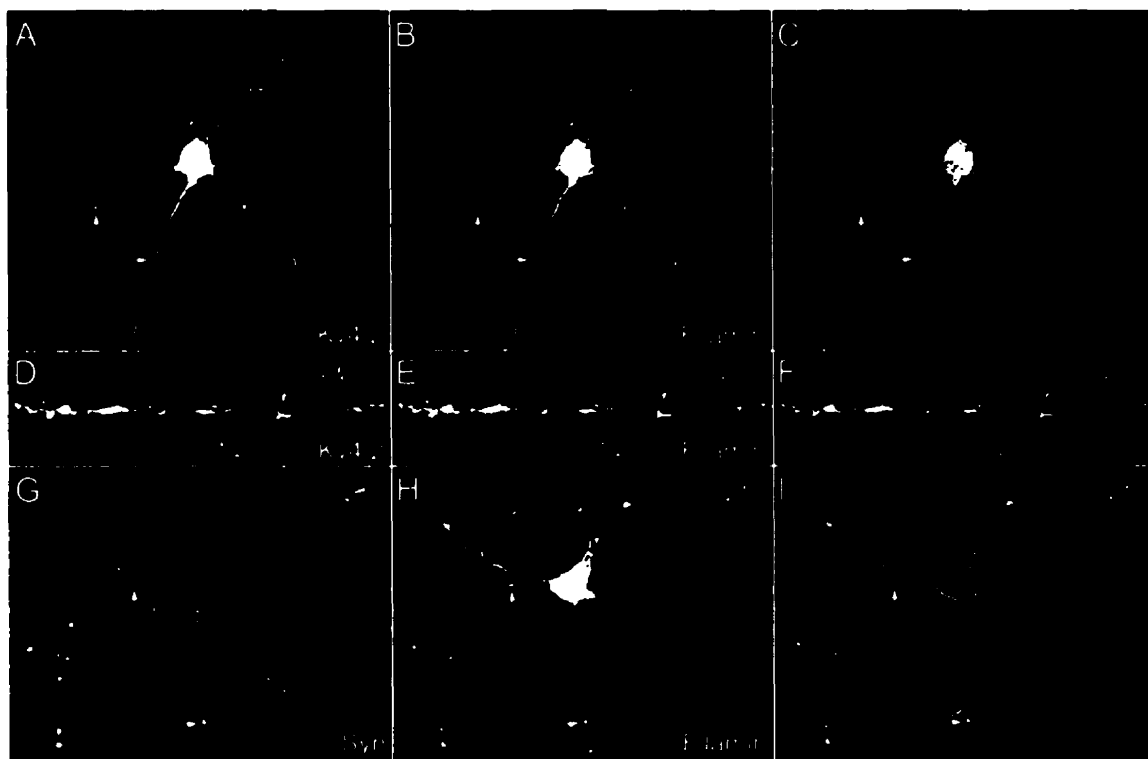
Kv4.2 Colocalizes with Filamin at Synapses

The experiments described above indicate that filamin localizes Kv4.2 to cellular specializations. Are filamin and Kv4.2 also colocalized at neuronal specializations? This question was addressed by cotransfecting cultured hippocampal neurons with HA-filamin and myc-Kv4.2. As shown in figure 4A-F, Kv4.2 and filamin display an overlapping distribution exhibiting a punctate staining pattern along dendrites of neurons. This punctate filamin localization matches closely that of the presynaptic marker synaptophysin (Figure 4G-I), indicating the specific concentration of filamin at synapses. Thus, at the light microscope level, filamin colocalizes with Kv4.2 at neuronal synapses.

Kv4.2 and Filamin Colocalize in Brain

Kv4.2 immunoreactivity is present at high levels in the granule cell layer of the cerebellar cortex exhibiting a somatodendritic localization (Sheng et al., 1992). As such, we used

Figure 4. Colocalization of Kv4.2 and Filamin at Synapses in Cultured Hippocampal Neurons. Cultured hippocampal neurons were doubly transfected with myc-Kv4.2 and HA-filamin. (A-C) Double immunolabeling of Kv4.2 and filamin using anti-myc (Cy3) and anti-HA (Oregon Green) antibodies shows that Kv4.2 and filamin colocalize in a punctate pattern along dendrites. Arrows indicate colocalization at the tips of dendritic spines. (D-F) High magnification imaging revealing the extent of Kv4.2 and filamin colocalization. (G-I) Double immunolabeling of filamin and synaptophysin using anti-synaptophysin (Cy3) and anti-HA (Oregon Green) antibodies reveals filamin localization to synapses, as determined by colocalization with the synaptic marker. Arrows indicate localization at the tips of dendritic spines.



high-resolution confocal imaging to determine if Kv4.2 and filamin colocalize in cerebellar sections using a previously characterized anti-Kv4.2 antibody (Barry et al., 1995). Figure 5A shows Kv4.2 is abundantly expressed in the cerebellar granule cell layer, consistent with Sheng et al. (1992), and that there is a striking overlap between Kv4.2 and filamin immunoreactivity in this cell layer. In order to determine if this colocalization represents a synaptic localization, we determined if Kv4.2 immunoreactivity correlated with that of the synaptic marker synaptophysin. Figure 5B shows that the Kv4.2 expression pattern highly correlates with that of synaptophysin. Thus, at the light microscope level, these data show that Kv4.2 and filamin are colocalized and concentrated at synaptic sites in the granule cell layer of the cerebellum, consistent with direct association of these proteins in vivo.

Association of Kv4.2 and Filamin In Vivo

To determine whether Kv4.2 and filamin interact in vivo, we performed coimmunoprecipitation experiments from rat cerebellum. Membrane fractions from rat cerebellar homogenates were solubilized and the supernatant was immunoprecipitated with two distinct anti-filamin antibodies. The immunoprecipitates were then resolved by SDS-PAGE, transferred to a PVDF membrane, and immunoblotted with the same anti-Kv4.2 antibody used in the immunohistochemical experiments performed on cerebellar sections (Figure 6). A band at ~ 74 KDa is seen upon anti-Kv4.2 immunoblotting indicating that Kv4.2 coimmunoprecipitates with filamin using either of the filamin antibodies as the immunoprecipitating antibodies. Kv4.2 was not precipitated when control IgG was used as the precipitating antibody, indicating the specificity of the

Figure 5. Colocalization of Kv4.2 and Filamin at Synapses in Cerebellum. Fresh-frozen 20 μm thick section of adult rat cerebellum were cryosectioned and double immunolabeled with (A), anti-Kv4.2 (Cy3) and anti-filamin (Oregon Green) antibodies and (B), anti-Kv4.2 (Cy3) and anti-synaptophysin (Oregon Green) antibodies. (A) Low magnification (left) and high magnification (right) images show that Kv4.2 and filamin colocalize in the cerebellar granule cell layer. (B) Low and high magnification images (inset in upper left panel indicates the region from which high magnification images were obtained) show that the Kv4.2 and synaptophysin distribution patterns overlap indicating that Kv4.2 is localized to synapses. G, granule cell layer; M, molecular layer; W, white matter. Bars: A = 50 μm , B= 100 μm .

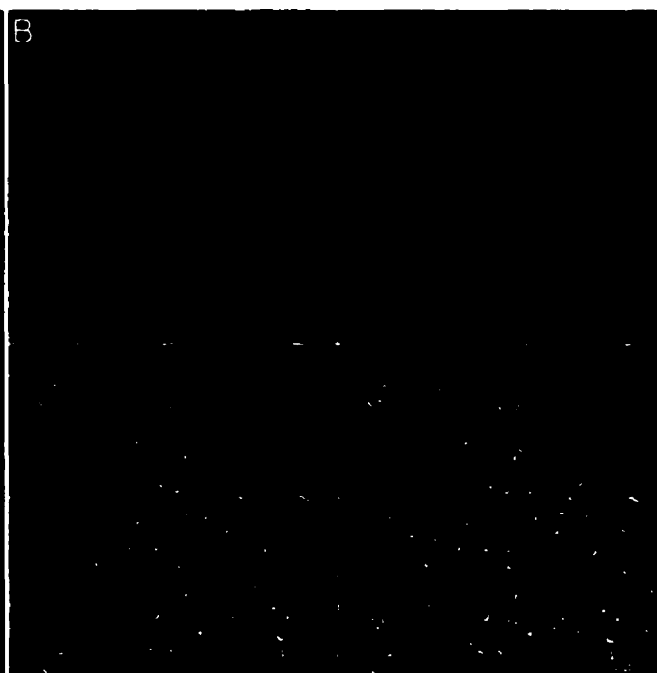
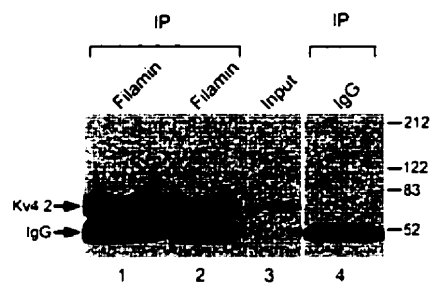


Figure 6. Biochemical Association of Kv4.2 and Filamin in Rat Brain.

Coimmunoprecipitation of Kv4.2 and filamin from cerebellum. Membrane fractions of cerebellar homogenate were solubilized and immunoprecipitated as indicated. The immunoblot shows that two different anti-filamin antibodies (lanes: 1, Sigma; 2, Serotec) specifically precipitate Kv4.2 as visualized by blotting with an anti-Kv4.2 antibody. Immunoprecipitation with control IgG (lanes 4) does not pull down Kv4.2 demonstrating the specificity of the immunoprecipitation. Input lane was loaded with 5% of the extract used for immunoprecipitation (lane 3).



coimmunoprecipitation. Moreover, competition of the anti-Kv4.2 antibody with the immunogenic peptide completely blocked the labeling of Kv4.2 band (data not shown). These data demonstrate that Kv4.2 forms a complex with filamin in brain.

Discussion

Here, we report a novel protein-protein interaction between Kv4.2 and filamin, a member of the α -actinin/spectrin/dystrophin family of actin-binding proteins. We have defined a PTPP motif in the C terminus (aa 601-604) of Kv4.2 that is required for filamin interaction. Deletion or mutation of this motif abolishes the interaction as determined by the yeast two-hybrid assay. We also show that Kv4.3, which contains the identical C-terminal tail PTPP motif, also interacts with filamin in the yeast two-hybrid assay. In addition, we demonstrate that Kv4.2 and filamin directly interact in an in vitro assay and can be coimmunoprecipitated from heterologous cells and rat brain extracts. Furthermore, Kv4.2 and filamin colocalize at cellular specializations; membrane in heterologous cells. Deletion or mutation of the Kv4.2 binding motif abolishes this colocalization indicating that filamin plays a role in Kv4.2 localization. Importantly, we show that Kv4.2 and filamin share an overlapping synaptic expression pattern (as defined by synaptophysin colocalization) in rat cerebellum and cultured hippocampal neurons. Taken together, these findings indicate that filamin is a Kv4.2-interacting cytoskeletal protein that colocalizes with Kv4.2 at neuronal synapses and plays an important role in the localization of Kv4.2 in heterologous cells.

What Determines Filamin Localization?

The data presented in this study and others indicate that filamin exhibits a restricted distribution within the cell, localized primarily at cellular specializations, eg., membrane ruffles (Burrige and Chrzanowska-Wodnicka, 1996; Schwarzman et al., 1999; Ohta et al., 1999). This restricted localization may be owing to its interaction with the adhesion

molecule integrin, a constituent protein of cellular specializations (BurrIDGE and Chrzanowska-Wodnicka, 1996). Interestingly, both integrin and filamin have been implicated as molecular components of the NMJ and $\beta 1$ integrin has been shown to play a physiologic role in the agrin-mediated signaling cascade that leads to AChR clustering (Meier and Wallace, 1998). Similarly, filamin has been implicated in stabilizing AChR clustering at the NMJ (Shadiak and Nitkin, 1991).

Integrins function exclusively as $\alpha\beta$ heterodimers, mediating adhesive interactions of cells with counter-receptors displayed by other cells or with the extracellular matrix. They also dynamically transduce information across the cell membrane bi-directionally. To date, filamin has been shown to interact with $\beta 1$, $\beta 2$ and $\beta 7$ integrin subunits through an NPXY motif in the β integrin C terminus (Sharma et al., 1995; Loo et al., 1998; Pfaff et al., 1998). Our results demonstrating a restricted localization of filamin and an accumulation of Kv4.2 at focal adhesions sites are consistent with a filamin/integrin interaction.

Does integrin determine filamin localization at the synapse? Many studies have implicated a role for integrin at the synapse although they have not received as much attention as the cadherin family of cell adhesion molecules. $\beta 1$ integrin participates in neurite outgrowth in vivo (Galileo et al., 1992), is required for chick neuroblast migration (Neugebauer et al., 1991), and has been purified from brain synaptic membranes (Bahr and Lynch, 1992). Electron microscopic analysis reveals a concentration of $\alpha 8\beta 1$ and $\beta 8$ immunoreactivity within perikarya and dendrites with a striking concentration in the spines and PSDs providing ultrastructural evidence that integrins may participate in the formation, maintenance, or plasticity of synapses (Einheber et al., 1996; Nishimura et al.,

1998). Association of $\beta 8$ with synaptic membranes was further supported by its enrichment in synaptosomal preparations as detected by immunoblotting (Nishimura et al., 1998).

Recently, a novel α -integrin termed *Volado* was identified in *Drosophila*. Reduced expression of the *Volado* integrin produces an impairment in memory that is reversible, indicative of a dynamic event (Grotewiel et al., 1998). These results, demonstrating a role for integrins in behavioral plasticity, fit well with studies showing integrin-dependent modulation of synaptic plasticity, eg peptide inhibitors of integrin binding have no effect on the formation of long-term potentiation but block the maintenance of LTP (Staubli et al., 1990; Bahr et al., 1997). Furthermore, the cytoplasmic tail of β integrin, responsible for its subcellular localization, has been shown to interact with another member of the spectrin/dystrophin family, α -actinin. Interestingly, α -actinin2 binds and colocalizes with the NMDA receptors at dendritic spines (Wyszynski et al., 1997). Thus, the localization of filamin at cellular specializations such as focal adhesion sites and synapses may be owing to its interaction with integrin.

Role of Filamin at the Synapse?

This study demonstrates that filamin colocalizes and interacts with Kv4.2 at synapses. Using the yeast two-hybrid assay we mapped the filamin interaction site on Kv4.2 to a proline-rich region (PTPP) at aa 601-604. This PTPP motif constitutes a consensus SH3-binding module (Pawson and Scott, 1997); however, no SH3 domains were found within filamin. Alternatively, the dependence of binding on prolines suggests a role for these aa

in establishing the appropriate secondary structure required for Kv4.2-filamin interaction. A similar proposal has been made for the interaction between group 1 metabotropic glutamate receptors and Homer proteins (Tu et al., 1998).

The postsynaptic localization of Kv4.2 is consistent with the involvement of this fast-transient K^+ channel in regulating the excitability of the postsynaptic membrane and thus the reception and integration of synaptic signals (Sheng et al., 1992; Alonso and Widmer, 1997). What is the importance of positioning this K^+ channel in such a restricted manner? The answer may lie not within the ion channel but the complex it is associated with. Modulatory enzymes precisely localized to the subsynaptic membrane could provide a rapid activity-dependent mechanism for the regulation of channel kinetics and thus postsynaptic excitability. In fact, a role for PKC in Kv4.2 and filamin modulation has been established (Nakamura et al., 1997; Glogauer et al., 1998). Interestingly, PKC has been shown to bind β integrin (Ng et al., 1999), while the interaction of β integrin with filamin has been clearly established (Sharma et al., 1995; Loo et al., 1998; Pfaff et al., 1998). Thus, through its interaction with Kv4.2 and β integrin, filamin may serve as a molecular scaffold to localize Kv4.2 to the postsynaptic membrane and/or mediate the assembly of a macromolecular complex linking Kv4.2 to the actin cytoskeleton and signaling molecules. A similar signaling complex has been described within which Yotiao, a scaffold protein that directly links the NMDA receptor with type I protein phosphatase and cAMP-dependent protein kinase, facilitates the regulation of channel activity (Westpal et al., 1999).

The ability of filamin to localize Kv4.2, through a C-terminal tail interaction, to cellular specializations in heterologous cells identifies it as a candidate protein involved

in Kv4.2 localization at the synapse. The importance of the Kv4.2 C-terminal tail in determining subcellular localization is not unique to this K⁺ channel. Using MDCK cells as a model for polarized cells, Scannevin et al. (1996) showed that a 130 aa domain within the C terminus of the Kv2.1 delayed rectifier K⁺ channel is essential for the proper subcellular localization of this channel. Further characterization of the Kv4.2/filamin interaction in neurons will be required to address the role of filamin in Kv4.2 localization at the neuronal synapse.

Materials and Methods

Yeast Two-Hybrid Screen and Analysis of Kv4.2-Filamin Interaction

Yeast two-hybrid screens were performed using the Y190 yeast strain harboring the reporter genes HIS3 and β -galactosidase (β -gal) under the control of upstream Gal4-binding sites (Clontech Laboratories, Palo Alto, Ca). The Kv4.2C1 bait was generated by incorporating unique Nco I and Xma I restriction sites, 5' and 3' respectively, using the polymerase chain reaction PCR and fused to the Gal4 DNA-binding domain in vector pAS2-1. This bait, pAS2-1/Kv4.2C1, was used to screen $\sim 3 \times 10^6$ clones from a human heart cDNA library constructed in the GAL4-activation domain vector pACT-2 (Clontech). Deletion variants of pAS2-1/Kv4.2C1 were constructed by PCR using specific primers and subcloned into pAS2-1 for yeast two-hybrid interactions. Mutations of pAS2-1/Kv4.2C1 were generated using QuikChange (Stratagene). The Kv4.3C bait was generated in a manner similar to Kv4.2C1. The HERGC bait was generated by incorporating unique Nco I and BamHI restriction sites, 5' and 3' respectively, by PCR and fused to the Gal4 DNA-binding domain in vector pAS2-1.

Expression Constructs

The GST-Kv4.2(aa 471-630) fusion construct was generated by digesting pAS2-1/Kv4.2C1 with BamHI and Sma I (aa 471-630) and subcloning it into pGEX-2T (Pharmacia). pCMV/myc-Kv4.2 was generated by subcloning full-length Kv4.2 into pCMV-myc (Stratagene). pSG-5/HA-filamin (filaminC, aa 2172-2705) was generated by subcloning the original pACT-2 library clone, containing a 5' HA epitope, into pSG-5 (Stratagene). pCMV/myc-Kv4.2/600 was constructed by PCR using specific primers and subcloned into pCMV-myc. pCMV/myc-Kv4.2/ATAA mutations was generated using

QuikChange (Stratagene).

Transfection and Immunocytochemistry in Heterologous Cells

COS7 cells were transfected with Lipofectamine (Gibco-BRL) on polylysine coated coverslips (for immunocytochemistry) or in 100 mm tissue culture dishes (for immunoprecipitation experiments). Cells were fixed, permeabilized, and immunolabeled 42h post-transfection as described (Petrecca et al., 1999). Rabbit anti-HA (Babco) was diluted 1:500 and mouse anti-myc (Santa Cruz) was used at a concentration of 2 µg/ml. Oregon Green-conjugated goat anti-rabbit (Molecular Probes) and Cy3-conjugated goat anti-mouse (Jackson ImmunoResearch) secondary antibodies were both used at a dilution of 1:100. Immunofluorescence was visualized with a BioRad MicroRadiance confocal microscope at an optical thickness of ~ 7 µm. Digital images were prepared using Adobe Photoshop.

Coimmunoprecipitations

For immunoprecipitation from COS7 cells extracts, cells plated on 100 mm dishes were washed in ice-cold phosphate-buffered saline (PBS) followed by solubilization in 1ml of ice-cold extraction buffer [50 mM Tris (pH 7.4), 150 mM NaCl, 1mM EDTA, 1% Nonidet P-40, 0.5% deoxycholate and 0.1% SDS supplemented with 1mM phenylmethylsulfonyl fluoride (PMSF) and 10 µg/ml each of pepstatin, aprotonin and leupeptin. The extraction was allowed to proceed with shaking for 3 h at 4°C. Insoluble material was pelleted by centrifugation at 60 000 g for 30 min and the supernatents were used for coimmunoprecipitation. Rabbit anti-HA antibody (1:200) was added to the 100

μl of detergent extract and was incubated with inversion for 2h at 4°C. Equilibrated protein A-Sepharose beads (Pharmacia) were added for a further 2h with inversion and then pelleted by centrifugation. Eluted proteins were resolved by SDS-PAGE, transferred to a PVDF membrane and visualized by immunoblotting with mouse anti-myc (1 μg/ml) and mouse anti-HA (1:500) antibodies followed by horseradish peroxidase conjugated goat anti-mouse antibody (1:5000, Jackson ImmunoResearch). Enhanced chemiluminescence was performed using ECL⁺ detection kit (Amersham). Cerebellar membrane preparations and solubilization were carried out according to Luo et al. (1997). Briefly, adult rat cerebellum from Sprague-Dawley rats was homogenized in ice-cold 10 mM Tris-HCl (pH 7.4) containing 320 mM sucrose, 1mM PMSF and 10 μg/ml each of pepstatin, aprotonin and leupeptin. The tissue homogenate was centrifuged at 700 g for 10 min at 4°C. The pellet was rehomogenized and centrifuged at 700 g and the supernatants were combined and centrifuged at 37 000 g for 40 min at 4°C. This pellet (P2) was resuspended in 10 mM Tris-HCl (pH 7.4) supplemented with protease inhibitors. Protein concentrations were determined using the Bradford assay. 400 μg of protein was then solubilized by the addition of 0.1 volumes of 10% sodium deoxycholate in 500 mM Tris-HCl (pH 9.0) and incubated for 30 min at 36°C. A 0.10 volume of 1% TritonX-100/50 mM Tris-HCl (pH 9.0) was then added and the preparation was dialyzed overnight at 4°C followed by centrifugation for 10 min at 100 000 g. The supernatant was then used for coimmunoprecipitation. Anti-filamin antibodies (Sigma, 1:50 ; Serotec, 1:20) were added to the clarified supernatant of the solubilized P2 fraction and were mixed by inversion for 2 h at 4°C. Equilibrated protein A-Sepharose beads were added and mixed by inversion for a further 2 h at 4°C. Eluted proteins were resolved by SDS-

PAGE, transferred to a PVDF membrane, and visualized by immunoblotting with an anti-Kv4.2 antibody generated against Kv4.2 residues 29-38: APPRQERKRT (1:400; Barry et al., 1995) followed by horseradish peroxidase conjugated secondary antibody (1:5000, Jackson ImmunoResearch). Enhanced chemiluminescence was performed using ECL⁺ detection kit (Amersham). For antibody controls, immunoprecipitations were performed using control IgG and the Kv4.2 antibody was blocked by preincubating with the immunogenic peptide (100 µg/ml).

Filter Overlay Assay

GST and GST-Kv4.2 (aa 471-630) fusion proteins, prepared from bacterial lysates, were purified using glutathione-Sepharose beads (Pharmacia). GST and GST-Kv4.2 were released from the beads and ~ 3 µg of each fusion protein was electrophoresed. The resolved proteins were transferred to a PVDF membrane and the denatured filter-bound proteins were renatured according to Wyszynski et al. (1999). Briefly, membranes were incubated in buffer A (10 mM HEPES, 60 mM KCl, 1mM EDTA, and 1 mM 2-mercaptoethanol) containing 6 M guanidine hydrochloride for 10 min at 4°C. Incubations were repeated for 10 min at 4°C using decreasing concentrations of guanidine hydrochloride (3, 1.5, 0.75, 0.38, 0.19, 0.1, and 0 M). pSG-5/filaminC (aa 2172-2705) was in vitro translated (Promega) in the presence of ³⁵S and used for the binding assay. The membrane was incubated with 10 µl of [³⁵S]filamin overnight at 4°C. The next day the membrane was brought to room temp., washed and submitted to autoradiography.

Neuron Culture, Transfection and Immunocytochemistry

Low density hippocampal neuronal cultures were prepared from hippocampi dissected from 3 day old Sprague-Dawley rats and stored in an oxygenated solution. The hippocampi were then exposed to an oxygenated papain solution for ~1 h, dissociated, spun through BSA, resuspended in growth medium (Neurobasal medium supplemented with B-27 (Gibco)) and plated on modified 35 mm culture dishes coated with poly-D-lysine and laminin. Transfections of HA-filaminC (aa 2172-2705) and myc-Kv4.2 were performed at 3 days in vitro using the calcium phosphate method as described (Xia et al., 1996). Ten days after transfection the neurons were fixed in methanol for 15 min at -20°C , blocked in 0.5% BSA for 30 min at room temp and were immunolabeled as described above. Synaptophysin SVP38 monoclonal (Sigma) was used at a dilution of 1:500. Immunofluorescence was visualized with a BioRad MicroRadiance confocal microscope at an optical thickness of $\sim 7\ \mu\text{m}$. Digital images were prepared using Adobe Photoshop.

Immunohistochemistry

Fresh frozen adult rat cerebellum was cryosectioned at a thickness of $20\ \mu\text{m}$ and thaw-mounted on Probe-On Plus slides (Fisher Scientific). Sections were air-dried at room temperature for 1 h and permeabilized and blocked in 0.2% Triton X100/0.5% BSA in PBS for 30 min. Sections were incubated with primary antibodies for 1 h, rinsed in PBS followed by incubation with secondary antibodies for 1h. Antibodies were used at the following dilutions: Kv4.2. 1:100; filamin (Sigma), 1:200; synaptophysin, 1:500. Immunofluorescence was visualized with a BioRad MicroRadiance confocal microscope at an optical thickness of $\sim 4\ \mu\text{m}$. Digital images were prepared using Adobe Photoshop.

CHAPTER 5

DISCUSSION

N-linked Glycosylation is Required for HERG Surface Membrane Expression

The experiments presented in chapter two demonstrate that N-linked glycosylation of HERG plays a crucial role in its cell surface membrane expression based on the following lines of evidence. First, treatment of HEK293 cells stably expressing HERG with tunicamycin, an N-linked glycosylation inhibitor, results in the absence of surface membrane expression and a pronounced intracellular localization. Second, mutation of each glycosylation site, N598Q and N629Q, either singly or in combination, leads to a complete loss of N-linked glycosylation as determined by immunoblot analysis. All three N-linked glycosylation mutant channels stably expressed in HEK293 cells failed to localize at the cell surface as determined by immunocytochemical analysis. Instead, they exhibited an intracellular localization, similar to that seen upon tunicamycin treatment. Lastly, electrophysiological analysis of all three mutant channels stably expressed in HEK293 cells failed to generate a current, indicative of a loss of surface membrane expression.

The most likely explanation of these findings is that N-linked oligosaccharides are required for the proper folding of HERG, and that in their absence, defective HERG processing occurs. N-linked oligosaccharides, upon addition to proteins, aid in the folding process by interacting with the ER-resident chaperone calnexin. This association retains the misfolded protein in the ER giving it an opportunity to fold properly, most likely in association with other ER-resident chaperones. The absence of oligosaccharides prevents such an interaction and leads to the rapid degradation of the misfolded protein. Along the same line, oligosaccharides may also play a role in HERG subunit coassembly. This is based on the observation that in the immunoblotting experiments of the N-linked

glycosylation mutant channels, an ~70kDa band can be observed at a greater intensity than seen for the wild-type channel. This band could represent unassembled subunits within the ER. The absence of oligosaccharides could alter their conformation such that they can no longer coassemble with the same efficiency as the native subunits.

Taken together, these results suggest that the absence of N-linked glycosylation results in protein misfolding and potentially a decrease in the efficiency of subunit assembly. The overall result is an intracellular retention of the protein and a loss of surface membrane expression.

Upon completion of this study, three groups have provided evidence to further support the role of N-linked glycosylation in HERG channel processing and surface membrane expression. Yoshida et al. (1999) reported their study of a 26 year-old patient who was admitted because of recurrent syncopal episodes that had started at the age of 15. A hyperventilation test during electrocardiographic recording provoked a torsade des pointes ventricular arrhythmia showing a markedly prolonged QT interval. Genomic DNA analysis was used to screen for mutations in *SCN5A*, *KVLQT1* and *HERG*. The results revealed that there were no mutations in either *SCN5A* or *KVLQT1*. A single point mutation was found in *HERG* that converted the asparagine at position 629, a N-linked glycosylation site, to lysine (N629K). Expression of these mutant channels in COS cells revealed that they were unable to generate a current. Moreover, coexpression of the wild-type and mutant channels revealed a HERG current density that was 9.2% of the wild-type channel, demonstrating a dominant negative effect. Thus, mutation of one N-linked glycosylation site leads to an absence of current generated by the mutant channel. The subcellular localization of this channel was not determined.

In the second study, Furantini et al. (1999) characterized a novel missense mutations, G601S, found in a HERG-associated LQT sufferer. Electrophysiological analysis revealed that the current density was only 15% that of the wild-type channel and immunocytochemical analysis revealed that the majority of the protein was retained in the ER. Importantly, immunoblot analysis revealed that the channel was incompletely glycosylated.

Lastly, Zhou et al. (1999) reinvestigated the N470D mutation. The effects of this mutation on channel function had been previously reported by Sanguinetti et al. (1996) who showed that when this mutant channel was expressed in *Xenopus* oocytes at room temperature a current was generated with an amplitude that was 30% that of the wild-type channel. When Zhou et al. (1999) expressed this mutant channel in HEK293 cells at 37°C they found that almost no HERG current was generated. When the cells were cooled to 24°C, however, the HERG current amplitude was greatly increased, 43 ± 8 pA for cells at cultured at 37°C as compared to 375 ± 66 pA for cells cultured at 24°C. Moreover, immunoblot analysis revealed that the mutant channel was fully glycosylated only when it was expressed in cells cultured at 24°C indicating that at 37°C the mutant channel had taken on a conformation within the ER that hindered the accessibility of the oligosaccharyl-transferase. The cooling process allowed the mutant channel to fold in a manner that no longer hindered this accessibility of this enzyme. The observation that mutations that disrupt protein folding can be temperature sensitive is not novel. The folding defect of the F508 CFTR protein is also temperature dependent. Lowering the temperature, to 30°C or less, of cells expressing the F508 CFTR protein causes a portion of the mutant protein to move to the plasma membrane (Brown et al., 1997).

Localization of NHE1 and the Identification of a Cytoskeletal Anchoring Protein

The findings presented in chapter three clearly demonstrate that NHE1 is predominantly localized at the intercalated disc of cardiomyocytes. The possible functional relevance of this localization was described within the discussion section of that chapter. The fact that such a restricted distribution for NHE1 exists suggests that associated proteins may be involved in either the targeting or the anchoring of NHE1 at the intercalated disc. Using the same rationale as described for identifying a Kv4.2 interacting protein, I generated a bait construct that encompassed the entire C-terminus of NHE1 and screened a human heart cDNA library. After screening $\sim 6 \times 10^6$ library clones, no positive clones were identified. A possible explanation for this negative result is that since the length of this bait construct is considerable, 352 amino acids, it may be taking on a conformation within the yeast nucleus that is hindering the accessibility of an interaction site. As such, I constructed five fragmented baits that together encompassed the entire C-terminus. Upon screening another $\sim 10 \times 10^6$ library clones in total, one positive clone was identified with a bait that included the last 132 amino acids (688-820). The clone identified encoded the C-terminal 48 amino acids of a novel protein with homology to the cytoskeletal protein talin, temporarily named NHE1-binding protein (NHE1BP1).

Two pieces of data make this finding interesting. First, NHE1 has been shown to colocalize with talin at focal adhesion sites in adherent fibroblast (Grinstein et al., 1993). Second, a deletion construct of NHE1 lacking the residues 566-635 was also able to localize to focal adhesion sites. Taken together, these data indicate that regions other than the central region of the C-terminus are responsible for NHE1 localization and that localization to cellular specializations may be dependent upon protein interactions with

the distal C-terminus. The fact that NHE1BP interacted with the a bait protein that was distal to amino acid 635 lends further support the notion that such a protein may be involved in the targeting or anchoring of the exchanger at cellular specializations.

To date, no cytoskeletal anchoring proteins have been reported to associate with NHE1. On the other hand, two protein associations with the C-terminal tail of the exchanger that exert regulatory effects have been identified. Lin et al. (1996) showed that a calcineurin B homologous protein (CHP) binds to NHE1 at a region within the C-terminal tail between amino acids 567 and 637. CHP binding to NHE1 was shown to inhibit exchanger activity in a phosphorylation-dependent manner. The region distal to the CHP binding site, 636-684, contains two domains capable of binding calmodulin. Binding of calmodulin is thought to play a role in transport regulation of the exchanger (Bertrand et al., 1994).

Implications of the Kv4.2/Filamin Interaction

The findings presented in chapter four of this thesis identify filamin as a Kv4.2 cytoskeletal associated protein. At least two functional implications of the Kv4.2/filamin interaction can be envisioned. First, and most obviously, is a role for filamin in the subcellular localization of Kv4.2. The data presented in chapter four demonstrate that filamin plays a direct role in the subcellular localization of Kv4.2 at cellular specialization in COS cells. Mutation or truncation of the region responsible for Kv4.2/filamin binding abolishes this localization. Similarly, these two proteins colocalize at synaptic sites in cerebellum and cultured hippocampal neurons. Furthermore, I have

found that these proteins colocalize at intercalated discs in cardiomyocytes (unpublished observations).

To determine if filamin plays a role in the subcellular localization of Kv4.2 *in vivo*, more direct experiments need be performed. Such experiments, however, are not without difficulty. The subcellular localization of filamin most likely involves its association with the integrin family of cell adhesion molecules. A culture system model for determining localization would most likely not be sufficient as the process of culturing neurons leads to a reorganization of the cytoskeletal architecture and may thus promote integrin, and thus filamin, mislocalization. Although, the results presented in chapter four reveal that filamin does localize at synaptic site, nonsynaptic localization of filamin is also observed. In contrast, filamin localization in cerebellar sections revealed an almost exclusive localization at synaptic sites. Instead, a more appropriate system would be one similar to that used by Arnold et al. (1999). This technique involves gene transfer, using biolistic techniques, to study the effects of various Kv4.2 mutations and truncations on its subcellular localization. By using thick brains slices, one can keep the transfected neurons in their native environment. Kv4.2 subcellular localization can then be determined using confocal microscopy.

Another related question is what is the functional implication of Kv4.2 clustering. This question is presently being addressed using electrophysiological analysis. In order to do so I have obtained a well-characterized filamin deficient melanoma cell line, M2, and its filamin repleted counterpart A7. The experimental plan is to transfect wild-type Kv4.2 cDNA into each of these cell lines in order to determine if the Kv4.2/filamin interaction results in a change in the current generated by Kv4.2. The initial preliminary

electrophysiological characterization of these cell lines revealed a promising finding. The M2 filamin-deficient cell line exhibited small transient outward currents when transfected with Kv4.2. In contrast, the Kv4.2 transfected A7 filamin repleted cell line exhibited transient outward currents that, upon initial observations, are three to four fold greater in amplitude than that seen in M2 transfected cells. (A. Shrier, unpublished observation). These preliminary data indicate that a Kv4.2/filamin interaction may have important effects on the current generated by this channel.

A second role for filamin in its association with Kv4.2 is that it may be acting as a scaffold protein mediating the assembly of a macromolecular signaling complex. A couple of important protein-protein interactions need be described in order to appreciate such a proposal. Filamin directly interacts with certain β -integrin subunits (Sharma et al., 1995; Loo et al., 1998; Pfaff et al., 1998). Beta-integrins also directly bind PKC (Ng et al., 1999). Moreover, filamin is directly phosphorylated by PKC (Glogauer et al., 1998). Taken together with the fact that Kv4.2 phosphorylation is also mediated by PKC leads one to speculate that filamin may be acting as the centerpiece in the organization of this signaling complex.

References

Abbott, G.W., Sesti, F., Splawski, I., Buck, M.E., Lehmann, M.H., Timothy, K.W., Keating, M.T., Goldstein, S.A. (1999). MiRP1 forms I_{Kr} potassium channels with HERG and is associated with cardiac arrhythmia. *Cell* 97, 175-187.

Ackerman, M.J., and Clapham, D.E. (1997). Ion channels – basic science and clinical disease. *N. Engl. J. Med.* 336, 1575-1600.

Akimoto, K., Furutani, M., Kasanuki, H., Imamura, S.-I., Furutani, Y., Takao, A., Monma, K., and Matsuoka, R. (1996). Coexistence of missense mutation of HERG and mitochondrial DNA in Japanese long QT family. *Circulation* 94, I-164.

Alberts, B., Bray, D., Lewis, J., Raff, M., Roberts, K., and Watson, J.D. (1994). *Molecular biology of the cell*. Third edition (Garland Publishing Inc., New York)

Alonso, G., and Widmer, H. (1997). Clustering of Kv4.2 potassium channels in postsynaptic membrane of rat supraoptic neurons: an ultrastructural study. *Neurosci.* 77, 617-621.

Arnold, D.B., and Clapham, D.E. (1999). Molecular determinants for subcellular localization of PSD-95 with an interacting K^+ channel. *Neuron* 23, 149-157.

Bahr, B.A., and Lynch, G. (1992). Purification of and Arg-Gly-Asp selective matrix receptor from brain synaptic plasma membrane. *Biochem. J.* 281, 137-142.

Bahr, B.A., Staubli, U., Xiao, P., Chun, D., Ji, Z.X., Esteban, E.T., and Lynch, G. (1997). Arg-Gly-Asp-Ser-selective adhesion and the stabilization of long-term potentiation: pharmacological studies and the characterization of a candidate matrix receptor. *J. Neurosci.* 17, 1320-1329.

Barhanin, J., Lesage, F., Guillemare, E., Fink, M., Lazdunski, M., and Romey, G. (1996). KvLQT1 and IsK (min K) proteins associated to form the I_{Ks} cardiac potassium current. *Nature* 385, 78-80.

Barry, D.M., Trimmer, J.S., Merlie, J.P., and Nerbonne, J.M. (1995). Differential expression of voltage-gated K^+ channel subunits in adult rat heart. Relation to functional K^+ channels? *Circ. Res.* 77, 361-369.

Bartel, P.L., and Fields, S. (1997). The yeast two-hybrid system. Oxford University Press, New York).

Benson, D.W., MacRae, C.A., Vesely, M.R., Walsh, E.P., Seidman, J.G., Seidman, C.E., and Satler, C.A. (1996). Missense mutation in the pore region of HERG causes familial long QT syndrome. *Circulation* 93, 1791-1795.

Beyer, E.C., Kistler, J., Paul, D.L., and Goodenough, D.A. (1989). Antisera directed against connexin43 peptides react with a 43-kD protein localized to gap junctions in myocardium and other tissues. *J. Cell Biol.* 108, 595-605.

Biemesderfer, D., Reilly, R.F., Exner, M., Igarashi, P., and Aronson, P.S. (1992). Immunocytochemical characterization of Na⁺-H⁺ exchanger isoform NHE-1 in rabbit kidney. *Am. J. Physiol.* 263, F833-F840.

Blanchard, E.M., and Solaro, R.J. (1984). Inhibition of the activation and troponin calcium binding of dog cardiac myofibrils by acidic pH. *Circ. Res.* 55, 382-391.

Bonifacino, J.S., and Lippincot-Schwartz, J. (1991). Degradation of proteins within the endoplasmic reticulum. *Curr. Opin. Cell Biol.* 7, 592-600.

Buckel, A., James, E., Jacobson, L., Biewenga, J., Beeson, D., and Vincent, A. (1998). Evidence for an association between human acetylcholine receptor and rapsyn. *Ann. NY Acad. Sci.* 841, 14-16.

Bunn, R.C., Jensen, M.A., and Reed, B.C. (1999). Protein interaction with the glucose transporter binding protein (GLUT1CBP) that provide a link between GLUT1 and the cytoskeleton. *Mol. Biol. Cell.* 10, 819-832.

Burridge, K., and Chrzanowska-Wodnicka, M. (1996). Focal adhesions, contractility, and signaling. *Annu. Rev. Cell. Dev. Biol.* 12, 463-519.

Burt, J.M., and Spray, D.C. (1988). Single channel events and gating behavior of the cardiac gap junction channel. *Proc. Natl. Acad. Sci. USA* 85, 3431-3434.

Cantiello, H.F., Stow, J.L., Prat, A.G., and Ausiello, D.A. (1991). Actin filaments regulate epithelial Na⁺ channel activity. *Am. J. Physiol.* 261, C882-C888.

Caride, A.J., Filoteo, A.G., Enyedi, A., Verma, A.K., and Penniston, J.T. (1996). Detection of isoform 4 of the plasma membrane calcium pump in human tissues by using isoform-specific monoclonal antibodies. *Biochem. J.* 316, 353-359.

Carl, S.L., Felix, K., Caswell, A.H., Brandt, N.R., Ball Jr., W.J., Vaghy, P.L., Meissner, G., and Ferguson, D.G. (1995). Immunolocalization of sarcolemmal dihydropyridine receptor and sarcoplasmic reticular triadin and ryanodine receptor in rabbit ventricle and atrium. *J. Cell Biol.* 129, 673-682.

Cartaud, A., Coutant, S., Petrucci, T.C., and Cartaud, J. (1998). Evidence for *in situ* and *in vitro* association between β -dystroglycan and the subsynaptic 43K rapsyn protein. *J. Biol. Chem.* 273, 11321-11326.

Cheng, S.H., Gregory, R.J., Marshall, J., Paul, S., Souza, D.W., White, G.A., O'Riordan, C.R., and Smith, A.E. (1990). Defective Intracellular Transport and Processing of CFTR Is the Molecular Basis of Most Cystic Fibrosis. *Cell* 63, 827-834.

Coetzee, W.A., Amarillo, Y., Chiu, J., Chow, A., Lau, D., McCormack, T., Moreno, H., Nadal, M.S., Ozaita, A., Pountney, D., Saganich, M., Vega-Saenz De Miera, E., and Rudy, B. (1999). Molecular diversity of K⁺ channels. *Ann. NY Acad. Sci.* 868, 233-285.

Cohen, S.A. (1996). Immunocytochemical localization of rH1 sodium channel in adult rat heart atria and ventricle. Presence in terminal intercalated disks. *Circulation* 94, 3083-3086.

Cohen, N.A., Brenman, J.E., Snyder, S.H., and Brecht, D.S. (1996). Binding of the inward rectifier K⁺ channel Kir 2.3 and PSD-95 is regulated by protein kinase A phosphorylation. *Neuron* 17, 759-767.

Cohen, A.R., Woods, D.F., Marfatia, S.M., Walther, Z., Chishti, A.H., and Anderson, J.M. (1998). Human CASK/LIN-2 binds syndecan-2 and protein 4.1 and localizes to the basolateral membrane of epithelial cells. *J. Cell Biol.* 142, 129-138.

Colledge, M., and Froehner, S.C. (1998). To muster and cluster: anchoring neurotransmitter receptors and synapses. *Proc. Natl. Acad. Sci. USA* 95, 3341-3343.

Craven, S.E., and Brecht, D.S. (1998). PDZ proteins organize synaptic signaling pathways. *Cell* 93, 495-498.

Crompton, M., and Heid, I. (1978). The cycling of calcium, sodium, and protons across the inner membrane of cardiac mitochondria. *Eur. J. Biochem.* 91, 599-608.

Curran, M.E., Splawski, I., Timothy, K.W., Vincent, G.M., Green, E.D., and Keating, M.T. (1995). A molecular basis for cardiac arrhythmia. HERG mutations cause long QT syndrome. *Cell* 80, 795-803.

Dausse, E., Berthet, M., Denjoy, I., Andre-Fouet, X., Cruaud, C., Bennaceur, M., Faure, S., Coumel, P., Schwartz, K., and Guicheney, P. (1996). A mutation in HERG associated with notched T waves in long QT syndrome. *J. Mol. Cell. Cardiol.* 28, 1609-1615.

Deal, K.K., Lovinger, D.M., and Tamkun, M.M. (1994). The brain Kv1.1 potassium channel: in vitro and in vivo studies on subunit assembly and posttranslational processing. *J. Neurosci.* 14, 1666-1676.

Deng, W.P., and Nickoloff, J.A. (1992). Site-directed mutagenesis of virtually any plasmid by eliminating a unique site. *Anal. Biochem.* 200, 81-88.

Duff, H.J. (1995). Clinical and in vivo antiarrhythmic potential of sodium-hydrogen exchange inhibitors. *Cardiovasc.Res.* 29, 189-193.

Dobson, C.M. (1999). Protein misfolding, evolution and disease. *TIBS* 24, 329-332.

Doria-Medina, C.L., Lund, D.D., Pasley, A., Sandra, A., and Sivitz, W.I. (1993). Immunolocalization of GLUT-1 glucose transporter in rat skeletal muscle and in normal and hypoxic cardiac tissue. *Am. J. Physiol.* 265, E454-E464.

Doyle, D.A., Lee, A., Lewis, J., Kim, E., Sheng, M., and MacKinnon, R. (1996). Crystal Structures of a Complexed and Peptide-Free Membrane Protein-Binding Domain: Molecular Basis of Peptide Recognition by PDZ. *Cell* 85, 1067-1076.

Duff, H.J., Brown, C.E., Cragoe Jr, E.J., and Rahmberg, M. (1991). Antiarrhythmic activity of amiloride: mechanisms. *J. Cardiovasc. Pharmacol.* 17, 879-888.

Duff, H.J., Mitchell, L.B., Kavanagh, K.M., Manyari, D.E., Gillis, A.M., and Wyse, D.G. (1989). Amiloride: antiarrhythmic and electrophysiological actions in patients with sustained ventricular tachycardia. *Circulation* 79, 1257-1263.

Edwards, D.N., Towb, P., and Wasserman, S.A. (1997). An activity-dependent network of interactions link the Rel protein Dorsal with its cytoplasmic regulators. *Development* 24, 3855-3864.

Einheber, S., Schnapp, L.M., Salzer, J.L., Capiello Z.B., and Milner, T.A. (1996). Regional and ultrastructural distribution of the $\alpha 8$ Integrin subunit in developing and adult rat brain suggest a role in synaptic function. *J. Comp. Neurol.* 370, 105-134.

Ek, J.F., Delmar, M., Perzova, R., and Taffet, S.M. (1994). Role of histidine 95 on the pH gating of the cardiac gap junction protein connexin43. *Circ. Res.* 74, 1058-1064.

Fafournoux, P., Noël, J., and Pouyssegur, J. (1994). Evidence that Na⁺/H⁺ exchanger isoforms NHE1 and NHE3 exist as stable dimers in membranes with a high degree of specificity for homodimers. *J. Biol. Chem.* 269, 2589-2596.

Fannon, A.M., and Colman, D.R. (1996). A model for central synaptic junctional complex formation based on the differential adhesive specificities of cadherins. *Cell* 17, 423-424.

Fiedler, K., and Simons, K. (1995). The role of N-glycans in the secretory pathway. *Cell* 81, 309-312.

Fink, A.L. (1999). Chaperone-mediated protein folding. *Physiol. Rev.* 79, 425-449.

Firek, L., and Weingart, R. (1995). Modification of gap junction conductance by divalent cations and protons in neonatal rat heart cells. *J. Mol. Cell. Cardiol.* 27, 1633-1643.

Fliegel, L., and Dyck, J.R.B. (1995). Molecular biology of the cardiac sodium/hydrogen exchanger. *Cardiovasc. Res.* 29, 155-159.

Fliegel, L., Dyck, J.R.B., Wang, H., Fong, C., and Haworth, R.S. (1993). Cloning and analysis of the human myocardial Na⁺/H⁺ exchanger. *Mol. Cell. Biochem.* 125, 137-143.

Fox, J.W., Lamperti, E.D., Eksioglu, Y.Z., Hong, S.E., Feng, Y., Graham, D.A., Scheffer, I.E., Dobyns, W.B., Hirsch, B.A., Radtke, R.A., Berkovic, S.F., Huttenlocher, P.R., and

Walsh, C.A. (1998). Mutations in filamin 1 prevent migration of cerebral cortical neurons in human periventricular heterotopia. *Neuron* 21, 1315-1325.

Frank, J.S., Mottino, G., Reid, D., Molday, R.S., and Philipson, K.D. (1992). Distribution of the Na^+ - Ca^{2+} exchange protein in mammalian cardiac myocytes: An immunofluorescence and immunocolloidal gold-labeling study. *J. Cell Biol.* 117, 337-345.

Froehner, S.C. (1993). Regulation of ion channel distribution at synapses. *Annu. Rev. Neurosci.* 16, 347-368.

Froehner, S.C., Luetje, C.W., Scotland, P.B., and Patrick, J. (1990). The postsynaptic 43K protein clusters muscle nicotinic acetylcholine receptors in *Xenopus* oocytes. *Neuron* 5, 403-410.

Fuhrer, C., Gautam, M., Sugiyama, J., and Hall, Z.W. (1999). Roles of rapsyn and agrin in interaction of postsynaptic proteins with acetylcholine receptors. *J. Neurosci.* 19, 6405-6416.

Fukushima, T., Waddell, T.K., Grinstein, S., Goss, G.G., Orlowski, J., and Downey, G.P. (1996). Na^+ / H^+ exchange activity during phagocytosis in human neutrophils: Role of Fc receptors and tyrosine kinases. *J. Cell Biol.* 132, 1037-1052.

Furutani, M., Trudeau, M.C., Hagiwara, N., Seki, A., Gong, Q., Zhou, Z., Imamura, S., Nagashima, H., Kasanuki, H., Takao, A., Momma, K., January, C.T., Robertson, G.A., and Matsuoka, R. (1999). Novel mechanism associated with an inherited cardiac arrhythmia. Defective protein trafficking by the mutant HERG (G601S) potassium channel. *Circulation* 99, 2290-2294.

Galileo, D.S., Majors, J., Horowitz, A.F., and Sanes, J.R. (1992). Retrovirally introduced antisense integrin RNA inhibits neuroblast migration in vivo. *Neuron* 9, 1117-1131.

Galli, A., and DeFelice, L.J. (1994). Inactivation of L-type Ca channels in embryonic chick ventricle cells: dependence on the cytoskeletal agents colchicine and taxol. *Biophys. J.* 67, 2296-2304.

Gao, T., Puri, T.S., Gerhardstein, B.L., Chien, A.J., Green, R.D., and Hosey, M.M. (1997). Identification and subcellular localization of the subunits of L-type calcium channels and adenylyl cyclase in cardiac myocytes. *J. Biol. Chem.* 272, 19401-19407.

Gautam, M., Noakes, P.G., Mudd, J., Nichol, M., Chu, G.C., Sanes, J.R., Merlie, J.P. (1995). Failure of postsynaptic specialization to develop at neuromuscular junctions of rapsyn-deficient mice. *Nature* 377, 232-236.

Gee, S.H., Madhavan, R., Levinson, S.R., Caldwell, J.H., Sealock, R., and Froehner, S.C. (1998). Interaction of muscle and brain sodium channels with multiple members of the syntrophin family of dystrophin-associated proteins. *J. Neurosci.* 18, 128-137.

Glogauer, M., Arora, P., Chou, D., Janmey, P.A., Downey, G.P., and McCulloch C.A.G.(1998). The role of actin-binding protein 280 in integrin-dependent mechanoprotection. *J. Biol. Chem.* 273, 1689-1698.

Grinstein, S., Woodside, M., Waddell, T.K., Downey, G.P., Orlowski, J., Pouyssegur, J., Wong, D.C.P., and Foskett, J.K.. (1993). Focal localization of the NHE-1 isoform of the Na^+/H^+ antiport: Assessment of effects on intracellular pH. *EMBO J.* 12, 5209-5218.

Grotewiel, M.S., Beck, C.D., Wu, K.D., Zhu, X.R., and Davis, R.L. (1998). Integrin-mediated short-term memory in *Drosophila*. *Nature* 391, 455-460.

Gut, A., Kappeler, F., Hyka, N., Balda, M.S., Hauri, H.-P., and Matter, K. (1998). Carbohydrate-mediated Golgi to cell surface transport and apical targeting of membrane proteins. *EMBO J.* 17, 1919-1929.

Gulbis, J.M., Mann, S., and MacKinnon, R. (1999). Structure of a voltage-dependent K^+ channel β subunit. *Cell* 97, 943-952.

Hall, R.A., Ostedgaard, L.S., Premont, R.T., Blitzer, J.T., Rahman, N., Welsh, M.J., and Lefkowitz, R.J. (1998a). The C-terminal motif found in the β_2 -adrenergic receptor, P2Y1 receptor and cystic fibrosis transmembrane conductance regulator determines binding to the Na^+/H^+ exchanger regulatory factor family of PDZ proteins. *Proc. Natl. Acad. Sci., USA* 95, 8496-8501.

Hall, R.A., Premont, R.T., Chow, C.W., Blitzer, J.T., Pitcher, J.A., Claing, A., Stoffel, R.H., Barak, L.S., Shenolikar, S., Weinman, E.J., Grinstein, S., and Lefkowitz, R.J. (1998b). The β_2 -adrenergic receptor interacts with the Na^+/H^+ -exchanger regulatory factor to control Na^+/H^+ exchange. *Nature* 392, 626-630.

Hammes, A., Oberdorf-Maass, S., Rother, T., Nething, K., Gollnick, F., Linz, K.W., Meyer, R., Hu, K., Han, H., Gaudron, P., Ertl, G., Hoffmann, S., Ganten U., Vetter, R., Schuh, K., Benkwitz, C., Simmer, H.G., and Neyses, L. (1998). Overexpression of the sarcolemmal calcium pump in the myocardium of transgenic rats. *Circ. Res.* 83, 877-888.

Hammond, C., and Helenius, A. (1995). Quality control in the secretory pathway. *Curr. Opin. Cell Biol.* 3, 592-600.

Harper, I.S., Bond, J.M., Chacon, E., Reece, J.M., Herman, B., and Lemasters, J.J. (1993). Inhibition of Na^+/H^+ exchange preserves viability, restores mechanical function, and prevents the pH paradox in reperfusion injury to rat neonatal myocytes. *Basic Res. Cardiol.* 88, 430-442.

Hartwig, J., and Stossel, T. (1975). Isolation and properties of actin, myosin, and a new action-binding protein in rabbit alveolar macrophages. *J. Biol. Chem.* 250, 5696-5705.

Hata, Y., Butz, S., and Sudhof, T.C. (1996). CASK: a novel dlg/PSD95 homolog with an N-terminal calmodulin-dependent protein kinase domain identified by interaction with neurexins. *J. Neurosci.* 16, 2488-2494.

Hebert, D.N., Zhang, J.-X., Chen, W., Foellmer, B., and Helenius, A. (1997). The number and location of glycans on influenza hemagglutinin determine folding and association with calnexin and calreticulin. *J. Cell Biol.* 139, 613-623.

Hille, B. (1991). Ionic channels of excitable membranes. Second edition (Sunderland, Massachusetts: Sinauer Associates).

Horio, Y., Hibino, H., Inanobe, A., Yamada, M., Ishii, M., Tada, Y., Satoh, E., Hata, Y., Takai, Y., and Kurachi, Y. (1997). Clustering and enhanced activity of an inwardly rectifying potassium channel, Kir4.1, by an anchoring protein PSD-95/SAP90. *J. Biol. Chem.* 272, 12885-12888.

Hosey, M.M., and Fields, J.Z. (1981). Quantitative and qualitative differences in muscarinic cholinergic receptors in embryonic and newborn chick hearts. *J. Biol. Chem.* 256, 6395-6399.

Hsueh, Y.P., Kim, E., and Sheng, M. (1997). Disulfide-linked head-to-head multimerization in the mechanism of ion channel clustering by PSD-95. *Neuron* 18, 803-814.

Irie, M., Hata, Y., Takeuchi, M., Ichtchenko, K., Toyoda, A., Hirao, K., Takai, Y., Rosahl, T.W., and Sudhof, T.C. (1997). Binding of neuroligins to PSD-95. *Science* 277, 1511-1515.

Irisawa, H., and Sato, R. (1986). Intra- and extracellular actions of proton on the calcium current of isolated guinea pig ventricular cells. *Circ. Res.* 59, 348-355.

Jan, L.Y., and Jan, Y.N. (1997). Cloned potassium channels from eukaryotes and prokaryotes. *Annu. Rev. Neurosci.* 20, 91-123.

Jing, j., Peretz, T., Singer-Lahat, D., Chikvashvili, D., Thornhill, W.B., and Lotan, I. (1997). Inactivation of a voltage-dependent K^+ channel by β subunit. *J. Biol. Chem.* 272, 14021-14024.

Jurevicius, J., and Fischmeister, R. (1997). Longitudinal distribution of Na^+ and Ca^{2+} channels and β -adrenoceptors on the sarcolemmal membrane of frog cardiomyocytes. *J. Physiol. (Lond.)* 503, 471-477.

Kaplan, S.H., Yang, H., Gilliam, D.E., Shen, J., Lemasters, J.J., and Cascio, W.E. (1995). Hypercapnic acidosis and dimethyl amiloride reduce reperfusion induced cell death in ischaemic ventricular myocardium. *Cardiovasc. Res.* 29, 231-238.

Karmazyn, M. (1988). Amiloride enhances postischemic ventricular recovery: possible role of Na^+/H^+ exchange. *Am. J. Physiol.* 255, H608-H615.

Karmazyn, M., and Moffat, M.P. (1993). Role of Na^+/H^+ exchange in cardiac physiology and pathophysiology: Mediation of myocardial reperfusion injury by the pH paradox. *Cardiovasc. Res.* 27, 915-924.

Karmazyn, M., Ray, M., and Haist, J.V. (1993). Comparative effects of Na^+/H^+ exchange inhibitors against cardiac injury produced by ischemia/reperfusion, hypoxia/reoxygenation, and the calcium paradox. *J. Cardiovasc. Pharmacol.* 21, 172-178.

Kass, R.S., and Davies, M.P. (1996). The roles of ion channels in an inherited disease: molecular genetics of the long QT syndrome. *Cardiovasc. Res.* 32, 443-454.

Keller, S.H., Lindstrom, J., and Taylor, P. (1998). Inhibition of glucose trimming with castanospermine reduces calnexin association and promotes proteasome degradation of the α -subunit of the nicotinic acetylcholine receptor. *J. Biol. Chem.* 273, 17064-17072.

Kentish, J.C., and Nayler, W.G. (1979). The influence of pH on the Ca^{2+} -regulated ATPase of cardiac and white skeletal myofibrils. *J. Mol. Cell. Cardiol.* 11: 611-617.

Kieval, R.S., Bloch, R.J., Lindenmayer, G.E., Ambesi, A., and Lederer, W.J. (1992). Immunofluorescence localization of the Na-Ca exchanger in heart cells. *Am. J. Physiol.* 263, C545-C550.

Kijima, Y., Saito, A., Jetton, T.L., Magnuson, M.A., and Fleischer, S. (1993). Different intracellular localization of inositol 1,4,5-trisphosphate and ryanodine receptors in cardiomyocytes. *J. Biol. Chem.* 268, 3499-3506.

Kim, E., DeMarco, S.J., Marfatia, S.M., Chishti, A.H., Sheng, M., and Strehler, E.E. (1998). Plasma membrane Ca^{2+} ATPase isoform 4b binds to membrane associated guanylate kinase (MAGUK) proteins via their PDZ (PSD-95/Dlg/ZO-1) domains. *J. Biol. Chem.* 273, 1591-1595.

Kim, E., Niethammer, M., Rothschild, A., Jan, Y.N., and Sheng, M. (1995). Clustering of Shaker-type K^{+} channels by interaction with a family of membrane-associated guanylate kinases. *Nature* 378, 85-88.

Kim, E., and Sheng, M. (1996). Differential K^{+} channel clustering activity of PSD-95 and SAP97, two related membrane-associated putative guanylate kinases. *Neuropharmacology* 35, 993-1000.

Kleyman, T.R. and Cragoe Jr, E.J. (1988). Amiloride and its analogs as tools in the study of ion transport. *J. Membr. Biol.* 105, 1-21.

Kornau, H.C., Schenker, L.T., Kennedy, M.B., and Seeburg, P.H. (1995). Domain interaction between NMDA receptor subunits and the postsynaptic density protein PSD-95. *Science* 269, 1737-1740.

Lagadic-Gossmann, D., Buckler, K.J. and Vaughan-Jones, R.D. (1992). Role of bicarbonate in pH recovery from intracellular acidosis in the guinea-pig ventricular myocyte. *J. Physiol. (Lond.)* 458, 361-384.

Lahey, T., Gorczyca, M., Jia, X., and Budnick, V. (1994). The *Drosophila* tumor suppressor gene *dlg* is required for normal synaptic bouton structure. *Neuron* 13, 823-835.

Lazdunski, M., Frelin, C., and Vigne, P. (1985). The sodium/hydrogen exchange system in cardiac cells: its biochemical and pharmacological properties and its role in regulating internal concentrations of sodium and internal pH. *J. Mol. Cell. Cardiol.* 17, 1029-1042.

Lin, J.W., Wyszynski, M., Madhavan, R., Sealock, R., Kim, J.U., and Sheng, M. (1998). Yotiao, a novel protein of neuromuscular junction and brain that interacts with specific splice variants of NMDA receptor subunit NR1. *J. Neurosci.* 18, 2017-2027.

Liu, S., Piwnica-Worms, D., and Lieberman, M. (1990). Intracellular pH regulation in cultured embryonic chick heart cells. Na^+ -dependent $\text{Cl}^-/\text{HCO}_3^-$ exchange. *J. Gen. Physiol.* **96**, 1247-1269.

Liu, S., Taffet, S., Stoner, L., Delmar, M., Vallano, M.L., and Jalife, J. (1993). A structural basis for the unequal sensitivity of the major cardiac and liver gap junctions to intracellular acidification: the carboxyl tail length. *Biophys. J.* **64**, 1422-1433.

Loo, D.T., Kanner, S.B., and Aruffo, A. (1998). Filamin binds to the cytoplasmic domain of $\beta 1$ -integrin. *J. Biol. Chem.* **273**, 23304-23312.

Lue, R.A., Brandin, E., Chan, E.P., and Branton, D. (1996). Two independent domains of hDlg are sufficient for subcellular targeting: the PDZ1-2 conformational unit and an alternatively spliced domain. *J. Cell Biol.* **135**, 1125-1137.

Luo, J., Wang, Y., Yasuda, R.P., Dunah, A.W., and Wolfe, B.B. (1997). The majority of N-methyl-D-aspartate receptor complexes in adult rat cerebral cortex contain at least three different subunits (NR1/NR2A/NR2B). *Mol. Pharmacol.* **51**, 79-86.

Magee, J., Hoffman, D., Colbert, C., and Johnston, D. (1998). Electrical and calcium signaling in dendrites of hippocampal pyramidal neurons. *Annu. Rev. Physiol.* **60**, 327-346.

Maletic-Savatic, M., Lenn, N.J., and Trimmer, J.S. (1995). Differential spatiotemporal expression of K⁺ channel polypeptides in rat hippocampal neurons developing in situ and in vitro. *J. Neurosci.* 15, 3840–51.

Maltsev, V.A., and Undrovinas, A.I. (1997). Cytoskeleton modulated coupling between availability and activation of cardiac sodium channel. *Am. J. Physiol.* 273, H1832-H1840.

Marti, A., Luo, Z., Cunningham, C., Ohta, Y., Hartwig, J., Stossel, T.P., Kyriakis, J.M., and Avruch, J. (1997). Actin-binding protein-280 binds the Stress-activated Protein Kinase (SAPK) activator SEK-1 and is required for tumor necrosis factor- α activation of SAPK in melanoma cells. *J. Biol. Chem.* 272, 2620-2628.

Mays, D.J., Foose, J.M., Philipson, L.H., and Tamkun, M.M. (1995). Localization of the Kv1.5 K⁺ channel protein in explanted cardiac tissue. *J. Clin. Invest.* 96, 282-292.

McDonough, A.A., Zhang, Y., Shin, V., and Frank, J.S. (1996). Subcellular distribution of the sodium pump isoform subunits in mammalian cardiac myocytes. *Am. J. Physiol.* 270, C1221-C1227.

Meier, T., and Wallace, B.G. (1998). Formation of the neuromuscular junction: molecules and mechanisms. *BioEssays* 20, 81-829.

Merlie, J.P., Sebbane, R., Tzartos, S., and Lindstrom, J. (1982). Inhibition of glycosylation with tunicamycin blocks assembly of newly synthesized acetylcholine receptor subunits in muscle cells. *J. Biol. Chem.* 257, 2694-2701.

Mishina, M., Tobimatsu, T., Imoto, K., Tanaka, K., Fujita, Y., Fukuda, K., Kurasaki, M., Takahashi, H., Morimoto, Y., Hirose, T. et al., (1985). Location of functional region of acetylcholine receptor alpha-subunits by site-directed mutagenesis. *Nature* 313, 364-369.

Mitic, L.L., and Anderson, J.M. (1998). Molecular architecture of tight junctions. *Annu. Rev. Physiol.* 60, 121-142.

Moffat, M.P., and Karmazyn, M. (1993). Protective effects of the potent Na/H exchange inhibitor methylisobutyl amiloride against post-ischemic contractile dysfunction in rat and guinea-pig hearts. *J. Mol. Cell. Cardiol.* 25, 959-971.

Murthy, A., Gonzalez-Agosti, C., Cordero, E., Pinney, D., Candia, C., Solomon, F., Gusella, J., and Ramesh, V. (1998). NHE-RF, a regulatory cofactor for Na^+/H^+ exchange, is a common interactor for merlin and ERM (MERM) proteins. *J. Biol. Chem.* 273, 1273-1276.

Myers, M.L., and Karmazyn, M. (1996). Improved cardiac function after prolonged hypothermic ischemia with the Na^+/H^+ exchange inhibitor HOE 694. *Ann. Thorac. Surg.* 61, 1400-1406.

Myers, M.L., Mathur, S., Li, G-H., and Karmazyn, M. (1995). Sodium-hydrogen exchange inhibitors improve postischaemic recovery of function in the perfused rabbit heart. *Cardiovasc. Res.* 29, 209-214.

Myers, M. (1990). Diuretic therapy and ventricular arrhythmias in persons 65 years of age and older. *Am. J. Cardiol.* 65, 599-603.

Nagaya, N., and Papazian, D.M. (1997). Potassium channel α and β subunits assemble in the endoplasmic reticulum. *J. Biol. Chem.* 272, 3022-3027.

Nakamura, T.Y., Coetzee, W.A., Vega-Saenz De Miera, E., Artman, M., and Rudy, B. (1997). Modulation of Kv4 channels, key components of rat ventricular transient outward K^+ current, by PKC. *Am. J. Physiol.* 273, H1775-H1786.

Neugebauer, K.M., Emmett, C. J., Venstrom, k.A., and Reichardt, L.F. (1991). Vitronectin and thrombospondin promote retinal neurite outgrowth: developmental regulation an role of integrins. *Neuron* 6, 345-358.

Ng, T., Shima, D., Squire, A., Bastiaens, P.I.H., Gschmeissner, S., Humphries, M.J., and Paker, P.J. (1999). PKC α regulates b1 integrin-dependent cell motility through association and control of integrin traffic. *EMBO J* 18, 3909-3923.

Niethammer, M., Kim, E., and Sheng, M. (1996). Interaction between the C terminus of NMDA receptor subunits and multiple members of the PSD-95 family of membrane-associated guanylate kinases. *J. Neurosci.* 16, 2157-2163.

Nishimura, S.L., Boylen K.P., Einheber, S., Milner, T.A., Ramos, D.M., and Pytela, R. (1998). Synaptic and glial localization of the integrin $\alpha v \beta 8$ in mouse and rat brain. *Brain Res.* 791, 271-282.

Numata, M., Petrecca, K., Lake, N., and Orlowski, J. (1998). Identification of a mitochondrial Na^+/H^+ exchanger. *J. Biol. Chem.* 273, 6951-6959.

Ohta, Y., Suzuki, N., Nakamura, S., Hartwig, J., and Stossel, T.P. (1999). The small GTPase RalA targets filamin to induce filopodia. *Proc. Natl. Acad. Sci, USA* 96, 2122-2128.

Olden, K., Parent, J.B., and White, S.L. (1982). Carbohydrate moieties of glycoproteins. A re-evaluation of their function. *Biochim. Biophys. Acta.* 650, 209-32.

Olivares, L., Aragon, C., Gimenez, C., and Zafra F. (1995). The role of N-glycosylation in the targeting and activity of the GLYT1 glycine transporter *J. Biol. Chem.* 270, 9437-9442.

Opdenakker, G., Rudd, P.M., Ponting, C.P., and Dwek, R.A. (1993). Concepts and principles of glycobiology. *FASEB J.* 7, 1330-1337.

Orchard, C.H., and Kentish, J.C. (1990). Effects of changes of pH on the contractile function of cardiac muscle. *Am. J. Physiol.* 258, C967-C981.

Orlowski, J. (1993). Heterologous expression and functional properties of the amiloride high affinity (NHE-1) and low affinity (NHE-3) isoforms of the rat Na/H exchanger. *J. Biol. Chem.* 268, 16369-16377.

Orlowski, J., and Grinstein, S. (1997). Na⁺/H⁺ exchangers in mammalian cells. *J. Biol. Chem.* 272, 22373-22376.

Orlowski, J., Kandasamy, R.A., and Shull, G.E. (1992). Molecular cloning of putative members of the Na/H exchanger gene family. cDNA cloning, deduced amino acid sequence, and mRNA tissue expression of the rat Na/H exchanger NHE- 1 and two structurally related proteins. *J. Biol. Chem.* 267, 9331-9339.

Page, E., and McCallister, L.P. (1973). Studies on the intercalated disk of rat left ventricular myocardial cells. *J. Ultrastruct. Res.* 43, 388-411.

Pawson, T., and Scott, J.D. (1997). Signaling through scaffold, anchoring, and adaptor proteins. *Science* 278, 2075-2080.

Petrecca, K., Amellal, F., Laird, D.W., Cohen, S.A., and Shrier, A. (1997). Sodium channel distribution within the rabbit atrioventricular node as analysed by confocal microscopy. *J. Physiol. (Lond.)* 501, 263-274.

Petrecca, K., Atanasiu, R., Grinstein, S., Orlowski, J., and Shrier, A. (1999). Subcellular localization of the Na^+/H^+ exchanger NHE1 in rat myocardium. *Am. J. Physiol.* 276, H709-H717.

Pfaff, M., Shouchun, L., Erle, D.J., and Ginsberg, M.H. (1998). Integrin β cytoplasmic domains differentially bind to cytoskeletal proteins. *J. Biol. Chem.* 273, 6104-6109.

Pierce, G.N., Cole, E.C., Liu, K., Massaeli, H., Maddaford, T.G., Chen, Y.J., McPherson, C.D., Jain, S., and Sontag, D. (1993). Modulation of cardiac performance by amiloride and several selected derivatives of amiloride. *J. Pharmacol. Exp. Ther.* 265, 1280-1291.

Pierce, G.N., and Meng, H. (1992). The role of sodium-proton exchange in ischemic/reperfusion injury in the heart. *Am. J. Cardiovasc. Pathol.* 4, 91-102.

Pierce, G.N., and Philipson, K.D. (1985). Na^+/H^+ exchange in cardiac sarcolemmal vesicles. *Biochim. Biophys. Acta* 818, 109-116.

Pond, A., and Nerbonne, J.M. (1996). A truncated form of HERG identified in human heart. *Circulation* 94, I-641.

Pond, A.L., Scheve, B.K., Benedict, A.T., Petrecca, K., Van Wagoner, D.R., Shrier, A., and Nerbonne J.M. Expression of distinct ERG proteins in rat, mouse and human heart: relation to functional I_{K_r} channels. *J. Biol. Chem.* In Press.

Pongs, O., Leicher, T., Berger, M., Roeper, J., Bähring, R., Wray, D., Giese, K.P., Silva, A.J., and Storm, J.F. (1999). Functional and molecular aspects of voltage-gated K^+ channel β subunits. *Ann. N Y Acad. Sci.* 868, 344-355.

Priori, S.G., Barhanin, J., Hauer, R.N.W., Haverkamp, W., Jongsma, H.J., Kleber, A.G., McKenna, W.J., Roden, D.M., Rudy, Y., Schwartz, K., Schwartz, P.J., Towbin, J.A., and Wilde, A.M. (1999). Genetic and molecular basis of cardiac arrhythmias: impact of clinical management: parts I and II. *Circulation* 99, 518-528.

Pucéat, M., Korichneva, I., Cassoly, R., and Vassort, G. (1995). Identification of band 3-like proteins and Cl^-/HCO_3^- exchange in isolated cardiomyocytes. *J. Biol. Chem.* 270, 1315-13.

Ray, K., Clapp, P., Goldsmith, P.K., and Spiegel, A.M. (1998). Identification of the sites of N-linked glycosylation on the human calcium receptor and assessment of their role in cell surface expression and signal transduction. *J. Biol. Chem.* 273, 34558-34567.

Reddy, P.S., and Corley, R.B. (1998). Assembly, sorting, and exit of oligomeric proteins from the endoplasmic reticulum. *Bioessays* 20, 546-554.

Roden, D.M., Lazzara, R., Rosen, M., Schwartz, P.J., Towbin, J., and Vincent, G.M. (1996). Multiple mechanisms in the long-QT syndrome. Current knowledge, gaps, and future directions. The SADS Foundation Task Force on LQTS. *Circulation* 94, 1996-2012.

Rosenmund, C., and Westbrook, G.L. (1993). Calcium-induced actin depolymerization reduces NMDA channel activity. *Neuron* 10, 805-814.

Rotin, D., and Grinstein, S. (1989). Impaired cell volume regulation in Na^+ - H^+ exchange-deficient mutants. *Am. J. Physiol.* 257, C1158-C1165.

Sanguinetti, M.C., Curran, M.E., Spector, P.S., and Keating, M.T. (1996). Spectrum of HERG K^+ - channel dysfunction in an inherited cardiac arrhythmia. *Proc. Natl. Acad. Sci. USA* 93, 2208-2212.

Sanguinetti, M.C., Curran, M.E., Zou, A., Shen, J., Spector, P.S., Atkinson, D.L., and Keating, M.T. (1996). Coassembly of KvLQT1 and minK (IsK) protein to form cardiac I_{Ks} potassium channel. *Nature* 384, 80-83.

Sanguinetti, M.C., Jiang, C., Curran, M.E., and Keating, M.T. (1995). A mechanistic link between an inherited and an acquired cardiac arrhythmia: HERG encodes the I_{Kr} potassium channel. *Cell* 81, 299-307.

Santacruz-Toloza, L., Huang, Y., John, S.A., and Papazian, D.M. (1994). Glycosylation of shaker potassium channel protein in insect cell culture and in *Xenopus* oocytes. *Biochemistry* 33, 5607-5613.

Satler, C.A., Walsh, E.P., Vesely, M.R., Plummer, M.H., Ginsburg, G.S., and Jacob, H.J. (1996). Novel missense mutation in the cyclic nucleotide-binding domain of HERG causes long QT syndrome. *Am. J. Med. Genet.* 65, 27-35.

Satler, C.A., Vesely, M.R., Duggal, P., Ginsburg, G.S., and Beggs, A.H. (1998). Multiple different missense mutations in the pore region of HERG in patients with long QT syndrome. *Hum. Genet.* 102, 265-272.

Sato, R., Noma, A., Kurachi, Y., and Irisawa, H. (1985). Effects of intracellular acidification on membrane currents in ventricular cells of the guinea pig. *Circ. Res.* 57, 553-561.

Scannevin, R.H., Murakoshi, H., Rhodes, K.J., and Trimmer, J.S. (1996). Identification of a cytoplasmic domain important in the polarized expression and clustering of the Kv2.1 K⁺ channel. *J. Cell. Biol.* 135, 1619-1632.

Schmidt, J.W., and Catterall, W.A. (1986). Biosynthesis and processing of the alpha subunit of the voltage-sensitive sodium channel in rat brain neurons. *Cell* 46, 437-444.

Scholz, W., and Albus, U. (1993). Na^+/H^+ exchange and its inhibition in cardiac ischemia and reperfusion. *Basic Res. Cardiol.* 88, 443-455.

Scholz, W., Albus, U., Counillon, L., Gögelein, H., Lang, H.J., Linz, W., Weichert, A., and Schölkens, B.A. (1995). Protective effects of HOE642, a selective sodium-hydrogen exchange subtype 1 inhibitor, on cardiac ischaemia and reperfusion. *Cardiovasc. Res.* 29, 260-268.

Scholz, W., Albus, U., Lang, H.J., Linz, W., Martorana, P.A., Englert, H.C., and Schölkens, B.A. (1993). Hoe 694, a new Na^+/H^+ exchange inhibitor and its effects in cardiac ischaemia. *Br. J. Pharmacol.* 109, 562-568.

Schulteis, C.T., Nagaya, N., Papazian, D.M. (1998). Subunit folding and assembly steps are interspersed during Shaker potassium channel biogenesis. *J. Biol. Chem.* 273, 26210-26217.

Schultz, J., Hoffmuller, U., Krause, G., Ashurst, J., Macias, M.J., Schmieder, P., Schneider-Mergener, J., and Oschkinat, H. (1998). Specific interactions between the syntrophin PDZ domain and voltage-gated sodium channels. *Nat. Struct. Biol.* 5, 19-24.

Schwarzman, A.L., Singh, N., Tsiper, M., Gregori, L., Dranovsky, A., Vitek, M.P., Glabe, C., St.George-Hyslop, P.H., and Goldgaber, D. (1999). Endogenous presenilin 1 redistributes to the surface of lamellopodia upon adhesion of Jurkat cells to a collagen matrix. *Proc. Natl. Acad. Sci, USA* 96, 7932-7937.

Sealock, R., Wray, B.E., Froehner, S.C. (1984). Ultrastructural localization of the Mr 43,000 protein and the acetylcholine receptor in Torpedo postsynaptic membranes using monoclonal antibodies. *J. Cell Biol.* 98, 2239-2244.

Shadiack, A.M., and Nitkin, R.M. (1991). Agrin induces α -actinin, filamin, and vinculin to co-localize with AChR clusters on cultured chick myotubes. *J. Neurobiol.* 22, 617-628.

Sharma, C.P., Ezzell, R.M., and Arnaout, M.A. (1995). Direct interaction of filamin (ABP-280) with the β 2-integrin subunit CD18. *J. Immunol.* 154, 3461-3470.

Sheng, M. (1996). PDZs and receptor/channel clustering: rounding up the latest aspect. *Neuron* 17, 575-8.

Sheng, M., Tsaur, M-L., Jan, Y.N., and Jan, L.Y. (1992). Subcellular segregation of two A-type K^+ channel proteins in rat central neurons. *Neuron* 9, 271-284.

Shi, G., Nakahira, K., Hammond, S., Rhodes, K.J., Schechter, L.E., and Trimmer, J.S. (1996). β subunits promote K^+ channel surface expression through effects early in biosynthesis. *Neuron* 16, 843-852.

Simske, J.S., Kaech, S.M., Harp, S.A., and Kim, S.K. (1996). LET-23 receptor localization by the cell junction protein LIN-7 during *C. elegans* vulval induction. *Cell* 85, 195-204.

Sobel, A., Weber, M., and Changeux, J.P. (1977). Large-scale purification of the acetylcholine-receptor protein in its membrane-bound and detergent-extracted forms from *Torpedo marmorata* electric organ. *Eur. J. Biochem.* 80, 215-224.

Sonyang, Z., Fanning, A.S., Fu, C., Xu, J., Marfatia, S.M., Chishti, A.H., Crompton, A., Chan, A.C., Anderson, J.M., and Cantley, L.C. (1997). Recognition of unique carboxyl-terminal motifs by distinct PDZ domains. *Science* 275, 73-77.

Sousa, M., and Parodi, A.J. (1995). The molecular basis for the recognition of misfolded glycoproteins by the UDP-Glc-glycoprotein glucosyltransferase. *EMBO J.* 14, 4196-4203.

Spray, D.C., White, R.L., Mazet, F., and Bennett, M.V. (1985). Regulation of gap junctional conductance. [Review]. *Am. J. Physiol.* 248, H753-H764.

Sweadner, K.J., Herrera, V.L.M., Amato, S., Moellmann, A., Gibbons, D.K., and Repke, K.R.H. (1994). Immunologic identification of Na⁺,K⁺-ATPase isoforms in myocardium: Isoform change in deoxycorticosterone acetate-salt hypertension. *Circ. Res.* 74, 669-678.

Staubli, U., Vanderklish, P., and Lynch, G. (1990). An inhibitor of integrin receptors blocks long-term potentiation. *Behav. Neural. Biol.* 53, 1-5.

Takagashi, Y., Rothery, S., Issberner, J., Levi, A., and Severs, N.J. (1997). Spatial distribution of dihydropyridine receptors in the plasma membrane of guinea pig cardiac myocytes investigated by correlative confocal microscopy and label-fracture electron microscopy. *J. Electron. Microsc.* 46, 165-170.

Tamarappoo, B.K., and Verkman, A.S. (1998). Defective aquaporin-2 trafficking in nephrogenic diabetes insipidus and correction by chemical chaperones. *J. Clin. Invest.* 101, 2257-2267.

Tanaka, T., Nagai, R., Tomoike, H., Takata, S., Yano, K., Yabuta, K., Haneda, N., Nakano, O., Shibata, A. et al., (1997). Four novel KVLQT1 and four novel HERG mutations in familial long-QT syndrome. *Circulation* 95, 565-567.

Tani, M., Shinmura, K., Hasegawa, H., and Nakamura, Y. (1996). Effect of methylisobutyl amiloride on $[Na^+]_i$, reperfusion arrhythmias, and function in ischemic rat hearts. *J. Cardiovasc. Pharmacol.* 27, 794-801.

Tatu, U., and Helenius, A. (1997). Interactions between newly synthesized glycoproteins, calnexin and a network of resident chaperones in the endoplasmic reticulum. *J. Cell. Biol.* 136, 555-565.

Toyofuku, T., Yabuki, M., Otsu, K., Kuzuya, T., Hori, M., and Tada, M. (1998). Direct association of the gap junction protein connexin-43 with ZO-1 in cardiac myocytes. *J. Biol. Chem.* *273*, 12725-12731.

Trudeau, M.C., Warmke, J.W., Ganetzky, B., and Robertson, G.A. (1995). HERG, a human inward rectifier in the voltage-gated potassium channel family. *Science* *269*, 92-95.

Tse, C.-M., Levine, S., Yun, C., Brant, S., Counillon, L.T., Pouyssegur, J., and Donowitz, M. (1993). Structure/function studies of the epithelial isoforms of the mammalian Na^+/H^+ exchanger gene family. *J. Membr. Biol.* *135*, 93-108.

Tse, C.-M., Ma, A.I., Yang, V.W., Watson, A.J.M., Levine, S., Montrose, M.H., Potter, J., Sardet, C., Pouyssegur, J., and Donowitz, M. (1991). Molecular cloning and expression of a cDNA encoding the rabbit ileal villus cell basolateral membrane Na^+/H^+ exchanger. *EMBO J.* *10*, 1957-1967.

Tu, J.C., Xiao, B., Yuan J.P., Lanahan, A.A., Leoffert, K., Li, M., Linden, D.J., and Worley, P.F. (1998). Homer binds a novel proline-rich motif and links group 1 metabotropic glutamate receptors with IP3 receptors. *Neuron* *21*, 717-726.

Undrovinas, A.I., Shander, G.S., and Makielski, J.C. (1995). Cytoskeleton modulated gating of voltage-dependent sodium channel in heart. *Am. J. Physiol.* *269*, H203-H214.

Vaughan-Jones, R.D. (1979). Regulation of chloride in quiescent sheep-heart Purkinje fibres studied using intracellular chloride and pH-sensitive micro-electrodes. *J. Physiol. (Lond.)* 295, 111-137.

Veh, R.W., Lichtinghagen, R., Sewing, S., Wunder, F., Grumbach, I.M., and Pongs, O. (1995). Immunohistochemical localization of five members of the Kv1 channel subunits: contrasting subcellular locations and neuron-specific co-localizations in rat brain. *Eur. J. Neurosci.* 7, 2189-2205.

Vincent, G.M. (1998). The molecular genetics of the long QT syndrome: genes causing fainting and sudden death. *Annu. Rev. Med.* 49, 263-274.

Waechter, C.J., Schmidt, J.W., and Catterall, W.A. (1983). Glycosylation is required for maintenance of functional sodium channels in neuroblastoma cells. *J. Biol. Chem.* 258, 5117-5123.

Wakabayashi, S., Shigekawa, M., and Pouyssegur, J. (1997). Molecular physiology of vertebrate Na^+/H^+ exchangers. *Physiol. Rev.* 77, 51-74.

Wallert, M.A., and Fröhlich, O. (1989). Na^+/H^+ exchange in isolated myocytes from adult rat heart. *Am. J. Physiol.* 257, C207-C213.

Wang, H., Kunkel, D.D., Schwartzkroin, P.A., and Tempel, B.L. (1994). Localization of Kv1.1 and Kv1.2, two K channel proteins, to synaptic terminals, somata, and dendrites in the mouse brain. *J. Neurosci.* *14*, 4588-4599.

Ward, C.L., and Kopito, R.R. (1995). Degradation of CFTR by the ubiquitin-proteasome pathway. *Cell* *83*, 121-127.

Warmke, J.W., and Ganetzky, B. (1994). A family of potassium channel genes related to eag in *Drosophila* and mammals. *Proc. Nat. Acad. Sci., USA* *91*, 3438-3442.

Weinman, E.J., Steplock, D., Tate, K., Hall, R.A., Spurney, R.F., and Shenolikar, S. (1998). Structure-function of recombinant Na/H exchanger regulatory factor (NHE-RF). *J. Clin. Invest.* *101*, 2199-2206.

Westpal, R.S., Tavalin, S.J., Lin, J.W., Alto, N.M., Fraser, I.D.C., Langeberg, L.K., Sheng, M., and Scott, J.D. (1999). Regulation of NMDA receptors by an associated phosphatase-kinase signaling complex. *Science* *285*, 93-96.

White, R.L., Doeller, J.E., Verselis, V.K., and Wittenberg, B.K. (1990). Gap junctional conductance between pairs of ventricular myocytes is modulated synergistically by H⁺ and Ca⁺⁺. *J. Gen. Physiol.* *95*, 1061-1075.

Woods, D.F., and Bryant, P.J. (1991). The Discs-large Tumor Suppressor Gene of *Drosophila* Encodes a Guanylate Kinase Homolog Localized at Septate Junctions Cell 66, 451–464.

Wyszynski, M., Lin, J., Rao, A., Nigh, E., Beggs, A.H., Craig, A.M., and Sheng, M. (1997). Competitive binding of α -actinin and calmodulin to the NMDA receptor. *Nature*, 385, 439-442.

Wyszynski, M., and Sheng, M. (1999). Analysis of ion channel associated proteins. *Method. Enzymol.* 294, 371-385.

Xie, Z., Xu, W., Davie, E.W., and Chung, D.W. (1998). Molecular cloning of human ABPL, an actin-binding protein homologue. *Biochem. Biophys. Res. Commun.* 251, 914-919.

Xu, L., Mann, G., and Meissner, G. (1996). Regulation of cardiac Ca^{2+} release channel (ryanodine receptor) by Ca^{2+} , H^+ , Mg^{2+} , and adenine nucleotides under normal and simulated ischemic conditions. *Circ. Res.* 79, 1100-1109.

Xue, Y.X., Aye, N.N., and Hashimoto, K. (1996). Antiarrhythmic effects of HOE642, a novel Na^+ - H^+ exchange inhibitor, on ventricular arrhythmias in animal hearts. *Eur. J. Pharmacol.* 317, 309-316.

Yasutake, M., Ibuki, C., Hearse, D.J., and Avkiran, M. (1994). Na^+/H^+ exchange and reperfusion arrhythmias: Protection by intracoronary infusion of a novel inhibitor. *Am. J. Physiol.* 267, H2430-H2440.

Yoshida, H., Horie, M., Otani, H., Takano, M., Tsuji, K., Kubota, T., Fukunami, M., and Sasayama, S. (1999). Characterization of a novel missense mutation in the pore of HERG in a patient with long QT syndrome. *J. Cardiovasc. Electrophysiol.* 10, 1262-1270.

Yu, F.H., Shull, G.E., and Orlowski, J. (1993). Functional properties of the rat Na/H exchanger NHE-2 isoform expressed in Na/H exchanger-deficient Chinese hamster ovary cells. *J. Biol. Chem.* 268, 25536-25541.

Yun, C.H., Lamprecht, G., Forster, D.V., and Sidor, A. (1998). NHE3 kinase A regulatory protein E3KARP binds the epithelial brush border Na^+/H^+ exchanger NHE3 and the cytoskeletal protein ezrin. *J. Biol. Chem.* 273, 25856-25863.

Yun, C.H., Oh, S., Zizak, M., Steplock, D., Tsao, S., Tse, C.M., Weinman, E.J., and Donowitz, M. (1997). cAMP-mediated inhibition of the epithelial brush border Na^+/H^+ exchanger, NHE3, requires an associated regulatory protein. *Proc. Natl. Acad. Sci. U S A* 94, 3010-3015

Zhang, J.Z., and Ismail-Beigi, F. (1998). Activation of Glut1 glucose transporter in human erythrocytes. *Arch. Biochem. Biophys.* 356, 86-92.

Zhang, J.F., and Siegelbaum, S.A. (1991). Effects of external protons on single cardiac sodium channels from guinea pig ventricular myocytes. *J. Gen. Physiol.* 98, 1065-1083.

Zhou, Z., Gong, Q., Epstein, M., and January, C.T. (1998a). Multiple mechanisms of HERG channel dysfunction in human long QT associated mutation. *Biophys. J.* 74, A26.

Zhou, Z., Gong, Q., Epstein, M., and January, C.T. (1998c). HERG channel dysfunction in human long QT syndrome. *J. Biol.Chem.* 273, 21061-21066.

Zhou, Z., Gong, Q., Ye, B., Fan, Z., Makielski, J.C., Robertson, G.A., and January, C.T. (1998b). Properties of HERG channels stably expressed in HEK 293 cells studied at physiological temperature. *Biophys. J.* 74, 230-241.

Ziff, E.B. (1997). Enlightening the postsynaptic density. *Neuron* 19, 1163-1174.

Zito, K., Fetter, R.D., Goodman, C.S., and Isacoff, E.Y. (1997). Synaptic clustering of Fasciclin II and Shaker: essential targeting sequences and role of Dlg. *Neuron* 19, 1007-1016.